# Synthesis of Conjugated Polymers for Organic Solar Cell Applications

Yen-Ju Cheng,* Sheng-Hsiung Yang, and Chain-Shu Hsu*

*Department of Applied Chemistry, National Chiao Tung University, 1001 Ta Hsueh Road, Hsin-Chu 30049, Taiwan*

*Received May 7, 2009*

## Contents



* To whom correspondence should be addressed. Phone: +886-3513-1523. Fax: +886-3513-1523. E-mail: yjcheng@mail.nctu.edu.tw (Y.-J.C.); cshsu@mail.nctu.edu.tw (C.-S.H.).

## 1. Introduction

Harvesting energy directly from sunlight using photovoltaic technology is considered as being one of the most important ways to address growing global energy needs using a renewable resource. Polymeric solar cells (PSCs) are a promising alternative for producing clean and renewable energy due to the fact that there is the potential to fabricate them onto large areas of lightweight flexible substrates by solution processing at a low cost.[1,2] Organic photovoltaic cells with a single-component active layer sandwiched between two electrodes with different work functions only led to very low power conversion efficiency due to poor charge carrier generation and unbalanced charge transport.[3]

A bilayer heterojunction configuration containing a p-type layer for hole transport and an n-type layer for electron transport has been implemented by Tang to improve the photocurrent of the solar cell device.[4] As shown in Figure 1, the general working principle in such solar cells first involves the photoexcitation of the donor material by the absorption of light energy to generate excitons. This Coulomb-correlated electron−hole pair, the exciton, diffuses to the donor−acceptor (D−A) interface where exciton dissociation occurs via an electron-transfer process. The fully separated free charge carriers transport to the respective electrodes in the opposite direction with the aid of the internal electric field, which in turn generates the photocurrent and photovoltage. Due to the fact that their limited lifetimes only allow excitons to diffuse a short distance, between 5 and 14 nm,[5−9] donor excitons created far away from the heterojunction interface decay to the ground state without the chance to reach the acceptor. This leads to the loss of absorbed photons and quantum efficiency. Consequently, the performance of bilayer heterojunction devices is greatly limited by the small area of charge-generating interface between the donor and acceptor.

To overcome this difficulty, the concept of a bulk heterojunction (BHJ) was introduced by the pioneering work of Yu et al.[10] By blending donor and acceptor materials together, an interpenetrating network with a large D−A

10.1021/cr900182s CCC: $71.50 
Published on Web 09/28/2009

Yen-Ju Cheng received his Ph.D. degree in chemistry from the National Taiwan University (NTU) in 2004 under the supervision of Professor Tien-Yau Luh. After spending another year as a postdoctoral assistant with Prof. Luh at NTU, he joined Prof. Alex K.-Y. Jen's group as a postdoctoral researcher at the University of Washington in 2005. In the summer of 2008, he joined the Department of Applied Chemistry, National Chiao Tung University, in Taiwan as an assistant professor. His current research interest is focused on the design, synthesis, and characterization of organic and polymeric functional materials for optoelectronic and photovoltaic applications.

Sheng-Hsiung Yang received his B.S. degree from the Department of Applied Chemistry in 1998 from National Chiao Tung University, Taiwan. He obtained his Ph.D. degree in material science from the University of Nantes, France, in 2004. His research interests include liquid crystalline polymers, organic light-emitting diodes, and self-assembly of conjugated materials. Currently he is a postdoctoral researcher on light-emitting polymers in Prof. Chain-Shu Hsu's laboratory.

Chain-Shu Hsu received his Ph.D. degree from Case Western Reserve University in 1987 and conducted his postdoctoral work at the National Tsing Hua University in Taiwan. He joined the Department of Applied Chemistry of the National Chiao Tung University, Taiwan, in 1988 as an associate professor and was promoted to full professor in 1991. Currently he is serving as a vice president and chair professor of the National Chiao Tung University. His research interests include liquid crystalline polymers and conjugated polymers, polymer light-emitting diodes, and organic photovoltaics. He has published more than 160 research papers and 18 patents. He is currently on the international advisory board of *Polymer* and editorial boards of the *Journal of Polymer Science, Polymer Chemistry*, and the *Journal of Polymer Research*. He received the Excellent Research Award of the National Science Council, Taiwan, in 1994, the Franco-Taiwan Scientific Award for nanomaterials in 2006, Teco and Hou Chin Tui Awards in 2007, and an Academic Award of the Ministry of Education, Taiwan, in 2008.

interfacial area can be achieved through controlling the phase separation between the two components in bulk. In this way, any absorbing site in the composite is within a few nanometers of the donor−acceptor interface, leading to much enhanced quantum efficiency of charge separation. The formation of a bicontinuous network creates two channels to transport holes in the donor domain and electrons in the acceptor domain, resulting in efficient charge collection.

Because the BHJ configuration only requires a single active layer to create an internal D−A heterojunction, the fabrication of the device can be greatly simplified by employing solution processing techniques without having to deal with the interfacial erosion problems always encountered in making the bilayer configuration. Figure 2 illustrates the standard BHJ solar cell architecture where an active layer of the BHJ composite is sandwiched between two electrodes. The current−voltage ($I-V$) characteristics under illumination and the essential parameters are shown in Figure 3.

The major breakthrough and rapid development of BHJ solar cells arose from the discovery of efficient photoinduced electron transfer in conjugated polymer−fullerene composites as reported by Sariciftci and co-workers.[11] Buckminsterfullerene ($C_{60}$) has proven to be an ideal n-type material due to its various intrinsic advantages. First, it possesses a relatively low-lying lowest unoccupied molecular orbital (LUMO) energy level which is thermodynamically favorable to accepting electrons from an excited p-type material.[12] Second, the triply degenerate $C_{60}$ LUMO enables it to be reduced by up to six electrons, which reflects its unique stabilization of negative charges. Third, kinetically, photoinduced electron transfer from a conjugated polymer to a $C_{60}$ derivative can occur on a time scale of 45 fs, which is several orders of magnitude faster than the radiative decay of photoexcitation or back electron transfer. As a result, the quantum efficiency of charge separation is approaching unity.[13] Through this ultrafast electron transfer which immediately quenches the highly reactive excited state of p-type materials, any possible photooxidation associated with oxygen can be reduced, thus dramatically improving the photostability of the conjugated polymers.[14,15] Finally, $C_{60}$ derivatives also exhibit very high electron mobility in field-effect transistors (FETs).[16] However, the tendency to crystallize and the poor solubility of $C_{60}$ in organic solvents hinder direct applications in inexpensive solution-based processing techniques unless the bare $C_{60}$ structure is functionalized with solubilizing moieties.[17−21] To date, one particular solublizing derivative synthesized by Wudl and Hummelen in 1995, namely, [6,6]-phenyl-$C_{61}$-butyric acid methyl ester (PCBM), is the most ubiquitously used acceptor for current BHJ solar cell research (Chart 1).[21] One apparent drawback of PCBM comes from its insufficient absorption in the visible region due to its structural symmetry which forbids low-energy transitions. The efficiency of BHJ devices can be further improved by replacing acceptor $C_{60}$ PCBM with its higher fullerene analogue $C_{70}$ PCBM ($PC_{71}BM$),[22,23] which has lower symmetry and allows more transitions (Chart 1).[24]

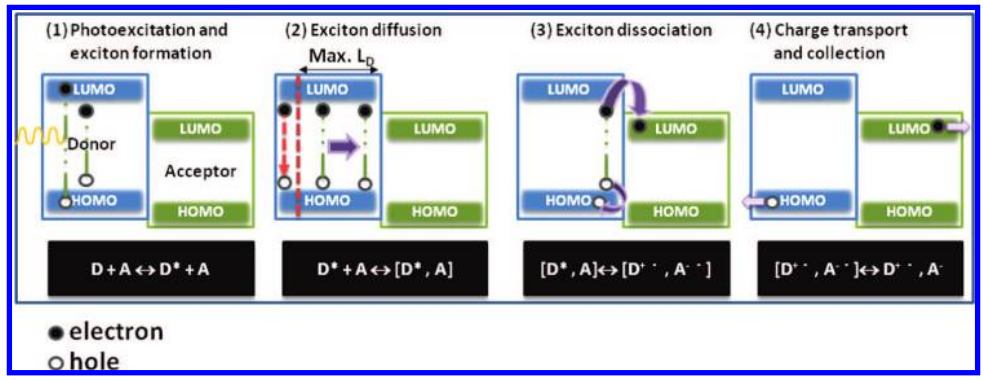


**Figure 1.** Working mechanism for donor−acceptor heterojunction solar cells. (1) Photoexitation of the donor to generate a Coulomb-correlated electron−hole pair, an exciton. (2) Exciton diffusion to the D−A interface. A distance longer than the maximum diffusion length (max $L_D$) will lead to relaxation of the exciton. (3) Bound exciton dissociation at the D−A interface to form a geminate pair. (4) Free charge transportation and collection at electrodes.

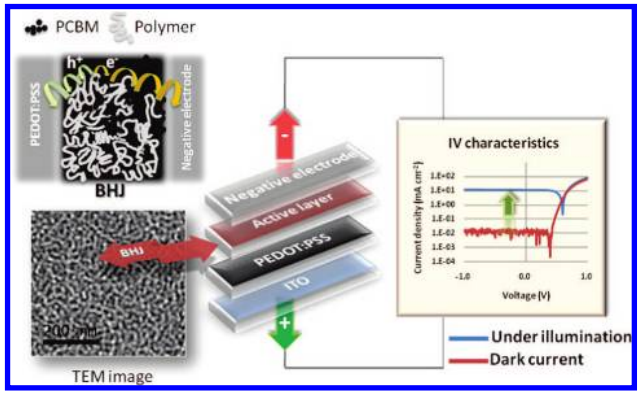


**Figure 2.** Architecture of a bulk heterojunction photovoltaic device using indium tin oxide (ITO) as the electrode and poly[3,4-(ethylenedioxy)thiophene]−poly(styrenesulfonate) (PEDOT:PSS) as the hole-conducting layer. The enlarged area shows the active layer consisting of a conjugated polymer−[6,6]-phenyl-$C_{61}$-butyric acid methyl ester (PCBM) composite with a bicontinuous interpenetrating morphology with domain sizes between 10 and 20 nm. (The bottom one is a TEM image, and the top one is a drawing illustration).

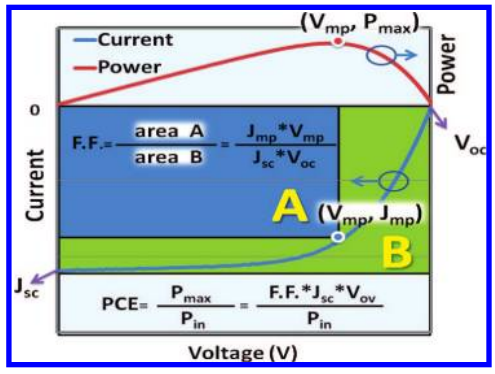


**Figure 3.** Current−voltage ($I$−$V$) characteristics and the corresponding power−voltage curve for a BHJ solar cell under illumination. Essential parameters determining the photovoltaic performance are shown: $J_{sc}$ is the short-circuit current, $V_{oc}$ is the open-circuit voltage, $J_{mp}$ and $V_{mp}$ are the current and voltage, respectively, at which a given device's electrical power output is the maximum, $P_{max}$, the fill factor (FF) is a graphic measure of the squareness of the $I$−$V$ curve, and the power conversion efficiency (PCE) is defined as the ratio of maximum power output ($P_{max}$) to power input ($P_{in}$).

Enhancement is mainly attributed to $C_{70}$'s stronger light absorption in the visible region than that of $C_{60}$.

Although $C_{60}$ derivatives currently fill an irreplaceable need for n-type materials, there is still an urgent need to develop ideal p-type materials. Conjugated polymers are novel materials that combine the optical and electronic properties of semiconductors with processing advantages. As well as having contributed to a wide range of applications such as in organic conductors, field-effect transistors and electroluminescent diodes, conjugated polymers continue to serve as the most promising p-type materials for producing organic solar cells with low weight, integrated flexibility, and low cost. Through a tremendous research effort over the past decade to create numerous novel conjugated polymers, device performance in BHJ solar cells has been steadily enhanced and power conversion efficiency (PCE) higher than 2% is becoming more and more commonplace. A most encouraging PCE of over 5% has been achieved not only for the well-known regioregular poly(3-hexylthiophene) but also for many newly developed low band gap conjugated polymers. Recent theoretical calculations further predict that a PCE for BHJ solar cells of over 10% is foreseeable if a perfect p-type material equipped with all required properties is available.[25−27] This indicates that the development of novel conjugated polymers will certainly play a pivotal role in driving this research.

**Chart 1. Chemical Structures of PCBM and $PC_{71}BM$**

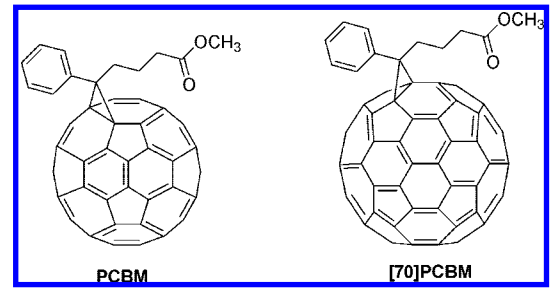


Several reviews have examined the use of conjugated polymers in solar cell applications.[28−32] In view of the rapid growth of this active field and the increasing number of publications in recent years, this review will not only cover the most important and representative conjugated polymers that have had a significant impact in the field but will also update the latest progress and development of materials with promising performance. Particular attention will be focused on synthetic approaches directed toward making these polymers as well as highlighting the useful and important building blocks leading to the necessary monomers. The principle of molecular design with band gap engineering, structure−property relationships, and device performances

will also be discussed although space limits any comprehensive or complete coverage.

## 2. Molecular Design and Engineering of Conjugated Polymers

The most critical challenges in developing ideal p-type materials are to design and synthesize a conjugated polymer that simultaneously possesses good film-forming properties, strong absorption ability, high hole mobility, and suitable HOMO−LUMO energy levels. A fundamental understanding of molecular design and the benefits of versatile polymer syntheses allow for the effective tailoring of the intrinsic properties of conjugated polymers to serve the desired purpose and address the application needs.

### 2.1. Requirement of Band Gap and HOMO−LUMO Energy Levels

The magnitude of the band gap and the energy positions of the HOMO and LUMO energy levels are the most important characteristics for determining the optical and electrical properties of a given conjugated polymer. These in turn greatly influence the ultimate photovoltaic performance. The first step in the photovoltaic mechanism which converts light energy to electrical energy in a device involves the absorption of sunlight by the photoactive materials. The wavelength of the maximum photon flux density of the solar spectrum is located at approximately 700 nm, which corresponds to a low energy of 1.77 eV. To fully exploit the endless source of solar energy, the absorption spectrum of a conjugated polymer needs to cover both the red and near-infrared ranges to match the greater part of the terrestrial solar spectrum and hence harvest the maximum photon flux. It is highly desirable to develop conjugated polymers with broader absorptions through narrowing their optical band gap. To efficiently absorb light, high overall extinction coefficients of the polymers are also of critical importance and should not be sacrificed as the optical band gaps become smaller. The low band gap conjugated polymers have been intensely studied for more than two decades to realize the ultimate goal of developing organic conducting metals without the need of doping. Through numerous manipulations and modifications of the chemical structures of conjugated polymers, band gaps as small as 0.5 eV can be achieved.[33] While the utility of renewable energy emerges as a global issue to address the energy crisis, conjugated polymers with low band gaps regain research interest due to their potential application in organic solar cells. The most straightforward way to reduce the band gap is simply by either raising the HOMO or lowering the LUMO level of the polymer or by compressing the two levels closer together simultaneously. Unfortunately, the optical property associated with light harvesting is not the only one under consideration in designing new p-type polymers. Following photoexcitation, the generated exciton diffuses to the D−A interface to achieve charge separation. To obtain high efficiencies from BHJ polymer solar cells, the n-type material properties of the fullerene derivatives employed should be taken into account throughout the development process. It has been demonstrated that the open-circuit voltage in BHJ solar cells with ohmic contacts is linearly dependent on the magnitude of the built-in potential, defined as the difference between the HOMO level of a p-type polymer and the LUMO level of an n-type PCBM.[34−36] The schematic energy profile and

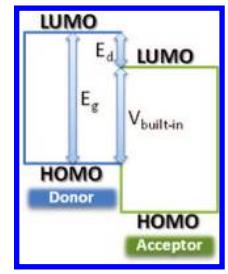


**Figure 4.** Energy diagram of donor and acceptor HOMO−LUMO levels showing three intercorrelated parameters. $E_g$ is the band gap of the polymer, $E_d$ is the LUMO energy difference inducing a downhill driving force for electron transfer, and $V_b$ is the built-in potential which has a linear relationship with the open-circuit voltage.

intercorrelated parameters of the donor−acceptor interface are shown in Figure 4. The donor with the lower HOMO level will better reach the theoretically attainable $V_{oc}$, whereas reduction in a polymer's band gap to broaden the absorption coverage by lifting up the HOMO level will inevitably result in a loss of $V_{oc}$. On the other hand, the LUMO level of p-type materials has to be at least 0.3 eV higher than that level of the fullerene derivatives to guarantee the formation of a downhill driving force for the energetically favorable electron transfer and overcome the binding energy of the intrachain exciton.[27,37,38] Lowering the LUMO level of a conjugated polymer to achieve a narrow band gap may result in the LUMO level eventually being lower than that of the fullerene, thus hampering the efficient electron transfer. A compromise is needed to balance the trade-off between the small band gap of the donor and the favorable energy HOMO−LUMO relationship between the donor and acceptor. As a result, the effort to find new p-type polymers for PSC is not solely directed to pursuing low band gaps but also to controlling the band gap by modulating the HOMO−LUMO levels to their optimal values.

### 2.2. Strategies for Band Gap Engineering

In terms of the formidable challenges and complex prerequisites needed for conjugated polymers used in solar cell applications, molecular engineering to carefully fine-tune the band gap is of critical importance. Before conjugated polymers are reviewed, it would be helpful to understand and discuss the general design strategies used to control their band gaps.[33,39,40] The skeleton of a polyaromatic conjugated polymer such as polyphenylene, poly(phenylenevinylene), and polythiophene can be simplified and defined as "a series of consecutive carbon−carbon double bonds linked together by a carbon−carbon single bond". There are two possible resonance structures for the ground state with nondegenerate energy (Figure 5). The first is called the aromatic form: here each thiophene or benzene unit maintains its aromaticity with confined $\pi$-electrons. Delocalization of the flowing $\pi$-electrons along the conjugated chain converts double bonds into single bonds and synchronously transforms single bonds into double bonds, leading to a resonance structure referred to as the quinoid form. Compared to the aromatic form, the quinoid form is energetically less stable and hence has a smaller band gap because adopting a quinoid structure requires destruction of the aromaticity and a loss in the stabilization energy. The ratio of the aromatic to quinoid population in a polyaromatic conjugated system can be correlated and represented by a geometrical parameter, i.e., bond length alternation (BLA), which is defined as the

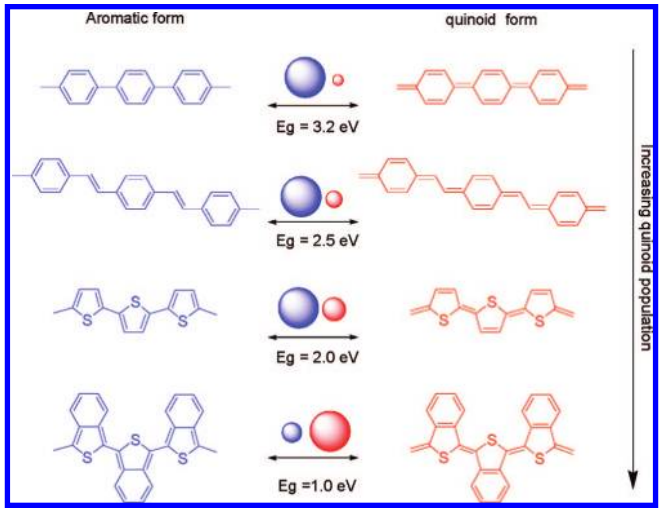


**Figure 5.** Aromatic and quinoid resonance forms of poly(*p*-phenylene), poly(*p*-phenylenevinylene), polythiophene, and polyisothianaphthene. The relative contribution of the mesomeric structures is represented by the size of the colored circles over the arrows.

average of the difference in length between adjacent carbon−carbon bonds in a polyene chain. The more the aromatic form prevails in the ground state, the larger the BLA value obtained.[41] As the quinoid contribution increases, the carbon−carbon single bonds between two adjacent rings adopt more double bond character and the BLA starts to decrease. Overall, the HOMO−LUMO band gap decreases linearly as a function of the increasing quinoid character with concomitant decreasing BLA value. It is apparent that the BLA is highly dependent on the aromatic stabilization resonance energy of the aromatic unit. A reduction in aromaticity of the aromatic units in the conjugated main chain allows a greater tendency to adopt the quinoid form through $\pi$-electron delocalization. Benzene rings with a high degree of aromaticity cause polyphenylene to have a high band gap of ca. 3.2 eV. By inserting a double bond to dilute the effect of the benzene rings and reduce the aromaticity, the band gap of poly(phenylenevinylene) is reduced to ca. 2.4 eV. Furthermore, thiophene has an even lower aromaticity than benzene, so polythiophene is even more likely to adopt a quinoid form, and consequently, it has a lower band gap of 2.0 eV. The most creative way to effectively increase the quinoid character of polythiophene is represented by polyisothianaphthene (PITN).[42] Again, this is because benzene has a larger aromatic resonance energy than thiophene (1.56 vs 1.26 eV, respectively). The main chain of PITN tends to favor the quinoid form to selectively maintain the benzene aromaticity, making PITN the first well-known conjugated polymer with a narrow band gap as low as 1 eV.[43,44] In a similar approach of quinoidization by aromatic exchange, poly(thieno[3,4-*b*]pyrazine) **P1**[45] or poly(thieno[3,4-*b*]-thiophene) **P2**[46] with primary thiophene rings fused with another aromatic pyrazine or thiophene ring at the $\beta$-position have also been synthesized to promote quinoid population and achieve low band gap conjugated polymers (Chart 2).

Additionally, molecular modification used to impose steric or electronic effects on conjugated main chains affords various useful strategies for reducing the band gap. Planarization between adjacent aromatic units allows parallel p-orbital interactions to extend conjugation and facilitate delocalization. This in turn leads to a decrease in the BLA and reduction of the band gap. The most straightforward way

**Chart 2. Chemical Structures of Poly(thieno[3,4-*b*]pyrazine) P1 and Poly(thieno[3,4-*b*]thiophene) P2**

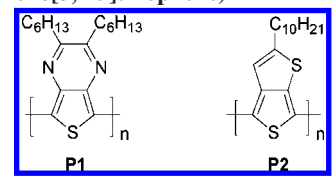


**Chart 3. Chemical Structures of Rigidified P3 and P4**

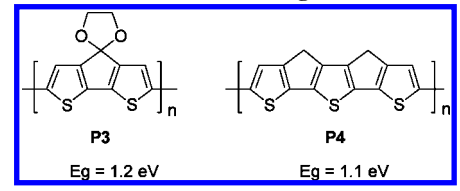


**Chart 4. Chemical Structures of P5 and P6 with Its Resonance Structure**

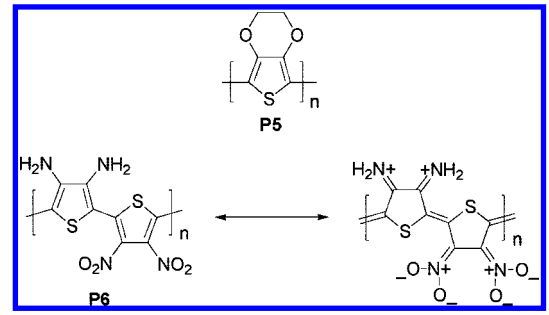


to surpass the rotational disorder due to steric hindrance is to tie and rigidify two adjacent aromatic units through covalent chemical bonding. This effect has been well demonstrated in a series of excellent work by Roncali and co-workers. For example, **P3**, where the bithiophene repeating unit is rigidified and bridged by the $sp^3$ carbon of a ketal group, exhibits a remarkably low band gap of 1.2 eV.[47,48] Extension of the bridged system from bithiophene to terthiophene for **P4** further decreases the band gap to 1.1 eV (Chart 3).[49]

In general, the energy difference between the HOMO and LUMO decreases as the length of conjugation increases. However, when the number of monomer units exceeds a certain value at which the effective conjugation length is saturated, the band gap starts to level off. Therefore, unlimited extension of the conjugation length results only in a limited reduction of the band gap.

Incorporation of electron-donating or electron-withdrawing substituents directly onto the aromatic unit in the main chain represents another effective way of perturbing the molecular orbitals through either inductive or mesomeric effects. In general, electron-donating groups raise the HOMO energy, while electron-withdrawing groups lower the LUMO energy, resulting in a decreased band gap. For example, poly[3,4-(ethylenedioxy)thiophene] (**P5**) with direct attachment of electron-donating alkoxy groups has a band gap of 1.5 eV, which is about 0.5 eV lower than that of the parent polythiophene.[50] For **P6** the dual effects of electron-donating amino groups and electron-withdrawing nitro groups on the neighboring thiophene units results in a dramatically reduced band gap of 1.1 eV due to its high degree of zwitterionic and quinoid character (Chart 4).[51]

A more powerful strategy in designing low band gap conjugated polymers is to alternate a conjugated electron-rich donor (D) unit and a conjugated electron-deficient

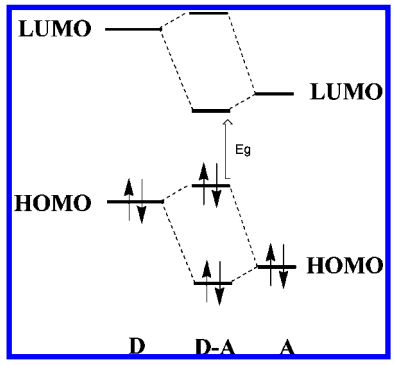


**Figure 6.** Orbital interactions of donor and acceptor units leading to a smaller band gap in a D−A conjugated polymer.

**Chart 5. Chemical Structures of P7 and P8**

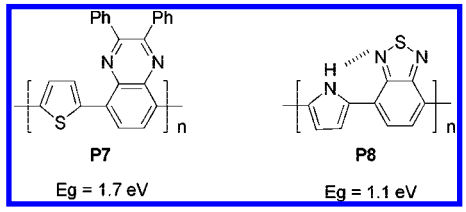


acceptor (A) unit in the same polymer backbone.[52] Through the introduction of push−pull driving forces to facilitate electron delocalization and the formation of quinoid mesomeric structures (D−A → $D^+$=$A^-$) over the conjugated main chain, the BLA can be significantly reduced. Photoinduced intramolecular charge transfer (ICT) correlated with the high-lying HOMO of the donor unit and the low-lying LUMO of the acceptor unit can also account for the reduced optical band gap. This can be elucidated in a more explicit and simpler way by introducing the concept of hybridization of the molecular orbital between the donor and acceptor in the D−A polymer.[53] As shown in Figure 6, according to the rules of perturbation theory, the HOMO of the donor segment will interact with the HOMO of the acceptor segment to yield two new HOMOs for the D−A polymer. Similarly, the LUMO of the donor will interact with that of the acceptor to produce two new LUMOs of the D−A polymer. After the electrons redistribute themselves from their original noninteracting orbitals to the new hybridized orbitals of the polymer, a higher lying HOMO and a lower lying LUMO are formed. This leads to a narrowing of the optical band gap. One evident experimental characteristic of an ICT absorption band is its sensitivity to solvent polarity. In general, the energy required for absorption decreases as the solvent polarity increases.

The copolymer **P7** with alternating electron-rich thiophene and electron-deficient quinoxaline moieties exhibits a band gap of 1.7 eV (Chart 5).[54] The degree of band gap reduction is strongly dependent on the strength of donor and acceptor segments embedded in the conjugated polymer. A judicial choice of the donor−acceptor combination allows for tuning the band gap to the desired magnitude.

With a stronger donor of pyrrole and a stronger acceptor of benzothiadiazole, copolymer **P8** shows a very low band gap of 1.1 eV in comparison with **P7**. Such a low band gap was also attributed to the presence of intramolecular hydrogen bonding, which results in conformational planarization assisted by supramolecular interaction.[55] Apart from the intrinsic properties of a conjugated polymer in the solution state, intermolecular interactions induced by secondary forces in the solid state promote interchain delocalization and

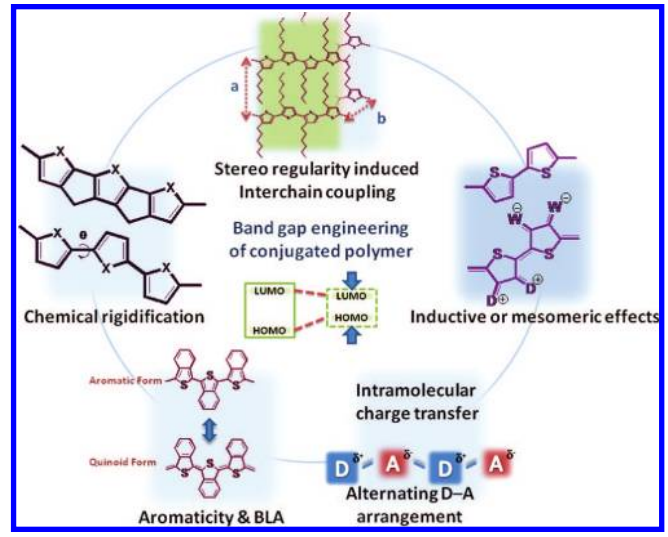


**Figure 7.** Illustration of band gap engineering strategies of conjugated polymers.

enable a dramatic reduction of the band gap. A highly stereoregular structure with an extended coplanar conjugated conformation is a prerequisite to attain a closely packed and ordered crystalline domain. The general strategies used to control the band gap of conjugated polymers are illustrated in Figure 7.

After photon absorption and exciton dissociation, the most critical factor regarding conjugated polymers in determining the photovoltaic performance is the charge-transport mobility. The molecular engineering strategies mentioned above are also closely related to the charge-transporting properties of conjugated polymers. Physical and chemical properties such as facile $\pi$-electron delocalization, ordered and planar intermolecular channels, and excellent electrochemical stability and reversibility will all facilitate the hole-transporting mobility.[56−58]

## 2.3. Solubility Issues

The targeted polymers should possess reasonable solubilities in organic solvents to ensure their solution-processability. It is rather frustrating if a new conjugated polymer made by tremendous synthetic efforts turns out to be insoluble and hence unprocessable. The degree of solubility of a given polymer is governed by several structural factors, including the degree of polymerization, the chain length of the aliphatic groups, the polarity of the attached substituents, backbone rigidity, polymer regioregularity, and intermolecular interactions. In addition to the processability, the solubility issue can directly influence many other important polymer physical parameters such as crystallinity, phase behavior, microscopic morphology, and contact between different active components, which ultimately determine the device performance of the final PVCs. Strong interchain $\pi-\pi$ stacking interactions are known to be the major contributing reason that most polyaromatic conjugated polymers are rendered insoluble. Introducing aliphatic side chains which are covalently attached to the conjugated main chain is an inevitable design for improving the solubility. Branched alkyl chains are more effective than their straight-chain counterparts for inducing solubility. It should be stressed that increasing the content of insulating alkyl chains relative to the hole-conductor portion in the polymer may result in deterioration in the charge mobility function. As a result, depending on the nature

**Chart 6. Catalytic Cycle of Transition-Metal-Catalyzed Reactions**

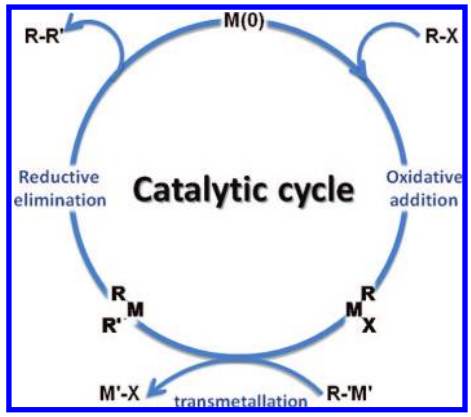


of the conjugated backbone, judicious choice of a suitable solubilizing group at an appropriate location is of crucial importance for fine-tuning the structure−property relationship.

## 2.4. General Routes for Synthesis of Conjugated Polymers

The construction of conjugated polymers lies essentially in the efficient carbon−carbon single bond formation between two unsaturated carbons in the aromatic units. In addition to electrochemical[59−61] or chemical[62] oxidative polymerizations, transition-metal-catalyzed cross-coupling reactions provide a particularly powerful arsenal for $Csp^2-Csp^2$ and $Csp-Csp^2$ bond formation.[63] The reaction, in general, involves a transition-metal-catalyzed oxidative addition reaction across the C−X bond of an electrophile and then transmetalation with a main group organometallic nucleophile, followed by a reductive elimination step leading to the carbon−carbon bond formation. Concomitantly the active catalyst is regenerated (Chart 6). The most commonly employed transition-metal catalysts are nickel- or palladium-based complexes, although other metals have also been used. The organometallic nucleophiles can be Grignard reagents (Kumada−Corriu),[64] stannyl (Stille),[65] boron reagents (Suzuki−Miyaura),[66] or copper (Sonogashira).[67] Thus, conjugation lengths can be extended through consecutive transformations in the catalytic cycle. When the electrophilic and nucleophilic centers of the monomeric substrates are readily accessible, regioregularity of the polymers can be easily achieved. Another advantage is that these reaction conditions are generally mild and can tolerate many functional groups. This is particularly important for synthesizing advanced functional conjugated polymers. Stille and Suzuki coupling reactions using two distinct monomers are the most efficient and widely used methods for preparing alternating copolymers. It is noteworthy that stannyl groups substituted on the benzene ring of the monomer substrate always give poor reactivity with aryl halides under Stille coupling conditions.[68] Therefore, Stille coupling is more suitable for thiophene-containing polymers using monomers with stannyl groups on the thiophene ring, whereas Suzuki coupling is more widely used for preparing benzene-containing polymers with boronic groups on the benzene ring of the monomer.

On the other hand, nickel-mediated Yamamoto dehalogenation coupling reactions also provide an alternative pathway for carrying out self-polymerizaiton of single monomers.[69] Traditional reactions such as the Wittig−Horner reaction or Knoevenagel condensation are particularly useful in the synthesis of vinylene-containing conjugated polymers via the carbon−carbon double bond formation between two respective monomers.

**Scheme 1. Synthesis of PPV (P9) via the Wessling Route**

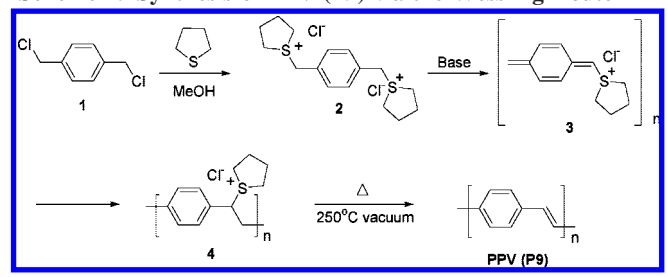


In the following section, we will review those conjugated polymers which are mainly classified according to the structures of the representative electron-rich fragments along the main chain.

# 3. p-Phenylenevinylene-Based Conjugated Polymers

## 3.1. Poly(*p*-phenylenevinylene) and Its Derivatives

Conjugated poly(*p*-phenylenevinylene)s (PPVs) have attracted a great deal of attention due to their conducting and photoluminescent properties. PPV is the first polymer reported for light-emitting diode applications.[70] Its derivatives remain the most popular conjugated polymers for this application and continue to generate considerable interest and much research for photovoltaic applications. Pure poly(*p*-phenylenevinylene) is insoluble and infusible and therefore difficult to process into the solid state. Initial attempts using a traditional Wittig reaction of *p*-xylylenebis(triphenylphosphonium chloride) and terephthalaldehyde to construct the double bonds only led to insoluble PPV with very low molecular weight.[71] A general methodology to circumvent this problem is to develop a synthetic route that involves a solution-processable polymer precursor. The synthesis of high-quality PPV films with high molecular weights was first developed by Wessling (Scheme 1).[72,73] Treatment of the bis(sulfonium halide) salt of *p*-xylene (**2**) with 1 equiv of base induces a 1,6-elimination to generate the quinodimethane-like intermediate **3**, which subsequently undergoes 1,6-polymerization to produce the sulfonium precursor polymer **4**. This water-soluble precursor can then be spin-cast into a thin film and converted in situ into conjugated PPV (**P9**) after thermal treatment in a vacuum to trigger a 1,2-elimination. The Wessling sulfonium precursor route has also been utilized to prepare a wide range of other PPV derivatives.[74,75] In a similar manner, various modified Wessling procedures using sulfur-based leaving groups such as sulfinyl, sulfonyl, and xanthate have all been reported for the synthesis of a range of PPV derivatives.[76−78]

Some of the drawbacks of this precursor approach include the generation of toxic side products during the solid-state elimination process, structural defects arising from incomplete thermal conversion or oxidation, and undefined molecular weights and distribution.[79] By incorporating long alkyl or alkoxy chains into the phenylene ring before polymerization to ensure the solubility, a one-step approach can be applied to make processable PPV derivatives which can then be cast into thin films directly without conversion for device fabrication.[80] Up until now, the most widely used method for the preparation of PPV derivatives is the Gilch route.

**Scheme 2. Synthesis of MEH-PPV (P10) via the Gilch Route**

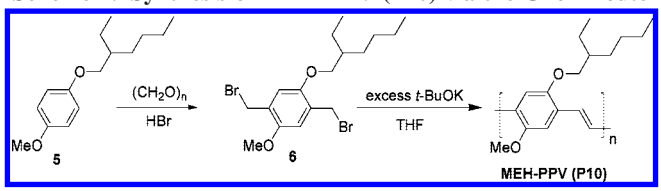


**Chart 7. Chemical Structure of MDMO-PPV (P11)**

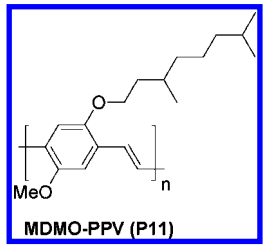


This involves the reaction of α,α′-dihalo-*p*-xylene **6** with 2 equiv of base to obtain conjugated PPV through a one-pot straightforward elimination−polymerization−elimination three-step procedure.[81−83] Because of the smaller size of the halide relative to sulfur-based leaving groups, this route allows PPV to introduce more bulky groups into the phenylene ring without affecting the reaction. A typical Gilch route to the synthesis of a representative solution-processable poly(2-methoxy-5-((2′-ethylhexyl)oxy)-1,4-phenylenevinylene) (MEH-PPV, **P10**) is depicted in Scheme 2.[83] By following the same synthetic route, poly(2-methoxy-5-((3′,7′-dimethyloctyl)oxy)-1,4-phenylenevinylene) (MDMO-PPV, **P11**) can also be synthesized (Chart 7). This route involves mild polymerization conditions, and the molecular weights of the polymers obtained are generally high.

In some cases gelation or precipitation of the polymeric products may occur during polymerization. Ferraris et al. developed a modified Gilch method for carrying out anionic polymerizations by the addition of monomer to the base solution along with using 4-methoxyphenol as the initiator to control the molecular weight.[83] The mechanism of the synthetic route to PPV via a quinodimethane intermediate has been a debatable subject: a radical vs an anionic pathway. The presence of radical trapping reagents during the reaction significantly reduces the molecular weight of PPV, implying a radical mechanism.[84,85] On the other hand, in the presence of an additive nucleophile as the initiator, an anionic polymerization pathway has been proposed.[86−88]

It has been shown that formation of structural defects in PPV will give rise to deteriorated emission efficiency. Regioregular, head-to-tail coupling of the asymmetric quinodimethane halide **8** results in 100% vinylene formation in **P12** between the neighboring phenylene units after elimination of **9**. However, it is known that the resulting polymer **P13** contains 1.5−2.2% structural defects due to head-to-head or tail-to-tail couplings in **10**. This leads to the sequential formation of corresponding acetylene and ethylene moieties which in turn attenuate the desired electronic and optical properties of PPV (Scheme 3).[89] By manipulating the substituents on the phenylene ring, the number of defects can be reduced to obtain high-performance polymers.[90,91]

Besides the elimination approach via a quinodimethane intermediate, other traditional Wittig-type[92] and Knoevenagel-type[93] polycondensations or palladium-catalyzed Heck coupling reactions have all been employed to prepare PPV derivatives.[94]

**Scheme 3. Illustration of Defect Formation during the Gilch Route**

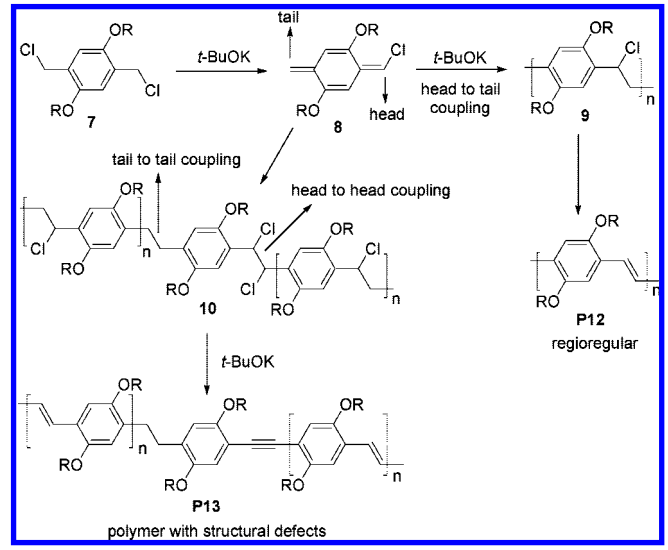


**Chart 8. Chemical Structure of Polymer BBL P14**

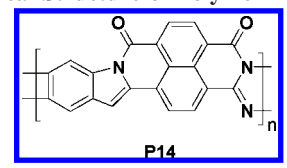


The substituent on the phenylene ring of PPV allows for the tuning of the band gap. The HOMO and LUMO levels of unsubstituted PPV are reported to be ca. −5.1 and −2.7 eV, respectively, with a band gap around 2.4 eV.[95] Introducing two alkoxy groups into the phenylene ring to perturb the molecular orbitals lowers the LUMO to −2.9 eV with an essentially unchanged HOMO level. Hence, the band gap is reduced to 2.2 eV.[95] Consequently, PPV emits a green-yellow light, while MEH-PPV exhibits a yellow-orange emission. Because PPV derivatives are the earliest conjugated polymers developed for organic electronics application, they were also frequently used as the active materials in bilayer heterojunction solar cells before the concept of bulk heterojunction configuration was widely accepted. For bilayer photovoltaic cells, PPV and MEH-PPV serve as the electron donor in conjunction with a poly(benzimidazobenzophenanthroline ladder) (BBL, **P14**) as the electron acceptor (Chart 8).[96] The bilayer device with the configuration ITO/PPV/**P14**/Al showed a $J_{sc}$ of 2.3 mA/cm$^2$, a $V_{oc}$ of 1.06 V, an FF of 47%, and a PCE value of 1.4%. While using MEH-PPV as the electron donor, the device achieved a PCE of 0.8% under the same conditions.[96] The better photovoltaic performance of PPV over MEH-PPV can be ascribed to the greater crystallinity and structural order of the PPV main chain compared to alkylated MEH-PPV. In addition, the fact that the complementary optical absorption of PPV/**P14** covers the 300−720 nm spectral range, whereas MEH-PPV/**P14** lacks absorption in the 350−460 nm range, also contributes.

Soluble MEH-PPV was also combined with PCBM for photovoltaic applications. The bilayer photovoltaic device with the configuration ITO/PEDOT:PSS/MEH-PPV/PCBM/Al showed a $J_{sc}$ of 2.1 mA/cm$^2$, a $V_{oc}$ of 0.75 V, an FF of 23%, and a PCE value of 0.46%.[97] A bulk heterojunction photovoltaic cell using MEH-PPV/PCBM as the active layer has also been characterized. It showed better PCE values in the range 1.1−1.3% than bilayer devices.[98] Furthermore, by stacking two independent single photovoltaic cells together

**Chart 9. Chemical Structures of $C_{60}$ Derivatives 11 and 12**

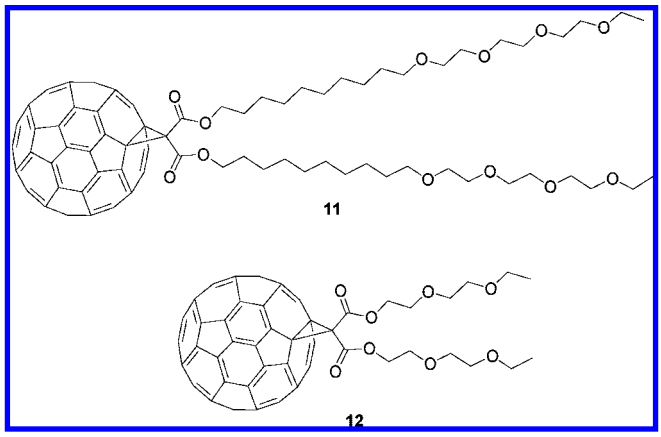


with the help of the transparent cathode LiF/Al/Au, the PCE of the multiple-device stacked structure can be dramatically improved 2-fold to 2.6%.[98] The cells can be stacked together and connected either in parallel or in series, resulting in doubled $J_{sc}$ or $V_{oc}$, respectively, compared to those of a single cell.

Two alternative soluble methanofullerene derivatives **11** and **12** have been developed to serve as electron acceptors and blended with MEH-PPV to fabricate photovoltaic devices. The chemical structures of the $C_{60}$ derivatives are shown in Chart 9. Due to a better compatibility of **11** with MEH-PPV, the MEH-PPV/**11** system shows a better device PCE of 0.49% than the MEH-PPV/**12** system, which has a PCE of 0.22%.[99] In addition to $C_{60}$ derivatives, different types of titanium oxide ($TiO_2$) were combined with MEH-PPV for photovoltaic applications.[100−104] However, their device performances were generally low, with PCE values lower than 0.5%.

MDMO-PPV is the most widely used PPV derivative to serve as the electron donor in combination with $C_{60}$ electron acceptor derivatives in organic BHJ photovoltaic cells. Devices based on blended MDMO-PPV:PCBM (1:4, w/w) were fabricated and reported by Shaheen and co-workers.[105] It was found that when chlorobenzene was used as the casting solvent instead of toluene to deposit the active layer, an optimal morphology with suppressed phase segregation and enhanced microstructure was obtained, resulting in increased charge carrier mobility for both holes and electrons in the active layer. Consequently, the device achieved a $J_{sc}$ of 5.23 mA/cm$^2$, a $V_{oc}$ of 0.82 V, and a high PCE of 2.5%.[105]

Regioregularity in MDMO-PPV also plays an important role in determining the device performance. As shown in Scheme 4, Tajima and co-workers synthesized a fully regioregular MDMO-PPV (**P15**) by the Wittig−Hornor reaction of a single monomer (**15**) comprised of aldehyde and phosphonate functionalities.[106] Regiorandom MDMO-PPV (**P16**), from dialdehyde **16** and diphosphnate monomers **17**, was also prepared for comparison. A PCE of 3.1%, a $J_{sc}$ of 6.2 mA/cm$^2$, a $V_{oc}$ of 0.71 V, and an FF of 70% were achieved with regioregular MDMO-PPV (**P15**). This is the highest efficiency reported for the PPV:PCBM system so far. In contrast, the device based on regiorandom MDMO-PPV (**P16**)/PCBM only achieved a PCE of 1.7%. It is concluded that higher crystallinity of the polymer for higher hole mobility and better mixing morphology between the polymer and PCBM contribute to the improvement of photovoltaic performance with regioregular MDMO-PPV.

Various physics and engineering aspects have been investigated for devices based on the MDMO-PPV/PCBM bulk heterojunction active layer system: photooxidation,[107] stacked cells,[108] active layer thickness,[109] NMR morphology studies,[110] and insertion of a hole-transporting layer between PEDOT and the active layer.[111] Apart from the PCBM organic acceptor, inorganic electron acceptors[112−115] such as metal oxides or quantum dots are also under active development and have been combined with conjugated MDMO-PPV to form hybrid organic−inorganic bulk heterojunction solar cells. Optimized photovoltaic devices using blends of MDMO-PPV:ZnO[113] or MDMO-PPV:cadmium selenide[115] exhibited moderate PCE values of 1.6% and 1.8%, respectively.

In addition to PPV homopolymer derivatives, two α,α′-dihalo-*p*-xylene monomers with different side chains can also be randomly copolymerized by the Gilch route to afford a variety of interesting PPV derivatives. The feeding ratio of two monomers can be varied to fine-tune the steric and electronic properties of the resultant polymer. Scheme 5 shows the synthesis of two different dendron-containing MEH-PPV derivatives. **P17** has 3,5-dialkoxybenzyl pendents,[116] while **P18** possesses electron-deficient oxadiazole segments as the side chain.[117] A solar cell device based on **P18**:PCBM (1:4, w/w) displayed a $J_{sc}$ of 4.93 mA/cm$^2$, a $V_{oc}$ of 0.81 V, an FF of 40%, and a PCE value of 1.6%. On the other hand, a device fabricated using a **P17**:PCBM (1:3, w/w) blend showed a $J_{sc}$ of 3.37 mA/cm$^2$, a $V_{oc}$ of 0.81 V, an FF of 42%, and a PCE value of 1.41%, which is slightly better than the corresponding MEH-PPV-based device with a PCE of 1.32% under the same condition.

A new PPV derivative (**P19**) with two triphenylamine groups attached directly to the 2,5-positions of the phenylene moieties was synthesized by the Wittig−Horner reaction of **22** and **23** to improve its hole-transporting properties and balance of charge transport in the active layer (Scheme 6).[118] Compared to **P20** with a band gap of 2.3 eV, **P19** exhibits a lower band gap of 2.0 eV and broader absorption spectrum due to the electronic band of the triphenylamino group at shorter wavelengths and a more red-shifted band at longer wavelengths arising from the 3-dimensional $\pi-\pi$ stacking. The bulk heterojunction polymer solar cells based on **P19**/PCBM (1:1, w/w) showed a PCE of 0.45%, which is much higher than that of the device based on **P20** (0.09%) without the triphenylamino side chains.

## 3.2. Cyano-Containing Poly(*p*-phenylenevinylene)s

In addition to introducing functional groups on the phenylene ring, the molecular orbital energy levels of PPV derivatives can also be tuned by incorporating electronic substituents into the conjugated vinylene bridges. By means of a facile Knoevenagel polycondensation between terephthaldehyde **24** and 1,4-bis(cyanomethyl)benzene **25** in the presence of the base *t*-BuOK, the CN-PPV derivatives containing a cyano group on each double bond are easily accessible (Scheme 7). Careful control of the reaction conditions is required to avoid a Michael addition which may lead to defected polymers. Alkoxy chains are introduced onto the aromatic rings to improve the solubility of the resulting polymers.

Compared to MEH-PPV, the replacement of vinylene linkages with cyanovinylene linkages in MEH-CN-PPV lowers both the LUMO and HOMO levels by ~0.5 eV, with little effect on the magnitude of the band gap. It should also be noted that, with additional cyano groups on the double bond, the conjugated backbone may twist as a result of steric hindrance. Additionally, CN-PPV displays high electron

**Scheme 4. Synthesis of Regioregular and Regiorandom MDMO-PPVs**

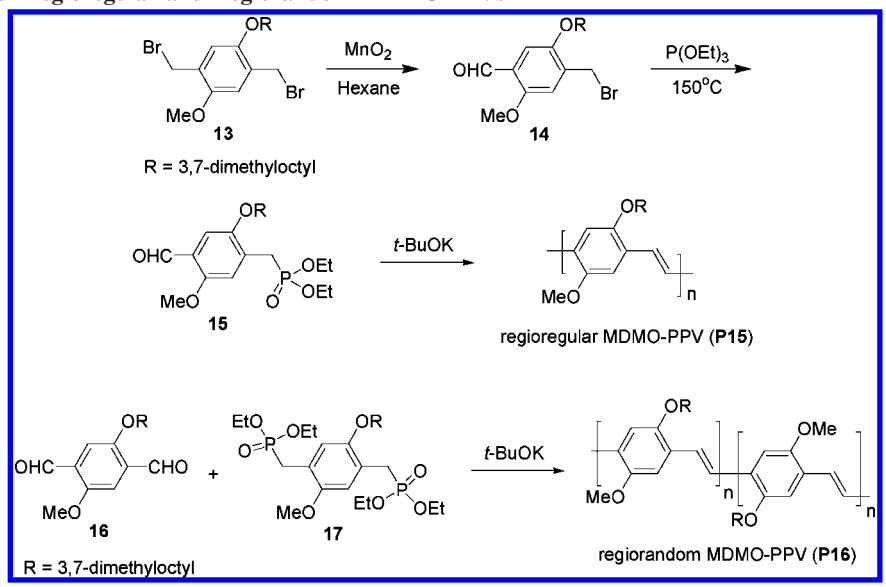


**Scheme 5. Synthesis of PPV Copolymers P17 and P18**

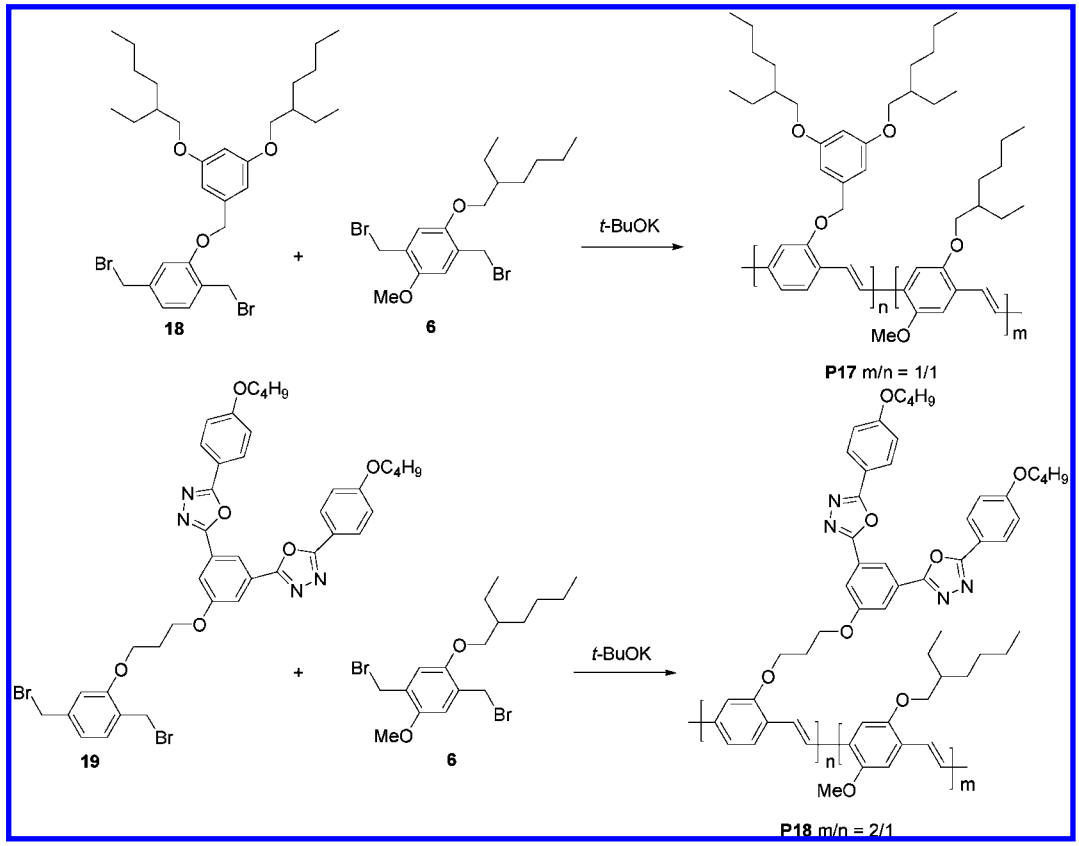


affinities and electron-transport properties as a result of the electron-withdrawing effect of the cyano side group and a low-lying LUMO level so that it can function as a suitable electron acceptor in photovoltaic devices in either a bilayer or bulk heterojunction configuration.[119−121] For example, a bilayer device consisting of **P21** as the n-type layer and polythiophene **P22** as the p-type layer, was constructed by a lamination technique followed by thermal annealing, achieving an overall PCE of 1.9%.[119] Alternatively, MEH-PPV has also been blended with **P23** as the electron donor−acceptor pair in a single-layer device, showing much better photovoltaic performance compared to similar devices with single components of either MEH-PPV or CN-PPV **P23**.[120] The chemical structures of **P22** and **P23** are shown in Chart 10. It is also noteworthy that CN-PPV derivatives with increased oxidation potential also improve the stability of PPV against singlet oxygen photooxidation.[122]

## 3.3. Cyano- and Thiophene-Containing Poly(*p*-phenylenevinylene)s

To effectively reduce the band gap of CN-PPV below 2 eV, electron-rich thiophene units with lower aromaticities have been incorporated into the main chain to form a D−A arrangement. Vanderzande et al. reported a series of copolymers based on the bis(1-cyano-2-thienylvinylene)phenylene

**Scheme 6. Synthesis of TPA-Containing P19 and Chemical Structure of P20**

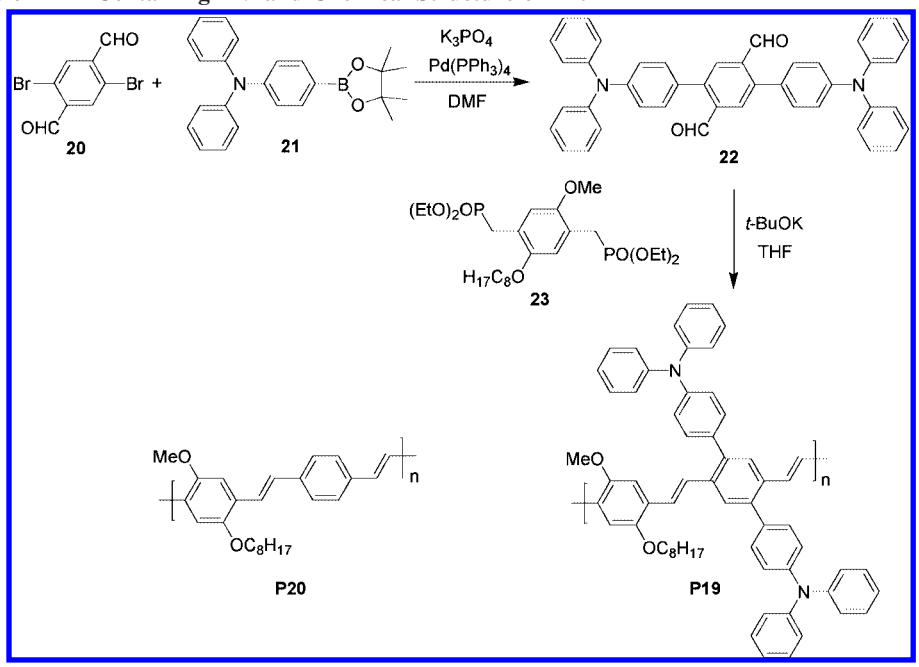


**Scheme 7. Synthesis of CN-PPV Copolymer P21 via a Knoevenagel Polycondensation**

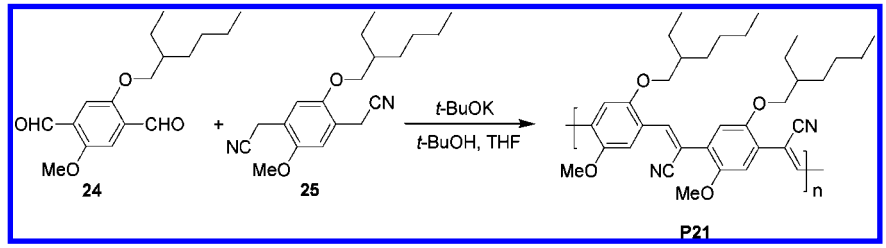


**Chart 10. Chemical Structures of P22 and P23**

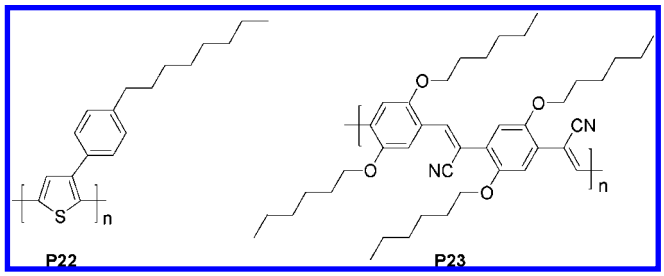


**Chart 11. Chemical Structures of P24−P27 Synthesized by Oxidative Polymerization of 31−34**

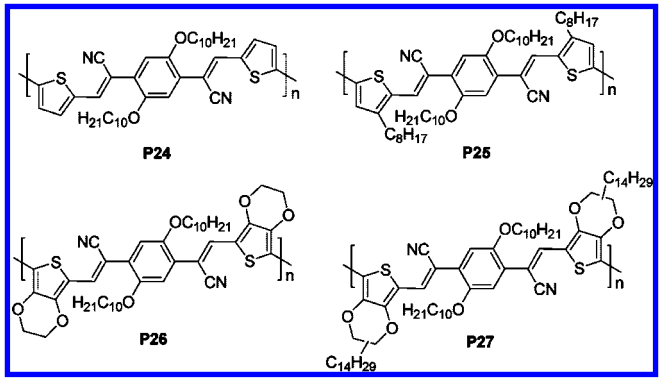


structure with different alkyl or alkoxy side chains on the thiophene rings (Chart 11).[123] The monomers were all prepared by Knoevenagel condensations to construct cyanovinylene linkages (Scheme 8). Each polymer was directly synthesized by $FeCl_3$ oxidative polymerization of the corresponding repeating unit monomer. The optical band gaps were determined to be 1.77, 1.72, 1.59, and 1.72 eV for **P24**, **P25**, **P26**, and **P27**, respectively. The decreasing trend in the band gap observed in **P24**−**P26** is attributed to the increasingly raised HOMO level due to the enhancement of the electron-donating effect from octyl to ethylenedioxy groups on the thiophene units. Moreover, such substitution effects have little influence on the LUMO level, which is mainly dominated by the presence of the cyanovinylene linkages. However, with additional bulky tetradecyl groups attached at the ethylenedioxy group, steric effects come into play. **P27** exhibited a higher band gap of 1.72 eV. This can be rationalized by the decrease in $\pi$ stacking interactions in the solid state as a result of the steric hindrance. The electron-rich nature of thiophene units in these polymers makes them good candidates to serve as electron donors in BHJ devices. Both **P25**/PCBM- and **P26**/PCBM-based photovoltaic devices achieved a PCE of around 0.14%. Optimization of the **P26**/PCBM device by thermal annealing showed a slight increase of PCE to 0.19%. The unsatisfactory results are related to the low hole mobility observed in the pure polymer films.

In a very similar manner, Reynold et al. also reported synthesizing a range of CN-PPV derivatives (**P28**−**P31**) containing dioxythiophene moieties in the main chain (Chart 12).[124,125] These donor−acceptor conjugated polymers possess narrow band gaps of about 1.5−1.8 eV and good solubilities in common organic solvents. The best photovoltaic device based on **P29**/PCBM (1:4, w/w) showed a PCE

**Scheme 8. Synthesis of Monomers 31−34 via Knoevenagel Condensations**

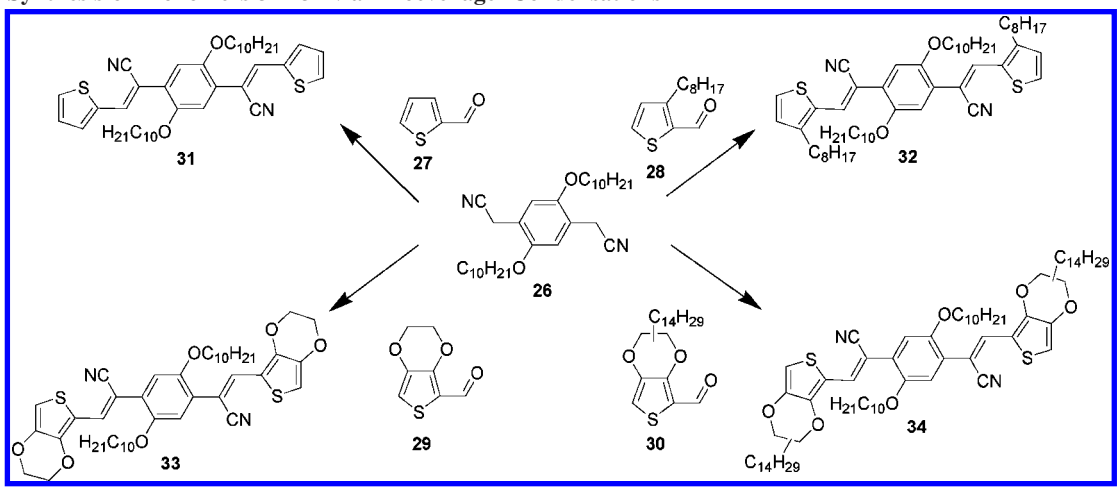

**Chart 12. Chemical Structures of P28−P31**

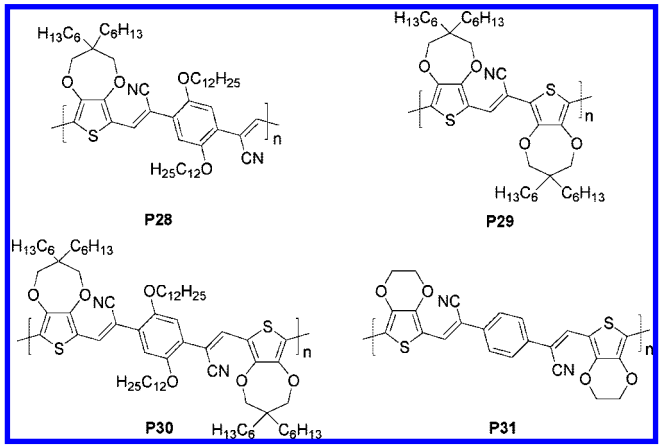

**Scheme 9. Synthesis of Acetylene-Containing P32 via a Wittig−Horner Reaction**

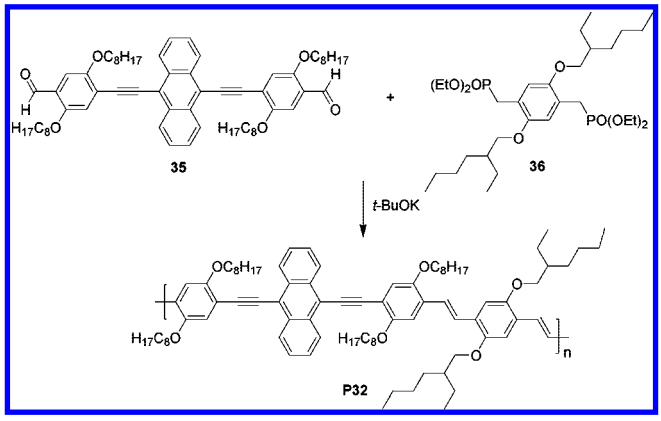

of 0.2%, which is very consistent with the results reported by Vanderzande et al.[123]

## 3.4. Acetylene-Containing Poly(*p*-phenylenevinylene)s

A number of PPV derivatives containing alternating arylene−ethynylene units were synthesized to evaluate their photovoltaic properties. The coplanar and rigid nature of the acetylene moiety in the polymer chain may have the potential to obtain a higher degree of packing and thus improve the photovoltaic performance of such devices. Scheme 9 shows the synthesis of the polymer **P32** via the Horner−Emmons reaction of the dialdehyde **35** and *p*-xylylenebis(diethyl phosphonate) **36** monomers in the presence of *t*-BuOK as the base.[126] Having coplanar electron-rich anthracene units and triple bond bridges, **P32** exhibits broader absorption, a lower HOMO level, and a smaller optical band gap of 1.9 eV, compared to MDMO-PPV. A device with the configuration of ITO/PEDOT/**P32**:PCBM (1:2, w/w)/LiF/Al, yielded a PCE value of up to 2% with a high $V_{oc}$ of 0.81 V. Chart 13 shows the chemical structures of a series of acetylene-containing PPV derivatives synthesized by similar procedures. For polymers **P35** and **P36**,[127] the introduction of a thiophene ring into the polymer backbone showed an improvement in the PCE ranging from 1.2% to 1.7%. This is higher than those for **P33** and **P34**,[128] based on the same device configuration of ITO/PEDOT/polymer:PCBM (1:3, wt %)/LiF/Al.

## 4. Fluorene-Based Conjugated Polymers

Fluorene-containing molecules represent an important class of aromatic systems that have received considerable attention due to their unique photophysical properties and potential for chemical modification. Fluorene and its derivatives are rigid, planar molecules that are usually associated with relatively large band gaps and low HOMO energy levels, rendering them highly stable toward photodegradation and thermal oxidation during device operation. Easy dialkylation at the 9-position and selective bromination at the 2,7-positions of fluorene allow versatile molecular manipulation to enhance solubility and extend conjugation easily by means of a transition-metal cross-coupling reaction. Due to their high fluorescence quantum yield, excellent hole-transporting properties, good film-forming properties, and exceptional chemical stability, polyfluorene-based (PF) conjugated polymers have been extensively studied and utilized specifically in the field of light-emitting diodes.[129,130] It is envisioned that the fluorene unit can emerge as a highly promising building block for the design of new p-type materials for photovoltaic applications. This is due to the fact that the low-lying HOMO levels and high hole mobility character of fluorene derivatives are expected to achieve higher open-circuit voltages and short-circuit currents, respectively. However, the optical band gap of poly(9,9-dialkylfluorene) is ca. 3.0 eV, which is too high for efficient sunlight harvesting where the maximum photon flux is around 1.7 eV. This problem can be solved by incorporating an electron-accepting unit into the main polyfluorene chain to form a donor−acceptor alternating arrangement and hence narrow-

**Chart 13. Chemical Structures of Acetylene-Containing PPV Derivatives P33−P36**

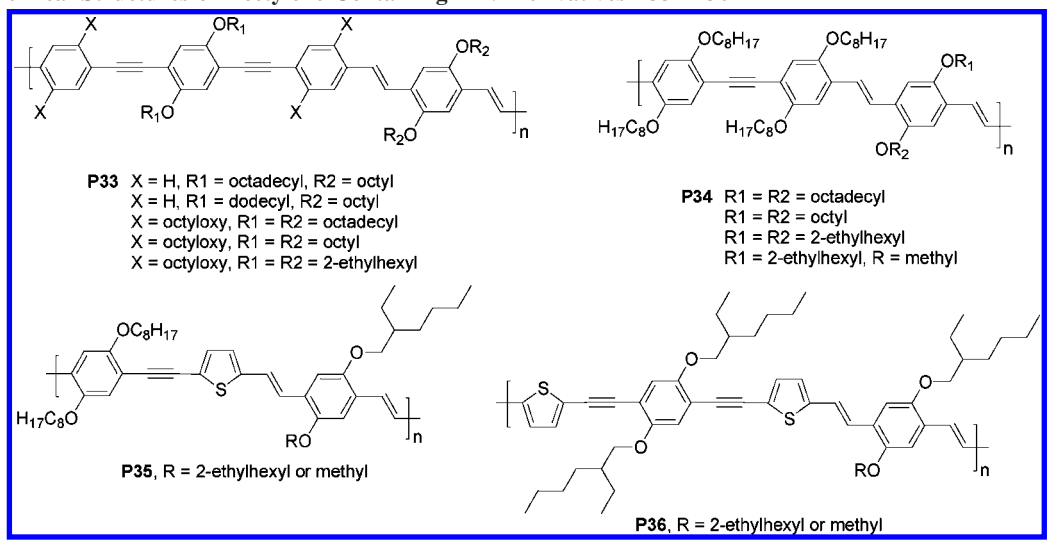


**Scheme 10. General Suzuki Coupling Reaction for the Synthesis of PF Copolymers**

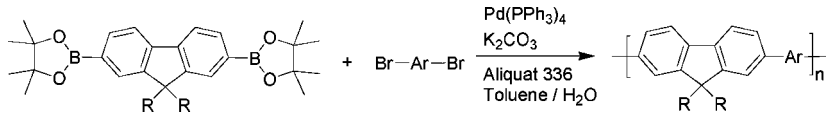


**Chart 14. Chemical Structure of Bithiophene-Containing PF Copolymer P37**

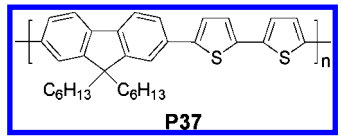


**Chart 15. Chemical Structure of Thieno[3,2-*b*]thiophene-Containing PF Copolymer P38**

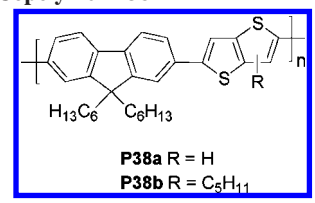


ing the band gap of the resulting copolymers for optimal sunlight collection.

To prepare PF-based copolymers, Suzuki coupling reactions are the most widely utilized. As far as the synthetic feasibility and reactivity are concerned, the 2,7-positions of the 9,9-dialkylfluorene unit are always functionalized with two boronic esters, whereas the dibromo functionality is placed at another coupling aromatic unit. In a typical Suzuki coupling reaction, a palladium complex such as $Pd(PPh_3)_4$ is used as the catalyst to carry out the polymerization in the presence of $K_2CO_3$ and a phase-transfer catalyst, Aliquat 336, in a solvent mixture (toluene/degassed water). During the polymerization process, the fluorenylboronic ester and the aromatic dibromide react with each other to give well-defined alternating PF copolymers. The molecular weights of the PF derivatives obtained are moderate ($M_n$ = 10000−50000) with low PDI values. A general Suzuki coupling reaction is shown in Scheme 10.

## 4.1. Fluorene-Based Copolymers Containing Electron-Rich Moieties

A conjugated polymer (**P37**) consisting of alternating fluorene and electron-rich bithiophene units was synthesized by Suzuki coupling and is shown in Chart 14.[131] The HOMO and LUMO levels of **P37** were estimated to be −5.41 and −2.52 eV, respectively. Through extended conjugation between the fluorene and thiophene units, the optical band gap of **P37** is reduced to 2.41 eV. Despite the fact that the **P37**:PCBM (1:4, w/w) blend film only absorbs light between 300 and 500 nm, a high $V_{oc}$ of 1.03 V and a moderate PCE value of 2.7% were obtained due to the high hole mobility of **P37** and well-defined nanophase segregation morphology. This makes it a promising high-energy-absorbing polymer for use in tandem bulk heterojunction solar cells.

Chart 15 depicts the chemical structure of alternating copolymers containing 9,9-dihexylfluorene and unsubstituted or alkylated thieno[3,2-*b*]thiophene units via Suzuki coupling. Compared with bithiophene-based **P37** (454 nm), **P38a** shows a blue-shifted absorption maximum at 430 nm in chloroform due to its shorter effective conjugation length. When a pentyl group is introduced into the $\beta$-position of thieno[3,2-*b*]thiophene in **P38b**, the absorption maximum is further blue-shifted to 388 nm as a result of steric-hindrance-induced main chain distortion. Photovoltaic cells with the configuration of ITO/PEDOT/**P38**:PCBM (1:1, w/w)/Ca/Ag were fabricated and characterized. The incident photon to current conversion efficiency (IPCE) value was found to be low, around 2%, leading to a limited PCE value, which might be due to the poor device fill factor and narrow absorption range of the polymers.[132]

Linearly fused arene- and heteroarene-based organic semiconductors have been intensively investigated for OFET and OLED applications.[133] Due to the extended and planar $\pi$-conjugated system, pentacene and its derivatives not only possess relatively low band gaps of 1.7 eV but also have achieved high thin-film transistor mobility. In terms of high charge mobility and an intrinsic low band gap, it is of great interest that incorporation of a pentacene unit into a conjugated polymer will generate a new class of promising p-type materials for photovoltaic applications.[134] In addition to pentacene, anthradithiophene, with two thiophenes on each

**Scheme 11. Synthesis of Pentacene- and Anthradithiophene-Containing PF Copolymers P39 and P40**

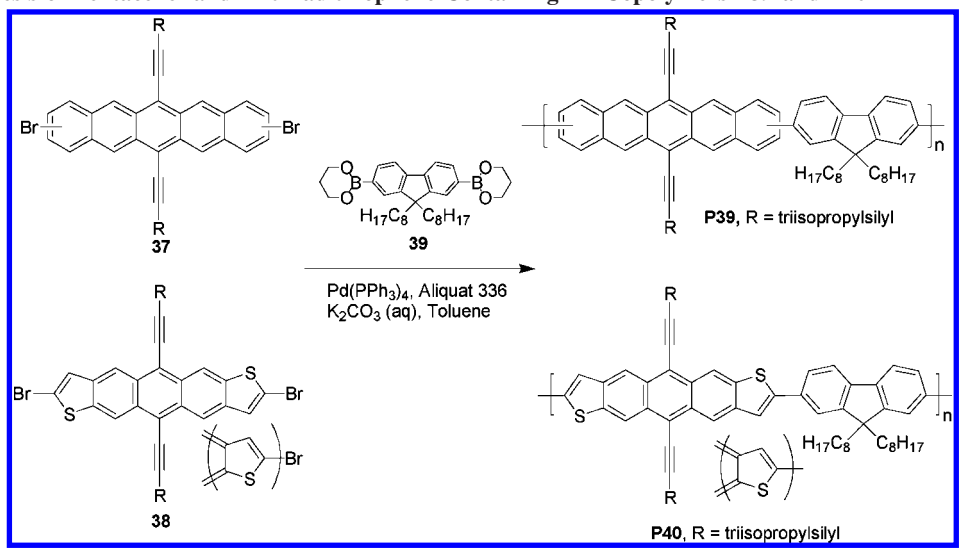


end of anthracene, is more stable than pentacene and can form a more coplanar structure with other conjugated units.[135] Two alternating high molecular weight polyfluorene-based polymers containing pentacene (**P39**) or anthradithiophene (**P40**) units were successfully synthesized by Suzuki coupling (Scheme 11).[136] The synthetic routes to (triisopropylsilyl)-ethynyl-substituted pentacene and anthradithiophene have been previously reported.[134,137] **P39** and **P40** show more red-shifted absorption spectra than their corresponding monomers **37** and **38** and have optical band gaps of 1.78 and 1.98 eV, respectively. Bulk heterojunction solar cells were fabricated using polymer **P40**:PCBM (1:3, w/w) as the active layer, giving a $J_{sc}$ of 2.35 mA/cm$^2$, a $V_{oc}$ of 0.75 V, and a PCE value of 0.68%. However, the device performance based on polymer **P39** was poor. A relatively low absorption coefficient at longer wavelengths may account for the poor performance.

## 4.2. Fluorene-Based Copolymers Containing Electron-Deficient Moieties

Electron-deficient 2,1,3-benzothiadiazole units have been widely incorporated into PF-based copolymers to alter the energy levels and fine-tune the emitting color over the entire visible region.[138] Chart 16 shows a series of 2,1,3-benzothiadiazole-containing PF derivatives (**P41**−**P49**) synthesized via Suzuki coupling reactions.

In spite of the high hole mobility and weak electron-transport nature of polyfluorene, alternating poly(9,9-dioctylfluorene-*co*-benzothiadiazole) (**P41**) exhibits a reduced LUMO level and thereby enhanced electron mobility ($10^{-3}$ cm$^2$/(V s)). This is a result of the high content of electron-deficient benzothiadiazole units and results in it being categorized as an electron-transport material.[139] When combined with the triarylamine-based polyfluorene **P50** (Chart 17) as the electron donor with a high hole mobility of $10^{-4}$ cm$^2$/(V s), **P41** serves as an electron acceptor in polymer/polymer bulk heterojunction photovoltaic devices.[140−142] They were fabricated by depositing the polymer blend **P41/P50** (1:1, w/w) as the active layer between ITO and Al electrodes, resulting in a low external quantum efficiency (EQE) value of 4% at an excitation energy of 3.2 eV.[140] The electron acceptor **P41** can also be added into a binary P3HT/PCBM system to act as the third component.[143] The photovoltaic performance of the ternary blend solar cell based on P3HT:PCBM:**P41** (1.0:0.6:1.4, wt %) showed a higher PCE value of 1.94% than that of the binary blend P3HT:PCBM (1:2, wt %) solar cell having the same donor−acceptor composition due to the additional light-harvesting effect of **P41**.

The charge-carrier-transporting properties of **P41** can be further modulated by copolymerizing fluorene with the 4,7-bis(3-hexylthiopen-5-yl)-2,1,3-benzothiadiazole unit to yield the polymer **P42**.[144] With two additional electron-rich thiophene rings attached to both sides of the benzothiadiazole unit, the hole mobility of **P42** is expected to be improved compared to that of **P41**. Therefore, **P42** shows an ambipolar nature and is capable of functioning as an efficient electron acceptor in blends with donor P3HT as well as an efficient electron donor in blends with acceptor PCBM. A polymer/polymer blend device based on P3HT:**P42** showed an enhanced PCE value from 0.14% to 1.2% after thermal annealing.

On the other hand, **P43**, which is structurally analogous to **P42**, serves as a promising electron donor in a photovoltaic device in combination with PCBM as the electron acceptor due to its higher hole mobility. The device with the configuration ITO/PEDOT/**P43**:PCBM (1:4, w/w)/LiF/Al showed a $J_{sc}$ of 4.66 mA/cm$^2$, a $V_{oc}$ of 1.04 V, an FF of 46%, and a PCE value of 2.2%.[145] The result is superior over the MDMO-PPV-based photovoltaic device due to **P43**'s ca. 50 nm red-shifted spectral coverage and much greater $V_{oc}$ value. The polymer **P44** contains 9,9-dioctylfluorene (DOF) and 4,7-di-2-thienyl-2,1,3-benzothiadiazole (DTBT) with different feeding ratios.[146] Two obvious absorption bands with maxima at 383 and 540 nm were observed. The shorter wavelength absorbance comes from the higher energy of the fluorene unit, whereas the lower energy band is attributed to intramolecular charge transfer from the electron-rich unit to the benzothiadiazole segment so that its intensity increases with increasing DTBT content. When the ratio of DOF to DTBT was 65:35 in **P44**, the best photovoltaic performance based on **P44**:PCBM (1:2, w/w) was obtained, showing a $J_{sc}$ of 5.18 mA/cm$^2$, a $V_{oc}$ of 0.95 V, and a PCE value of 2.24%. As shown in Scheme 12, **P44** with a comonomer ratio of 65:35 was synthesized by a Suzuki copolymerization of **40**−**42**.[147]

By mixing chloroform/chlorobenzene as the cosolvent, a finer and more uniform domain of the **P45a**:PCBM (1:3, w/w) thin layer was formed. The resulting photovoltaic

**Chart 16. Chemical Structures of 2,1,3-Benzothiadiazole-Containing PF Copolymers P41−P49**

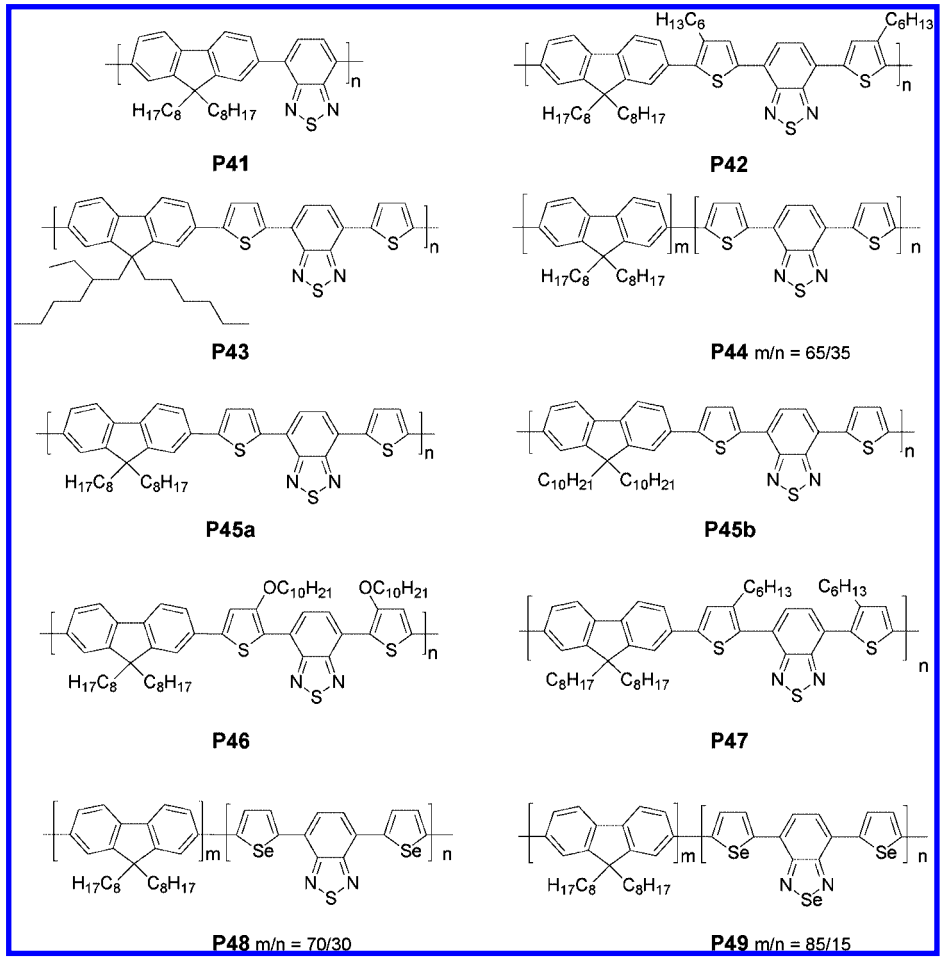


**Chart 17. Chemical Structures of Triarylamine-Based PF P50**

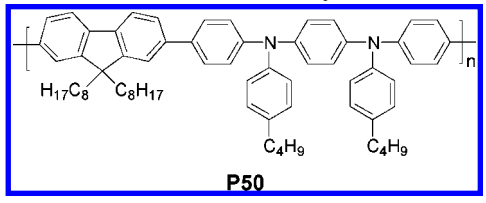


device had a $J_{sc}$ of 6.3 mA/cm$^2$, a $V_{oc}$ of 1.01 V, an FF of 44%, and a high-energy conversion record of 2.84%.[148] Apart from PCBM, CdSe nanoparticles were also used as the electron acceptor. A photovoltaic device based on **P45a**:CdSe showed a spectral response extending to 650 nm and gave a PCE value of 2.4%.[149] Furthermore, when the dioctyl chains in **P45a** were replaced by didecyl chains in the fluorene unit of **P45b**, a device based on **P45b**/PCBM showing the highest PCE value of 4.2% with a $V_{oc}$ of 0.99 V, a $J_{sc}$ of 7.7 mA/cm$^2$, and an FF of 0.54 was reported.[150]

The long alkoxy group can be introduced to the $\beta$-positon of the thiophene unit in the polymer **P46** to strengthen its electron-donating ability.[151] **P46** exhibited a significantly red-shifted absorption maximum of 581 nm and smaller band gap of 1.78 eV relative to its alkyl counterpart **P47**[152] with 525 nm and 2.06 eV due to the stronger donating strength of thiophene and thus more efficient intramolecular charge transfer. The solar cell based on a **P46**/PCBM (1:4, w/w) blend reached a $J_{sc}$ of 4.31 mA/cm$^2$, a $V_{oc}$ of 0.76, an FF of 0.48, and a PCE of 1.6%. The efficiency can be further improved to 2.4% by using $PC_{71}BM$ as the acceptor to strengthen the light-harvesting ability.[23]

It has been shown that selenium-containing heterocycles such as selenophene and benzoselenadiazole have stronger abilities to lower the band gaps of conjugated polymers than their sulfur analogues thiophene and benzothiadiazole.[153] Diselenophene-ylbenzothiadiazole and diselenophene-ylbenzoselenadiazole units have both been incorporated into the polyfluorene main chain to furnish **P48** and **P49**, respectively.[154] The optical band gaps deduced from the onset absorption are about 1.85 eV for **P48** and 1.77 eV for **P49**. Both of them have a relatively low-lying HOMO level of −5.5 eV. The best photovoltaic performance for a device based on **P49**/PCBM (1:4, w/w) reached a $J_{sc}$ of 2.53 mA/cm$^2$ and a very high $V_{oc}$ of 1.0 V and PCE of 1%. However, a device based on **P48**/PCBM (1:4, w/w) showed only 0.1% under the same conditions. This result can be attributed to the fact that **P49** has a weaker CT absorption band in the longer wavelength than **P48**. The syntheses of **P48** and **P49** are similar to that of **P44**.

Donor−acceptor polyfluorene-based polymers containing dithiophene-ylbenzothiadiazole units have shown larger $V_{oc}$ values (about 0.8−1.0 V) than P3HT (0.6−0.7 V) and broader absorption coverage (300−650 nm) than MDMO-PPV derivatives (425−575 nm), achieving moderate to good power conversion efficiency in the average range of 2−3% in BHJ devices. In terms of chemical feasibility and tunability, considerable effort has been directed to the design and synthesis of new polyfluorene-based polymers integrating a series of alternative electron-accepting aromatic units. Scheme 13 shows the synthesis of alternating PF derivatives containing electron-accepting thieno[3,4-*b*]pyrazine units.

**Scheme 12. Synthesis of Copolymer P44**

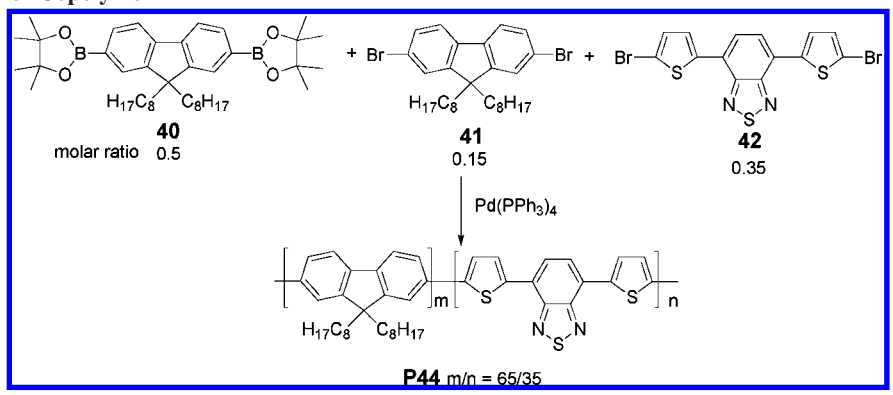


**Scheme 13. Synthesis of Thieno[3,4-*b*]pyrazine-Containing PF Copolymer P51**

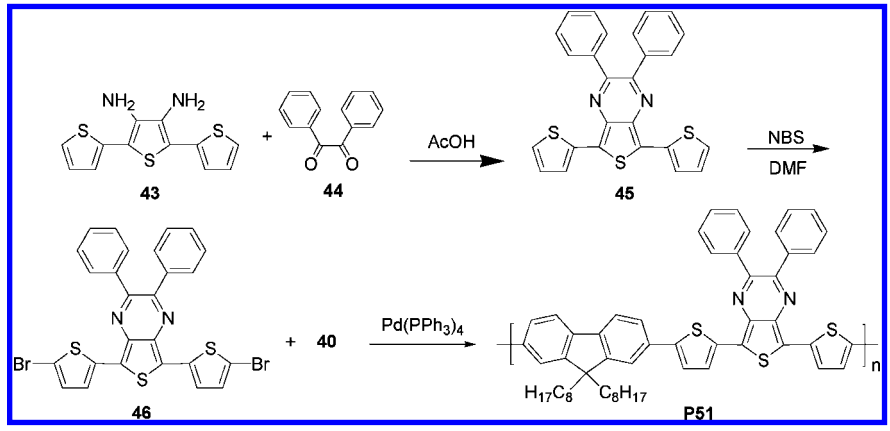


**Scheme 14. Synthesis of Alkoxylated Thieno[3,4-*b*]pyrazine-Containing PF Copolymer P52**

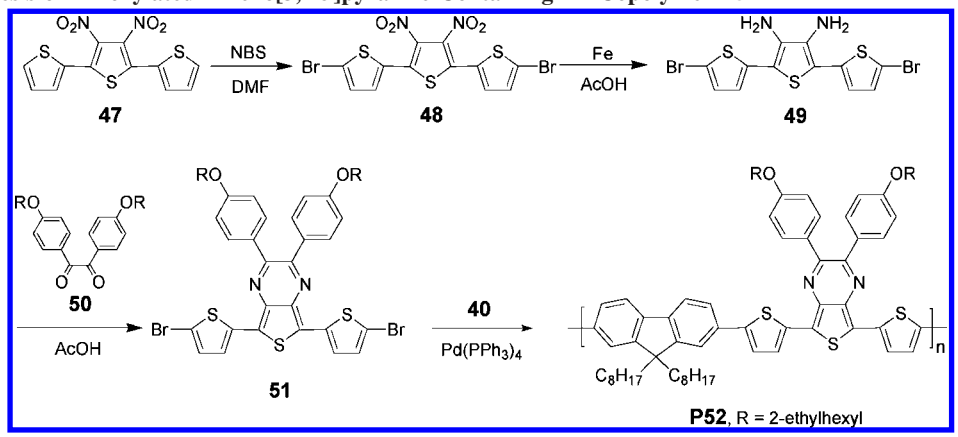


Imine formation of the diamino **43** with the 1,2-diketone **44** led to the cyclization product **45** containing the thieno[3,4-*b*]pyrazine unit. *N*-Bromosuccimide (NBS) bromination of **45** yielded the monomer **46**, which was allowed to polymerize with **40** to give **P51**.[155,156] The HOMO and LUMO levels of **P51** were estimated to be −5.6 and −3.6 eV, respectively, determining an electrochemical band gap of 2.0 eV. The absorption spectrum of **P51** covers a broad range from 300 to 850 nm. A device with the configuration of ITO/PEDOT/**P51**:PCBM (1:6, w/w)/LiF/Al was fabricated to measure its photovoltaic performance. When the ratio of **P51** to PCBM was increased to 1:6, the resulting device showed a photocurrent extended to 850 nm, achieved a $J_{sc}$ of 3.0 mA/cm$^2$ and a $V_{oc}$ of 0.78 V, and had the highest PCE value of 0.96%.

The polymer **P52** has a conjugated backbone similar to that of **P51**, with two additional (2-ethylhexyl)oxy substituents on the pendent phenyl rings of the thieno[3,4-*b*]pyrazine unit. The synthesis of the monomer **51** was obtained through a series of steps: bromination of the thiophene ring in **47** and reduction of the nitro groups in **48** followed by imine formation of **49** with 1,2-diketone **50**, finally leading to **P52** through a Suzuki coupling (Scheme 14).[157] Photovoltaic devices with the configuration ITO/PEDOT/**P52**:PCBM (1:3, w/w)/LiF/Al were fabricated, showing a $J_{sc}$ of 8.88 mA/cm$^2$, a $V_{oc}$ of 0.59 V, an FF of 42%, and a highest PCE value of 2.2%. Compared to polymer **P51**, the introduction of two alkoxy side chains into **P52** not only increased the solubility to produce a higher molecular weight ($M_n$ = 40000) but also shifted the HOMO/LUMO energy levels to −5.0/−3.4 eV, respectively, with subsequent lowering of the electrochemical band gap to 1.6 eV. The high molecular weight of **P52** leads to a higher FET hole mobility of the **P52**/PCBM blend by 2 orders of magnitude compared to that of **P51**/PCBM ($8 \times 10^{-4}$ vs $8 \times 10^{-6}$ cm$^2$/(V s)). In addition, the higher LUMO also facilitates the electron transfer from **P52** to PCBM, which

**Scheme 15. Synthesis of [1,2,5]Thiadiazolo[3,4-*g*]quinoxaline-Containing PF Copolymer P53**

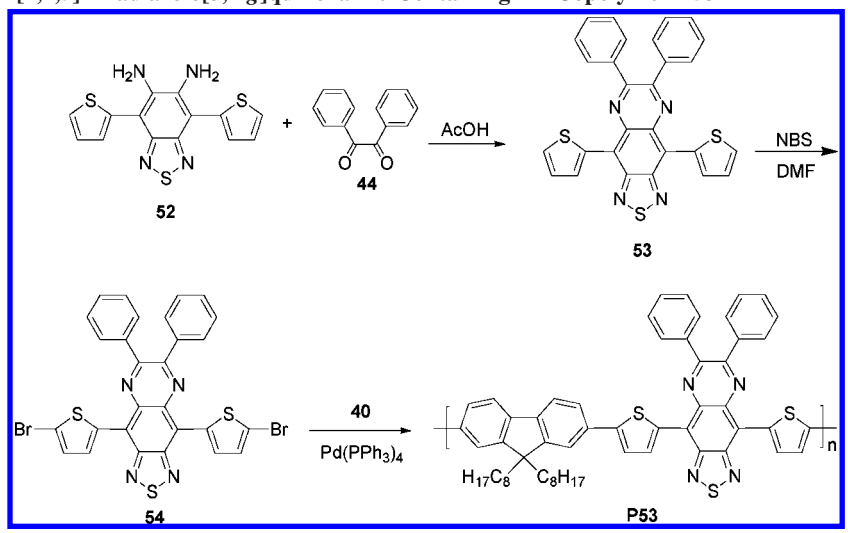


**Chart 18. Chemical Structure of Fullerene Derivative BTPF**

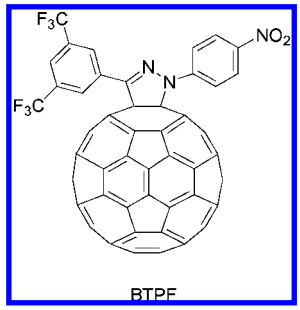


is evidenced by complete PL quenching in the film of the **P52**/PCBM blend. The **P52** absorption range covers 500−800 nm and absorbs more solar simulated light. The maximum EQE value of about 40% at 650 nm for the **P52** device also helps explain its better photovoltaic performance compared to the **P51** device (with a maximum EQE value of 15% at 600 nm).

The polymer **P53**, which contains [1,2,5]thiadiazolo[3,4-*g*]quinoxaline units in the main chain was synthesized by a synthetic route similar to that of **P51**, as shown in Scheme 15.[156] It was observed that no photoluminescence quenching could be detected for the **P53**:PCBM blended film compared with a film of pristine **P53**. This indicates that the strong electron-accepting ability of the thiadiazoloquinoxaline unit leads to stronger electron affinity and a lower LUMO level in **P53** and in turn prohibits favorable electron transfer from **P53** to PCBM. Indeed, the **P53** LUMO level is determined to be −4.0 eV, which is even lower than the −3.8 eV reported for PCBM. However, a partial photoluminescence quenching was observed on mixing **P53** with another $C_{60}$ derivative (BTPF)[158] which has a lower LUMO level at ca. −4.1 eV that can facilitate electron transfer (Chart 18). A device with the configuration ITO/PEDOT/**P53**:BTPF (1:4, w/w)/LiF/Al was fabricated and evaluated. It showed an onset photocurrent at 1000 nm and a maximum EQE value of 9.7% at 840 nm with a $J_{sc}$ of 2.1 mA/cm$^2$ and a $V_{oc}$ of 0.5 V.[159]

Polymer **P54**, the acceptor part of which consists of the pyrazino[2,3-*g*]quinoxaline unit, was also prepared by a similar procedure, as shown in Scheme 16.[160] The HOMO and LUMO levels were estimated to be −5.7 and −3.9 eV, respectively, with an electrochemical band gap of 1.8 eV. A device with the configuration ITO/PEDOT/**P54**:PCBM (1:3, w/w)/LiF/Al showed a $J_{sc}$ of 4.8 mA/cm$^2$, a $V_{oc}$ of 0.82 V, and FF of 41%, and a PCE value of 1.7%. To intensify **P54**'s absorption valley around 500 nm, $PC_{71}BM$ was used to replace PCBM as the electron acceptor capable of collecting photons in that region, resulting in 33% enhancement of $J_{sc}$ (6.5 mA/cm$^2$) and thereby a higher PCE value of 2.3%.

## 4.3. Fluorene-Based Copolymers Containing Phosphorescent Complexes

Considering the limited diffusion length of singlet excitons generated by the photoexcitation of donor materials, the bulk heterojunction strategy dominates over a bilayer heterojunction device because the exciton can travel a shorter distance to meet the electron acceptors before recombination occurs. The diffusion length of an exciton is highly dependent on its mobility and lifetime. One of the most promising ways to improve the efficiency of charge generation is to utilize triplet excitons which possess an inherently longer lifetime, which strengthens the diffusion ability of the exciton to reach the donor−acceptor interface. Holdcroft and co-workers reported a poly(fluorene-*co*-phenylpyridine)-based polymer (**P55**) containing an iridium complex tethered to the main chain.[161] The polymer was synthesized using Suzuki coupling as shown in Scheme 17. The corresponding non-Ir polymer **P56** was also prepared for comparison (Scheme 18). Upon excitation, **P56** only shows a fluorescence $\lambda_{max}$ at 422 nm, whereas in **P55** energy transfer takes place from the main chain to the iridium complex. This produces a peak of phosphorescence at 596 nm with a triplet lifetime of 0.26 $\mu$s. The phosphorescence can be completely quenched by blending with PCBM, which is indicative of efficient electron transfer from the triplet exiciton of the polymer to PCBM. Both polymers, blended with PCBM (1:4, w/w), were made into photovoltaic devices. **P55** showed a 10 times higher maximum EQE at 350 nm than its non-Ir counterpart (10.3% vs 1.1%), as well as a higher PCE of 0.07% compared to 0.002%. This clearly demonstrates the benefits of the longer triplet exciton diffusion length. It is expected that the device performance can be further improved by choosing a polymer having a lower band gap main chain to harvest more solar energy.

**Scheme 16. Synthesis of Pyrazino[2,3-*g*]quinoxaline-Containing PF Copolymer P54**

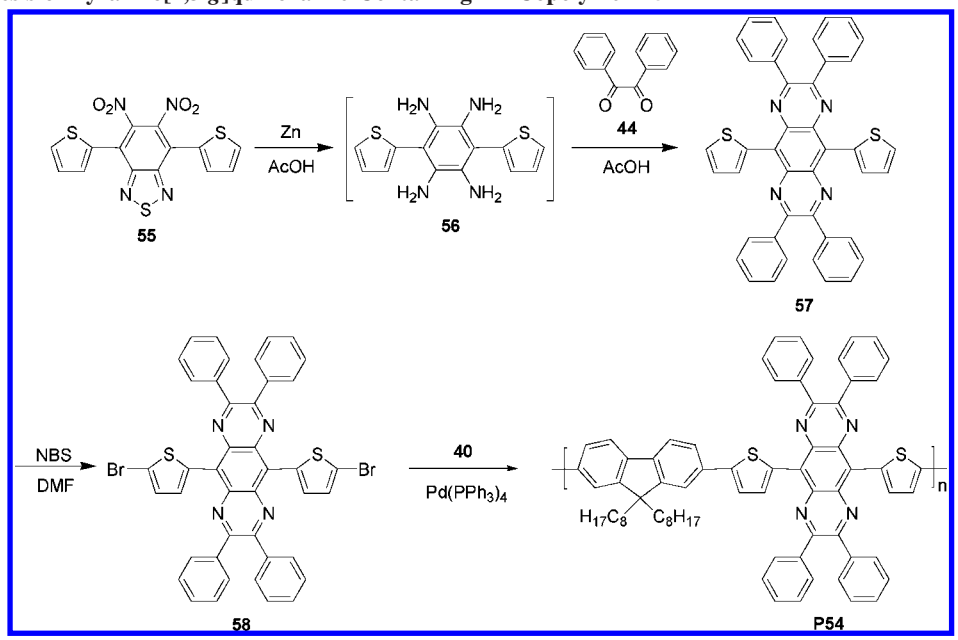


**Scheme 17. Synthesis of PF Copolymer P55 with a Pendent Ir Complex**

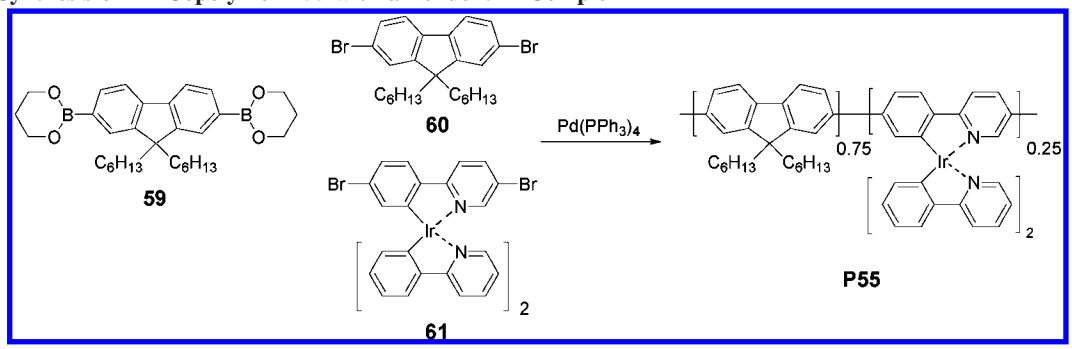


**Scheme 18. Synthesis of PF Copolymer P56 without a Pendent Ir Complex**

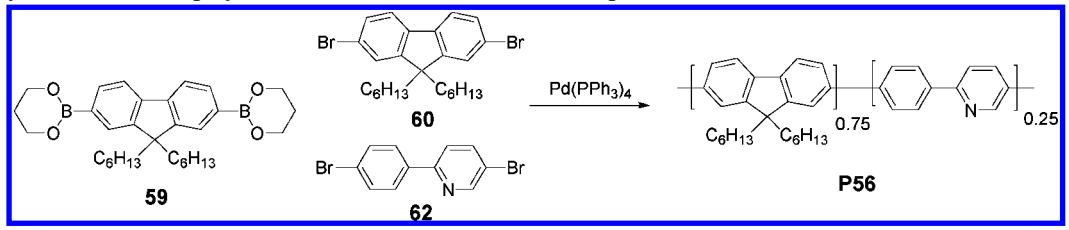


## 5. Carbazole-Based Conjugated Polymers

Carbazole, also known as 9-azafluorene, is one of the most attractive heterocyclic units for electronic applications in the field of conjugated polymers. Despite being structurally analogous to fluorene, the central fused pyrrole ring, with its donating nitrogen, makes tricyclic carbazole fully aromatic and electron-rich. The replacement of carbon by nitrogen in the fluorene skeleton avoids the susceptibility to oxidation of the 9-position toward ketone formation leading to undesired electronic and optical properties. The availability of nitrogen in carbazole to functionalization with an alkyl chain also ensures sufficient solubility. As a result, carbazole derivatives have been widely used as p-type semiconductors due to their ability to form stable radical cations, as well as their excellent thermal and photochemical stabilities, relatively high charge mobility, and easy availability. For example, poly(*N*-vinylcarbazole) (PVK), a nonconjugated linear polymer with pendent carbazole units, acts not only as a superb photoconductor[162] but also as a hole-transporting and electron-blocking material.[163] In addition, it serves as a large band gap host in polymer light-emitting devices.[164] Alternatively, conjugated poly(carbazole) derivatives have been successfully applied in organic field-effect transistors.[165] These properties make the carbazole unit a promising candidate for incorporation into low band gap polymers for solar cell applications.[166]

### 5.1. Poly(2,7-carbazole)-Based Polymers

In general, the carbazole unit can be connected and extended in a symmetrical manner through either the 3,6-positions or 2,7-positions to yield linear conjugated polymers. Connecting carbazole via the 3,6-positions results in a *meta*-linkage of phenylene with limited conjugation. On the other hand, the 2,7-positions lead to a *para*-linkage and a higher effective conjugation length.[167] It appears that 2,7-linked carbazole-based conjugated polymers for use as donor materials in photovoltaic devices are much more promising

**Scheme 19. Synthesis of Poly(3,6-carbazole) P57**

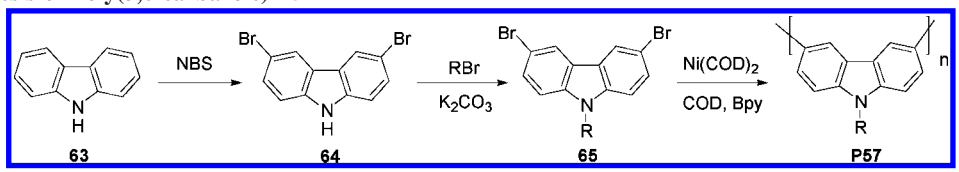


**Scheme 20. Synthesis of 2,7-Dibromocarbazole (68)**

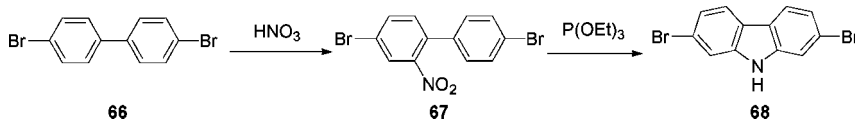


**Scheme 21. Synthesis of Alkylated Poly(2,7-carbazole) Homopolymer P58 and Chemical Structure of Perylene Diimide 71**

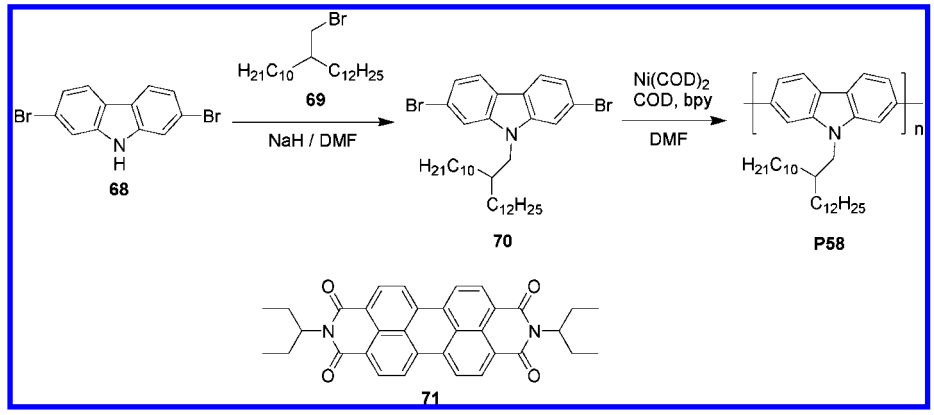


in terms of better charge migration along the more conjugated main chain. As shown in Scheme 19, bromination of carbazole **63** by NBS takes place regioselectively and quantitatively at the 3,6-positions, which are *para* to the directing nitrogen, to obtain **64**. After *N*-alkylation with an alkyl halide under basic conditions, poly(3,6-carbazole) **P57** with a high molecular weight can be synthesized using a Yamamoto coupling.[168]

In contrast, the preparation of 2,7-dibromocarbazole is not that straightforward.[169] However, Mullen et al. developed a facile route to its synthesis in two steps (Scheme 20).[170] Nitration of 4,4′-dibromobiphenyl (**66**) by nitric acid gave **67**. A Cadogan reductive cyclization of **67** using triethyl phosphate afforded 2,7-dibromocarbazole (**68**).[171]

Due to their poor solubilities, poly(2,7-carbazole) homopolymers generally have low molecular weights, which limits their use in thin-film devices. **P58**, a soluble and processable poly(2,7-carbazole) with a branched 2-decyltetradecyl substituent on the nitrogen, was designed and synthesized by a $Ni(COD)_2$-mediated Yamamoto coupling polymerization (Scheme 21).[172] The resultant polymer has a lower HOMO level, −5.6 versus −5.2 eV, than P3HT. This implies a better environmental stability toward air oxidation and the ability to obtain a higher $V_{oc}$. In spite of the relatively large band gap of 3.0 eV along with limited absorption, **P58** can be blended with the electron acceptor perylene diimide **71**, which has a low band gap of 2.0 eV, to form a bulk heterojunction solar cell. A simple device with the configuration ITO/**P58**:**71** (1:4, w/w)/Ag was fabricated to evaluate its photovoltaic performance, showing a $J_{sc}$ of 0.26 mA/cm$^2$, a $V_{oc}$ of 0.71 V, an FF of 37%, and a PCE value of 0.63%.

The band gap of poly(2,7-carbazole) can be reduced by incorporating an electron-accepting unit to generate a new class of D−A poly(2,7-carbazole)-based polymers. The copolymer **P59,** comprised of alternating 2,7-carbazole units

**Scheme 22. Synthesis of Poly(2,7-carbazole) P59 Containing 2,1,3-Benzothiadiazole Units**

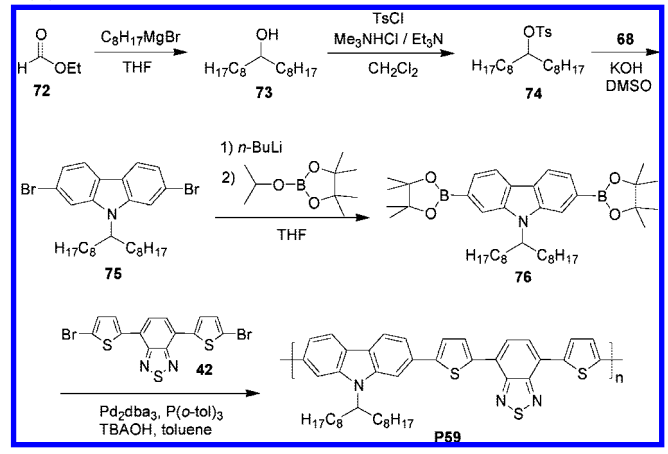


and DTBT moieties, was synthesized by Leclerc and co-workers. Scheme 22 shows the synthesis of **P59** via a Suzuki coupling reaction.[173] **P59** has an optical band gap of 1.88 eV from its absorption edge. The HOMO and LUMO levels were estimated to be −5.5 and −3.6 eV, respectively. The photovoltaic device based on **P59**:PCBM (1:4, w/w) showed a $J_{sc}$ of 6.92 mA/cm$^2$, a $V_{oc}$ of 0.89 V, an FF of 63%, and a PCE value of 3.6%. The result makes poly(2,7-carbazole) derivatives among the best conjugated polymers reported to date.

Leclerc and co-workers further reported a series of poly(2,7-carbazole) derivatives (**P60**−**P64**) using different electron-deficient moieties (Chart 19).[174] **P60**, **P62**, and **P59** have three different symmetric electron-withdrawing units, respectively, with benzene as the core. The corresponding compounds **P61**, **P63**, and **P64** all have asymmetric electron-withdrawing units with pyridine as the core. These copolymers were all synthesized via a Suzuki coupling reaction in

**Chart 19. Chemical Structures of Alternating Poly(2,7-carbazole) Copolymers P60−P64**

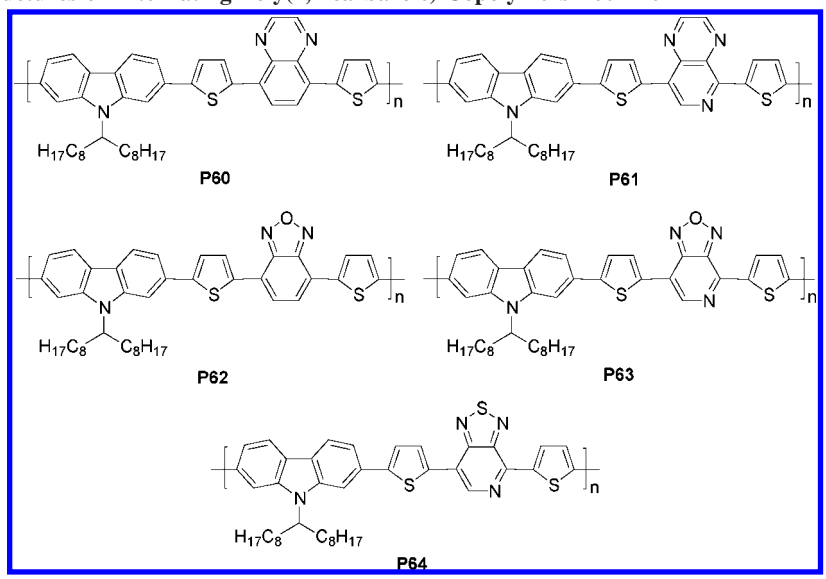


**Scheme 23. Synthesis of Poly(2,7-carbazolenevinylene) Derivative P65**

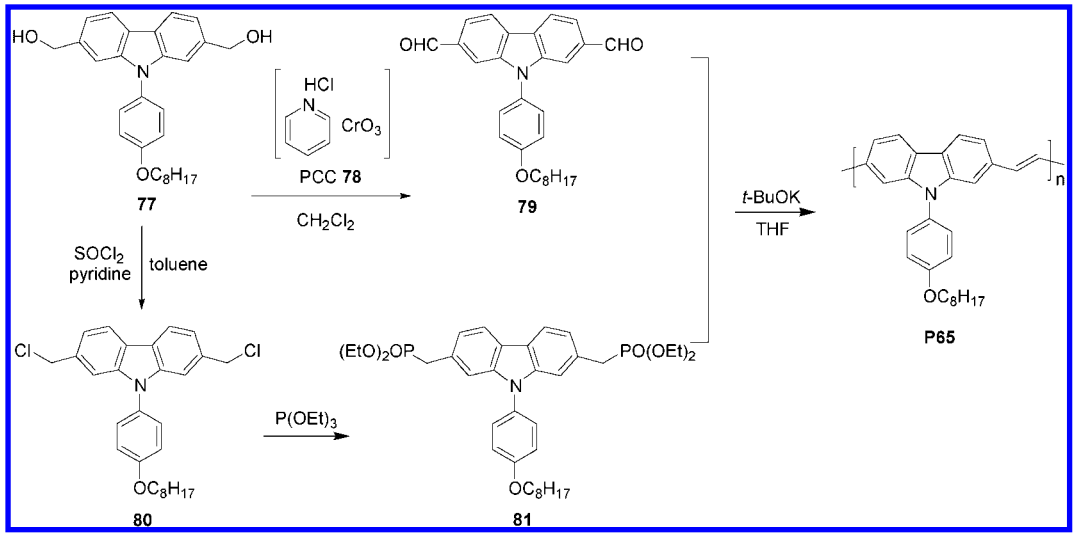


a manner similar to that of polymer **P59**. Cyclic voltammetric analysis shows that the HOMO levels of these polymers, ranging from −5.55 to −5.46 eV, are mainly determined by the carbazole unit. However, the LUMO level is dependent on the nature of the electron-withdrawing unit. Compared to benzene-based acceptors, the corresponding pyridine-based ones are more electron-withdrawing, resulting in lower LUMO levels by ca. 0.25 eV. It was found by X-ray analysis that polymers with symmetric benzene-based acceptors have better structural organization in the solid state than those with asymmetric acceptors. This greatly affects their photovoltaic performance. On the basis of the polymer/PCBM (1:4, w/w) blend in the device, **P60**, **P62**, and **P59** all show higher PCE values, 1.8%, 2.4%, and 3.6%, respectively, than their corresponding counterparts **P61**, **P63**, and **P64**, 1.1%, 0.8%, and 0.7%. It should be noted that these poly(carbazole)-based polymers generally deliver a higher $V_{oc}$ of ca. 0.8−1.0 V.

Schemes 23 and 24 show the synthetic routes to a series of poly(2,7-carbazolenevinylene) (PCV) polymers using different polymerization methods.[175] **P65** is a PCV homopolymer with an (octyloxy)benzyl side group on the nitrogen of the carbazole unit. The polymers **P66**−**P68**, on the other hand, are PCV copolymers incorporating different lengths of oligothiophenes into the main chain. To obtain high molecular weights, an *all-trans* double bond configuration, and low contamination, the Horner−Emmons reaction was employed to synthesize the polymers **P65**−**P68** by reacting the dialdehyde and corresponding diphosphonate derivatives in the presence of excess amounts of *t*-BuOK in anhydrous THF. However, polymer **P69** was prepared by the Stille cross-coupling reaction of the dibromo monomer **86** and distannyl compound **87** in the presence of $Pd_2(dba)_3$ and $AsPh_3$ in THF. The polymers **P65**−**P69** have optical band gaps of 2.3, 2.2, 2.1, 2.0, and 1.7 eV, respectively, indicating that the band gap of this polymer series decreases as the number of thiophene rings increases. The HOMO energy level is also proportionally lowered with increasing conjugation length of the backbone with the exception of polymer **P69**. It should be noted that the thienyl *S*,*S*-dioxide unit in **P69** is no longer aromatic and has two localized C═C and two S═O double bonds,[176] which results in greater electron affinity and a significantly lower LUMO level. Bulk heterojunction photovoltaic cells having the sandwiched structure ITO/PEDOT/polymer:PCBM (1:4, w/w)/Al were fabricated. Among them, **P69** showed the best photovoltaic performance: a $J_{sc}$ of 1.56 mA/cm$^2$, a $V_{oc}$ of 0.8 V, an FF of 54.6%, and a PCE value of 0.8%. The other four polymers

**Scheme 24. Synthesis of 2,7-Carbazolenevinylene-Based Copolymers P66−P69**

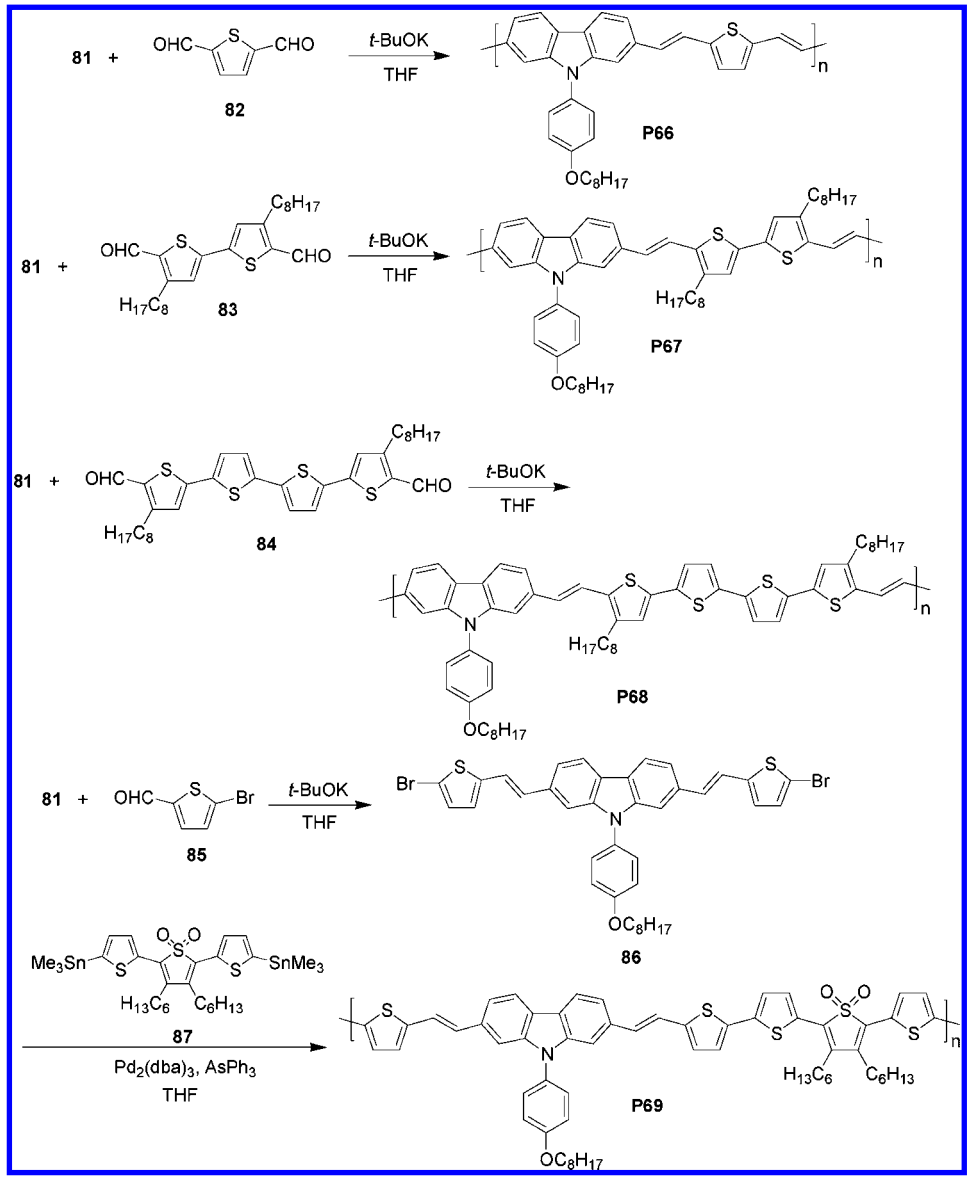


showed PCE values ranging from 0.2% to 0.4% following the same fabrication and characterization protocol.

## 5.2. Indolo[3,2-*b*]carbazole-Based Polymers

Indolo[3,2-*b*]carbazole can be regarded as two carbazoles fused together. It is envisaged that indolo[3,2-*b*]carbazole-based materials will have stronger donating abilities than carbazole while inheriting the advantages of carbazole such as hole-transporting properties and enhanced photostability and thermal stability. For the indolo[3,2-*b*]carbazole-based small molecule and homopolymer a very high mobility in FET has been achieved.[177,178] There are many intrinsic advantages making indolo[3,2-*b*]carbazole a promising electron-rich building block for the construction of a new class of donor−acceptor conjugated polymers. First, the penta-fused heterocyclic unit of indolocarbazole provides a large coplanar $\pi$-conjugated system. Second, the low-lying HOMO feature of indolocarbazole is expected to be beneficial for obtaining a high $V_{oc}$. The arylamine-type structure of indolocarbazole is known to be a good hole transporter. As a result, the copolymer **P70**, composed of an electron-accepting benzothiadiazole oligothiophene and an electron-donating indolocarbazole unit, has been synthesized by the Suzuki coupling of **88** and **89** (Scheme 25).[179] Both long and branched aliphatic chains must be introduced onto the nitrogen atom to ensure sufficient solubility of the polymer. The indolocarbazole polymerization site is at the 3,9-positions so that the fully conjugated main chain of the polymer can be obtained. A strong peak located at 538 nm in the absorption spectrum in chloroform is due to the intramolecular charge-transfer transition. Compared to the solution state, the absorption edge in the solid state is significantly red-shifted by 100 nm, indicating very strong interchain packing induced by planarization of the aryl rings. According to DSC measurements, **P70** has a strong tendency to crystallize, as evidenced by an exothermic crystallization peak at 209 °C without showing a glass transition. The HOMO level remains low at 5.17 eV, which is crucial to obtaining a high $V_{oc}$ and air stability. The device based on a blend of **P70**/PCBM (1:2, w/w) in the active layer exhibited a high $V_{oc}$ of 0.69, a $J_{sc}$ of 9.17 mA/cm$^2$, and a high PCE of 3.6%. The preparation of the 3,9-indolo[3,2-*b*]carbazole unit is shown in Scheme 26. Treatment of 1,4-cyclohexadione (**91**) with (3-bromophenyl)hydrazine (**90**) formed the bishy-

**Scheme 25. Synthesis of Indolocarbazole-Based P70 by Suzuki Coupling**

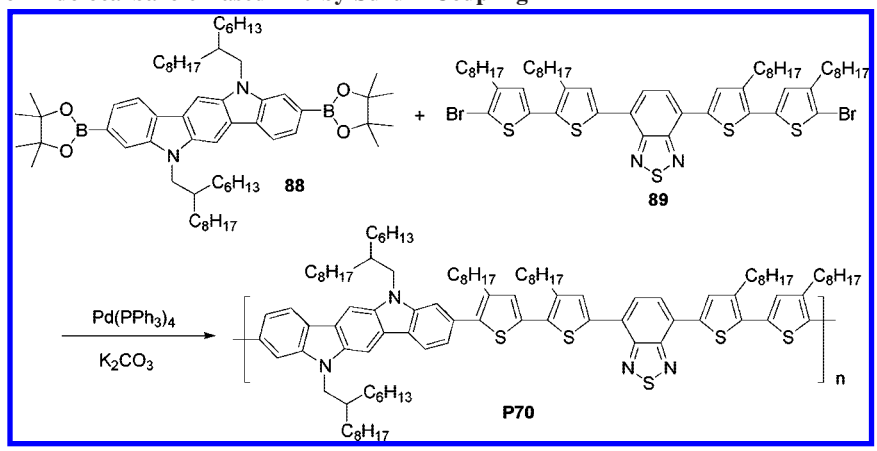


**Scheme 26. Synthetic Route toward Monomer 88**

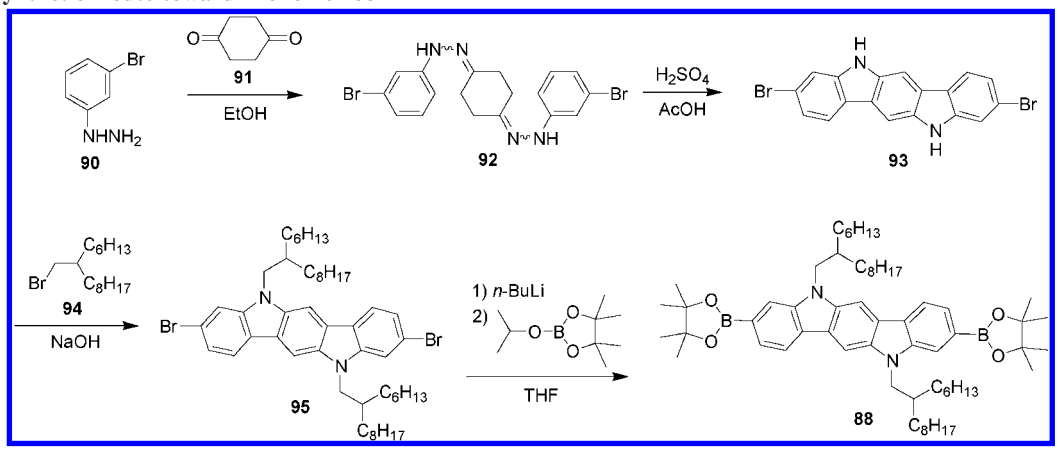


drazone **92**, which underwent a double Fischer indole cyclization and reduction under acidic conditions ($H_2SO_4$/AcOH), resulting in the formation of **93**.[180] After *N*-alkylation of **93** to introduce an aliphatic chain, the dibromo functionality in **95** was then converted to diboronic ester to produce the final monomer **88**.

Chen and co-workers also reported four alternating D−A copolymers (**P71**−**P74**) combining either 3,9-indolo[3,2-*b*]carbazole or 2,8-indolo[3,2-*b*]carbazole as the donor unit and 2,3-didodecylthienopyrazine or 2,3-bis(4-((2-ethylhexyl)-oxy)phenyl)quinoxaline as the accepting unit.[181] The synthesis of **P71**−**P74** is shown in Scheme 27. The absorption maxima of **P71** are more red-shifted than those of **P73** both in solution (552 vs 544 nm) and in the solid state (582 vs 557 nm), resulting in a lower optical band gap (1.79 vs 1.89 eV). These results can be rationalized by the fact that the 3,9-linkage of indolocarbazole can form a fully *p*-phenylene conjugated main chain, whereas the 2,8-linkage generates a less conjugated *m*-phenylene relationship between indolocarbazole and thienopyrazine. Moreover, compared to **P73**, **P71** has a lower HOMO level, implying that the 3,9-based copolymers have better air stability than the corresponding 2,8-based copolymers. The **P71**/PCBM-based solar cell device exhibited a better PCE of 0.66% than the **P73**/PCBM one with a PCE of 0.22%. On the other hand, however, **P72** shows a slight blue shift of its $\lambda_{max}$ and a larger band gap than that of **P74**. This is just the trend opposite that observed in the **P71** and **P73** pair. This might be attributed to the fact that the quinoxaline unit causes a larger steric effect in the 3,9-linkage than in the 2,8-linkage. It is also worthy to note that, in the 2,8-linkage, the nitrogen atom on the benzene ring now is *para* to the quinoxaline unit so that intramolecular charge transfer from the donating nitrogen to the acceptor unit may be facilitated and may contribute to the lower band gap. On the basis of a solar cell device with a blend of polymer/PCBM (1:4, w/w), the PCE of **P74** reached 0.87% and can be further improved to 1.4% when using $PC_{71}BM$ as the acceptor, outperforming the **P72**/PCBM-based device with a PCE of 0.32%.

## *6. Thiophene-Based Conjugated Polymers*

### 6.1. Poly(3-alkylthiophene) and Its Derivatives

Polythiophene represents the most important conjugated polymer utilized in a broad spectrum of applications such as conducting polymers, light-emitting diodes, field-effect transistors, and plastic solar cells due to its excellent optical and electrical properties as well as exceptional thermal and chemical stability. Early synthesis of poly(3-alkylthiophene) involved chemical oxidation or electrochemical polymerization in the pursuit of soluble and processable polythiophenes.[60,182,183] However, these processes suffered from the gross defect that the structure of the polymer is somewhat undirected and undefined.[184] Because 3-alkylthiophene is an asymmetrical molecule, there are three relative orientations available when the two thiophene rings are coupled between the 2- and 5-positions. The first of these is the 2−5′ or head-to-tail coupling (HT), the second is 2−2′ or head-to-head coupling (HH), and the third is 5−5′ or tail-to-tail coupling (TT). Containing a mixture of the possible couplings mentioned above results in a regioirregular poly(3-alkyl-

**Scheme 27. Synthesis of P71−P74 by Suzuki Coupling from Corresponding Monomers 96−99**

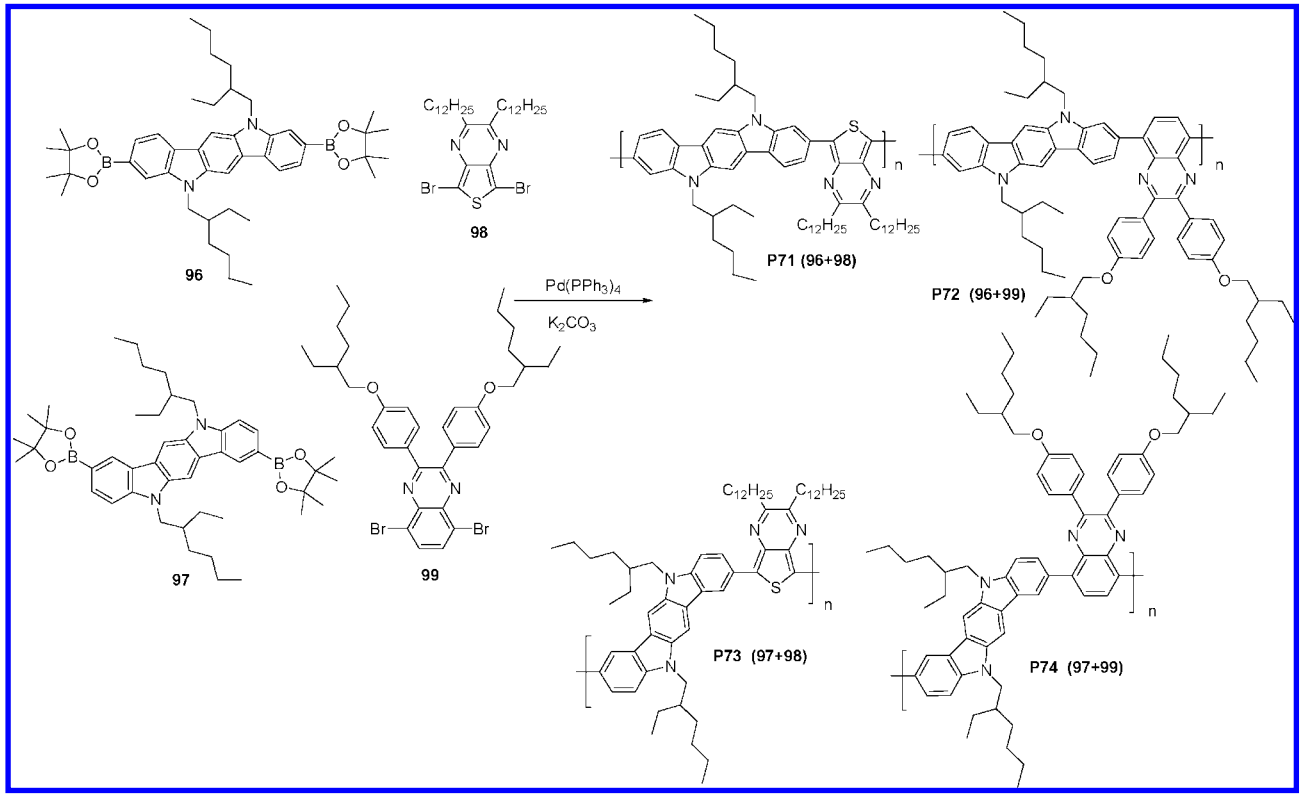


**Scheme 28. Synthesis of Regioregular Poly(3-alkylthiophene) P75 by the McCullough Route**

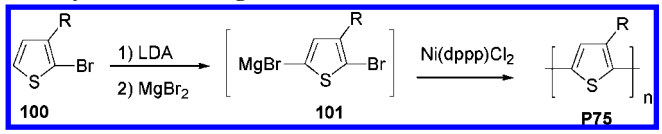


**Scheme 29. Synthesis of Regioregular Poly(3-alkylthiophene) P76 by the Rieke Route**

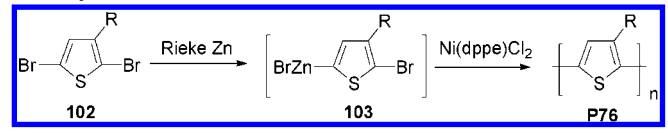


thiophene) in which a large number of thiophene rings twisted out of conjugation in a manner of HH coupling due to steric repulsion between alkyl chains. Overall this reduces the electrical conductivity of the polymer. On the other hand, coupling each thiophene unit in a consecutive head-to-tail manner during the polymerization affords a regioregular poly(3-alkylthiophene) which is capable of adopting a coplanar conformation, resulting in a lower energy. This arrangement produces a highly conjugated polymer having a lower band gap.

The first synthesis of regioregular head-to-tail coupled poly(3-alkylthiophene)s (P3ATs) was reported by McCullough early in 1992.[185,186] As shown in Scheme 28, the regioregular polymerization of 3-alkylthiophene **P75** can be controlled by selective lithiation of 2-bromo-3-alkylthiophene **100** with lithium diisopropylamide (LDA) followed by transmetalation using magnesium bromide to yield the organomagnesium intermediate **101**. The use of a Ni(dppp)$Cl_2$ catalyst for the polymerization of this intermediate gives the corresponding poly(3-alkylthiophene) **P75** with over 90% head-to-tail regioselectivity.

The second synthetic approach to HT-PAT was subsequently developed by Rieke.[187,188] Highly reactive zinc undergoes a selective oxidative addition to 2,5-dibromo-3-alkylthiophene **102** to yield 2-(bromozincio)-3-alkyl-5-bromothiophene intermediate **103** in quantitative yields. In the presence of Ni(dppe)$Cl_2$ as the catalyst this metalated intermediate undergoes regioselective polymerization to yield the desired HT-PAT **P76** product (Scheme 29).

Later on, McCullough reported another method for the synthesis of regioregular poly(3-alkylthiophene)s by Grignard metathesis (GRIM).[189,190] Treatment of 2,5-dibromo-3-hexylthiophene (**104**) with a variety of alkyl Grignard reagents resulted in two metalated regioisomers (**105** and **106**) in an 85:15 ratio via a magnesium exchange reaction (Scheme 30). This ratio appears to be independent of the reaction time, temperature, and Grignard reagent employed. Introduction of a catalytic amount of Ni(dppp)$Cl_2$ to this isomeric mixture afforded poly(3-hexylthiophene) (**P77**), which contained greater than 95% regioregularity.

McCullough and Yokozawa independently demonstrated that the Grignard metathesis polymerization of regioregular 3-alkylthiophene proceeds by a living chain growth mechanism instead of the traditionally accepted step growth polycondensation. As a result, low polydispersities (ca. 1.2−1.3) and well-defined molecular weights can be controlled by the feed ratio of monomer to the Ni catalyst.[191−194] Their proposed mechanism is shown in Scheme 31. First, two Grignard nucleophilic additions to a nickel catalyst generate the intermediate **109**. A reductive elimination involving carbon−carbon bond formation in **109** accompanied by Ni migration and insertion into the terminal C−Br bond keeps the living chain capable of further reacting with compound **107**. Propagation via consecutive coupling between the polymer with a Ni complex at the chain end and compound **107** elongates the conjugated backbone. Because this reaction can be accomplished both at room temperature and on a large scale, the Grignard metathesis/Kumada−Corriu

**Scheme 30. Synthesis of Regioregular Poly(3-hexylthiophene) P77 by Grignard Metathesis and Kumada−Corriu Coupling**

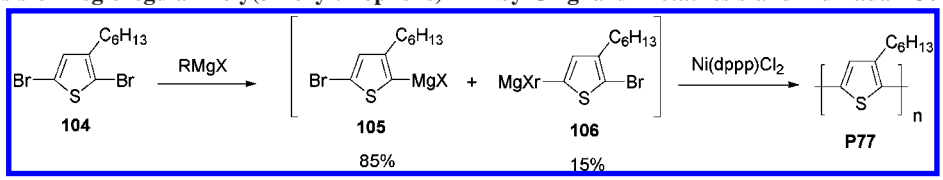


**Scheme 31. Mechanism of Chain Growth Polymerization Proposed by Yokozawa et al**

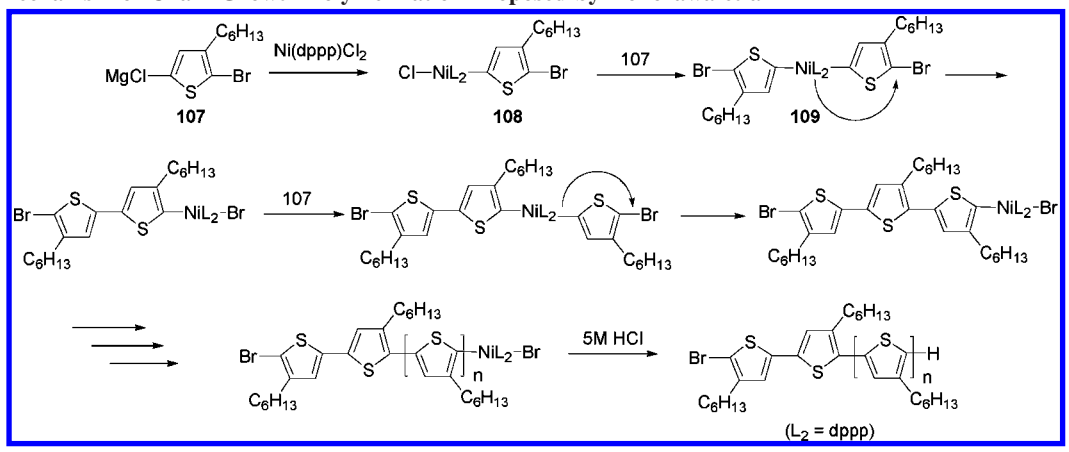


coupling has become the most widely used method for producing poly(3-alkylthiophene)s with predetermined high molecular weights. The beneficial features of GRIM are obtaining monodispersed samples of P3ATs without resorting to time-consuming polymer fractionation techniques and refining the properties of P3ATs by eliminating molecular weight distribution variations. Moreover, it is possible to keep the polydispersity constant when trying to determine if one polymer performs better than another.

Increasing regioregularity in poly(3-hexylthiophene) (P3HT) through these advanced metal-catalyzed reactions leads to various beneficial outcomes including a red shift in absorption in the solid state with an intensified extinction coefficient and an increase in the mobility of the charge carriers.[195] Regioregular poly(3-hexylthiophene) possesses HOMO and LUMO levels at −5.2 and −3.2 eV, respectively, with an optical band gap of ca. 2.0 eV. To date, a combination of poly(3-hexylthiophene) as the electron donor and PCBM as the electron acceptor in the active layer represents the most efficient bulk heterojunction solar cell with power conversion efficiency approaching 5%. The success of the P3HT/PCBM system is largely associated with careful control and optimization of the active layer morphology. It has been demonstrated that device performance based on P3HT/PCBM can be dramatically improved by judicious choice of the casting solvent,[196] by external treatment of solvent annealing[197−199] and thermal annealing,[200−202] or by forming P3HT nanofibers prior to deposition.[203] Thermal annealing of the P3HT/PCBM composite provides an external energy to drive reorganization of the polymer chains, which ultimately leads to a nanoscale phase separation with a bicontinuous interpenetrating D−A network.[204] As a result of this higher degree of nanoscale P3HT crystallinity, better charge transport and maximum interfacial area for efficient charge generation are obtained. However, prolonged thermal annealing causes regioregular P3HT to further crystallize and thereby tends to destroy the optimal morphology as a result of continuous phase segregation between P3HT and PCBM to form a macroscale domain larger than the exciton diffusion length. Fréchet and coworkers found that a slight decrease of the regioregularity of P3HT to weaken the crytallization formation not only

**Scheme 32. Synthesis of P78 for Lowering the Regioregularity by the Incorporation of a Dihexylthiophene Repeat Unit**

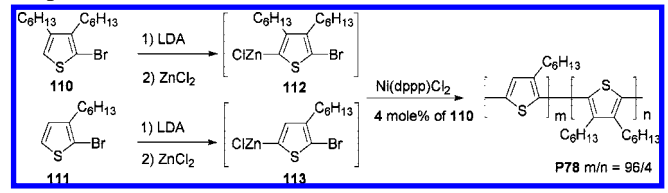


retains the device efficiency but also enhances the thermal stability of morphology in the solar cells.[205] Polythiophene **P78** with a regioregularity lower than 91% was synthesized by the copolymerization of 2-bromo-3-hexylthiophene (**111**) with a small amount of the 2-bromo-3,4-dihexylthiophene (**110**) unit using a modified McCullough route (Scheme 32). After 30 min of annealing at 150 °C, the resulting devices, using 96% regioregular P3HT and PCBM or **P78**/PCBM, showed PCEs of 4.3% and 4.4%, respectively. However, the PCE of P3HT/PCBM further fell to 2.6% when the annealing time was increased to 300 min, whereas the PCE of **P78**/PCBM remained at 3.5% under identical conditions.

A later more straightforward study, on the influence of the regioregularity of P3HT on polymer−fullerene solar cell performance, was carried out by systematically comparing three samples of P3HT having regioregularities of 86%, 90%, and 96%.[206] It was found that in blends with PCBM all three polymers were able to achieve solar cells with PCEs of about 4% and exhibit the same order of magnitude of charge mobility ($10^{-4}$ $cm^2/(V\ s)$). Most importantly, the P3HT with the lower regioregularity possessed superior thermal stability over those with higher regioregularities. This was ascribed to the suppression of the crystallization-driven phase separation through introduction of a controlled amount of disorder into the polymer backbone. This result is consistent with previous observations. Another example illustrating the effect of alkyl substitution patterns in thiophene copolymers was presented by the comparison of polymers **P79** and **P80**, which have identical compositions and similar molecular weights and polydispersities.[207] Polymer **P79**, synthesized by the Stille copolymerization of distannyl monomer **114**

**Scheme 33. Synthesis of P79 and P80**

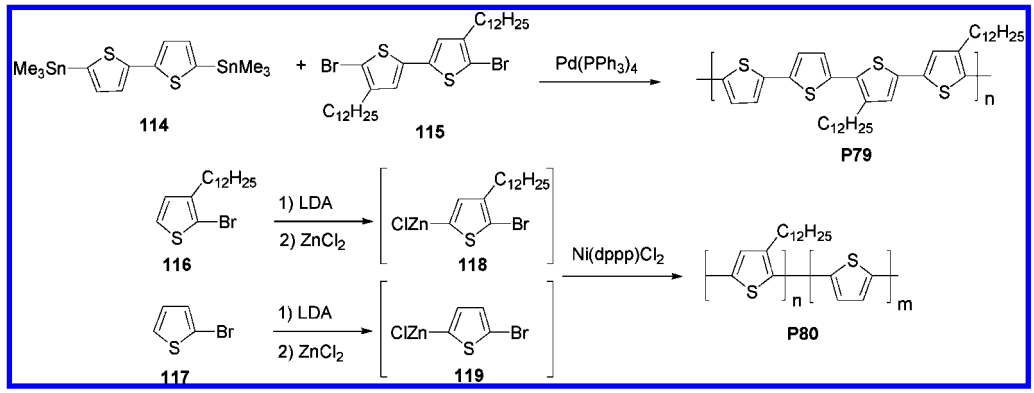


and dibromo monomer **115**, has a perfect regioregular alternating arrangement, whereas **P80** made by the McCullough route has a random sequence distribution (Scheme 33). X-ray diffraction measurements of the polymers were performed after spin-coating and thermal annealing at 100 °C for 30 min. Due to its longer alkyl chain interdigitation and structurally well-defined nature, **P79** crystallizes into a three-dimensional highly ordered structure[208] and exhibits an even higher degree of crystallinity than P3HT, which is known to have disordered noninterdigitated side chains.[209] On the contrary, **P80** exhibits amorphous character as a result of its random structure. The best device PCE of **P80** blended with PCBM (30:70, w/w) was 1.84%. However, the optimal PCE of **P79** blended with PCBM (25:75, w/w) only reached 0.54%, which is much lower than that of P3HT. These results indicate that increasing the crystallinity of the polymer to be higher than that of P3HT turns out to have a detrimental effect, because a higher crystallinity makes **P79** unable to form bicontinuous donor−acceptor networks at all and the longer alkyl chains further lower the miscibility with PCBM. Therefore, the random, amorphous polymer with the more favorable active layer morphology outperforms its more highly ordered analogues by more than 3-fold. These results clearly demonstrate that highly crystalline conjugated polymers are advantageous for achieving high mobility in field-effect transistors because polymers constitute the only component. However, the addition of another component such as fullerene into a BHJ solar cell renders the morphology, a bulk property, more important than the polymer crystallinity.

The length of the solubilizing group in the conjugated thiophene unit also plays an important role in determining the balance between crystallinity and miscibility in the bid to achieve optimal morphology. A systematic study of a series of regioregular poly(3-alkylthiophene)s, with different butyl, hexyl, octyl, decyl, and dodecyl side groups, has been conducted.[210] It was found that chain lengths longer than eight carbons facilitate diffusion rates of PCBM in the polymer matrix during the thermal annealing. This leads to a larger scale of phase separation, reduced interfacial area, and thereby lower device performance. Poly(3-butylthiophene) lacks suitable solubility in chloroform. Ultimately, the hexyl group in P3HT demonstrated an optimal balance with the best device performance in the poly(3-alkylthiophene) family. Moreover, the efficiency of the BHJ device also greatly depends on the molecular weight[211−213] and polydispersity[214] of the P3HT. It has been shown that only P3HT with a number-average molecular weight greater than 10000 can achieve a power conversion efficiency over 2.5%.[211] High molecular weight P3HT exhibits a bathochromic shift of the long-wavelength maxima and a prominent shoulder at 600 nm in the solid-state absorption spectrum. This indicates the formation of a lamellar structure and interchain aggregates, whereas the lower molecular weight with a shorter conjugation length results in reduced intermolecular interactions with a concomitant decrease in hole mobility.

**Scheme 34. Synthesis of P81 and P82**

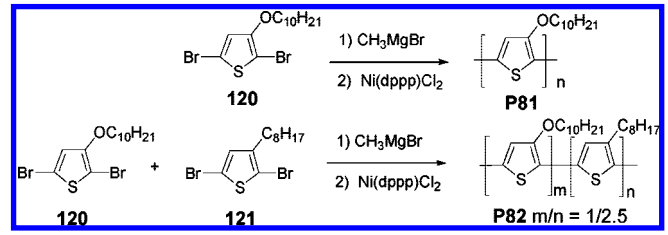


The major function of the aliphatic chain substituent is to provide adequate solubility of polythiophenes with weak electronic interactions with the main chain. Nevertheless, alkoxy chains introduced into the 3-position of polythiophenes not only serve as solubilizing groups but also greatly perturb the molecular orbitals involved in tuning the band gap.[215] Regioregular poly(3-(decyloxy)thiophene) (**P81**) was synthesized by a GRIM synthesis of 2,5-dibromo-3-(decyloxy)thiophene (**120**) (Scheme 34).[151] Despite the fact that the resultant polymer showed a lower band gap of 1.6 eV, due to electron-donating effects elevating the HOMO level, the resulting poor solubility and film-forming properties and air instability restricted its performance in solar cell devices. Therefore, the high head-to-tail regioregular copolymer **P82** was synthesized by reacting **120** with 2,5-dibromo-3-octylthiophene (**121**) via the McCullough method. Compared to that of P3HT, the absorption maximum of **P82** in the solid state was dramatically red-shifted to 621 nm. The electrochemical band gap of **P82** was determined to be 1.64 eV. However, **P82**/PCBM (1:1, w/w) also showed very poor photovoltaic performance with a PCE of 0.054%.

## 6.2. Poly(3-hexylselenophene)

Poly(3-hexylselenophene) (P3HS, **P83**) is an analogue of poly(3-hexylthiophene) with selenium replacing the sulfur atom. It can be synthesized successfully in a regioregular manner by employing a McCullough-type Ni coupling reaction of **123** made by bromination of **122** (Scheme 35).[216] It was found by Heeney and co-workers that poly(3-hexylselenophene) has a smaller band gap of 1.6 eV than P3HT through lowering the LUMO level without elevating the HOMO level. These are promising properties for obtaining profound absorption at lower energy while maintaining

**Scheme 35. Synthetic Route to Poly(3-hexylselenophene) (P83) by Grignard Metathesis and Kumada−Corriu Coupling**

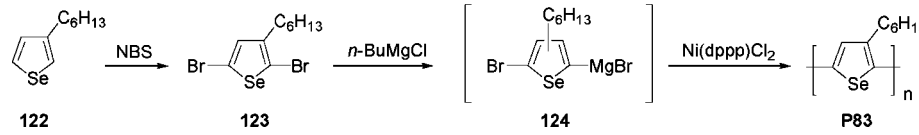


**Scheme 36. Synthesis of P84 by a Stille Coupling Reaction**

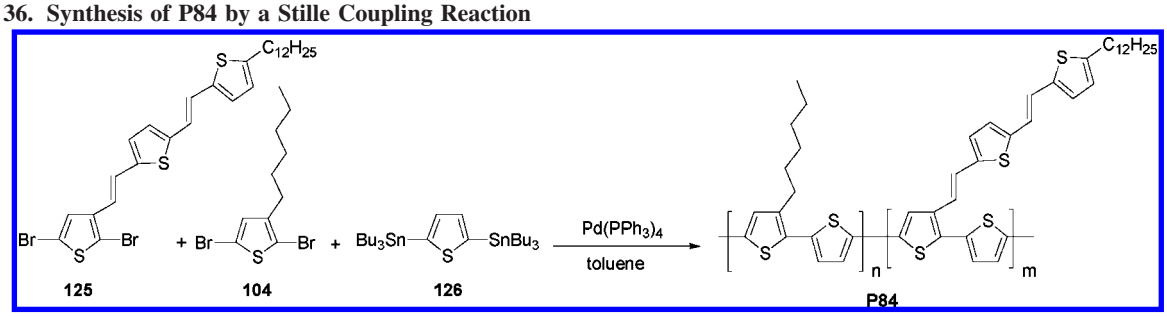


**Scheme 37. Synthesis of P85 by Grignard Metathesis**

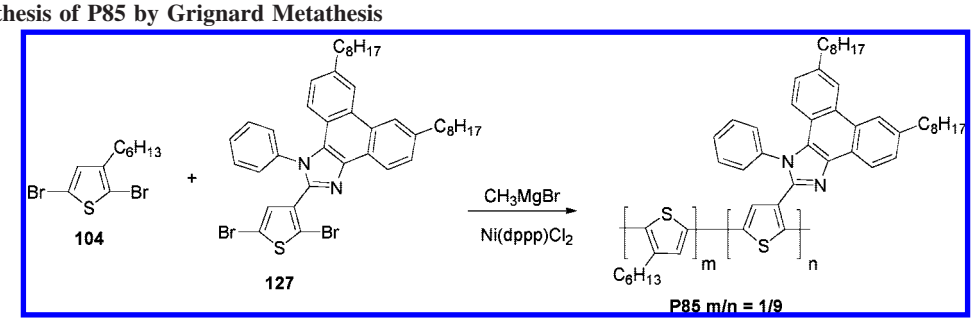


an open-circuit voltage comparable to that of P3HT. As a result, P3HS shows a much greater red-shifted absorption maximum at 630 nm in the solid state compared to 550 nm for P3HT. It was also found that P3HS is more resistant to photooxidation than P3HT. It has been suggested that one of the photooxidation mechanisms is through electron transfer from excited P3HS to oxygen, generating a superoxide anion that reacts with the conjugated backbone. The low-lying LUMO of P3HS can reduce the electron-transfer rate and therefore accounts for the better photostability of P3HS. The lower LUMO can be attributed to the smaller ionization potential of selenium. Moreover, P3HS displays crystalline morphology and thus has an FET charge mobility similar to that of P3HT under the same measurement conditions. The solar cell device based on P3HS/PCBM (1:1, w/w) produced a PCE of 2.7% after optimal thermal annealing, which is comparable to that of a P3HT/PCBM device.[217]

## 6.3. Polythiophenes with Conjugated Side Chains

An alternative design strategy to intensify the absorption ability of p-type polymers is to introduce additional absorptive chromophores directly and conjugatively attached to the main chain backbone.[218,219] Li et al. designed and synthesized, by Stille coupling, a series of polythiophene derivatives **P84** having conjugated bi(thienylenevinylene) side chains (Scheme 36). It has been shown that extension of a conjugated side chain to the polythiophene main chain leads to strong and broad absorption covering both the UV and visible regions from 350 to 650 nm. In addition, the **P84** HOMO level is lower by 0.2 eV than that of P3HT, resulting in a higher $V_{oc}$ of the PSC. The solar cell device based on a blend of **P84** ($m/n = 0.59$) as the donor and PCBM as the acceptor (1:1, w/w) reached a PCE of 3.18%; this is superior to that of the device based on P3HT under the same conditions.

Wei and co-workers reported a new regioregular 3-hexylthiophene copolymer (**P85**) incorporating (octylphenanthrenyl)imidazole moieties directly conjugated with 90% thiophene units at the 3-position.[220] This polymer was synthesized by Grignard metathesis and a Ni-catalyzed reaction of **104** with **127** (Scheme 37). The electron-accepting ability of this moiety induces efficient intramolecular charge transfer from the donor thiophene main chain to the conjugated acceptor side chain: this reduces the optical band gap slightly to 1.9 eV. In addition, charge separation is also facilitated through sequential transfer of electrons from the main chains to the side chains and then to PCBM. Consequently, the electron-transfer probability from this polymer to PCBM is twice as high than that from pure P3HT. Using a blending of **P85**/PCBM (1:1, w/w) in a solar cell device gives a high PCE of 3.45%. The synthesis of monomer **127** is shown in Scheme 38. The 1,2-diketone compound **130** was synthesized by NBS bromination of **128** to form **129**, which was then oxidized by $CrO_3$ to give **130**. The phenanthrenylimidazole core in compound **131** was generated under acidic conditions through a cyclization reaction of **130** with aniline, ammonium acetate, and 3-formylthiophene. The nickel-catalyzed Kumada–Corriu reaction of **131** afforded compound **132** with two attached octyl side chains. Subsequent NBS bromination yielded the final monomer **127**.

Charge mobility of conjugated polymers plays a critical role in high-performance polymer solar cells. In addition to intramolecular charge transport along the conjugated main chains, it is known that intermolecular hopping between adjacent main chains is the limiting step in the charge-transport process. Increased molecular weight or controlled regioregularity of conjugated polymers has been shown to induce higher hole mobility as a result of improved conjugation and $\pi-\pi$ stacking interactions. A series of polythiophenes **P86**, cross-linked by different amounts of con-

**Scheme 38. Synthetic Route toward Monomer 127**

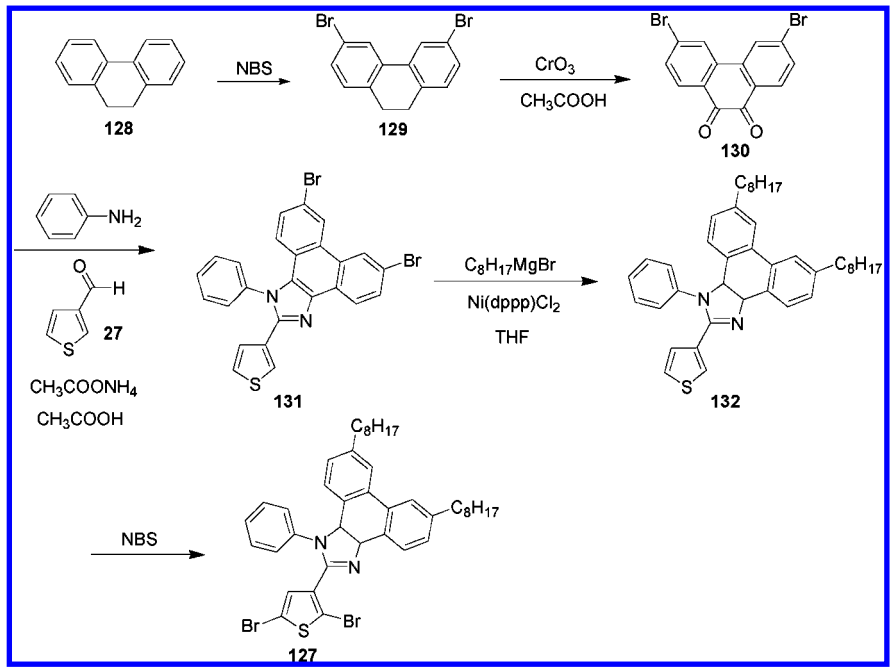


**Scheme 39. Synthesis of P86 by a Stille Coupling Reaction**

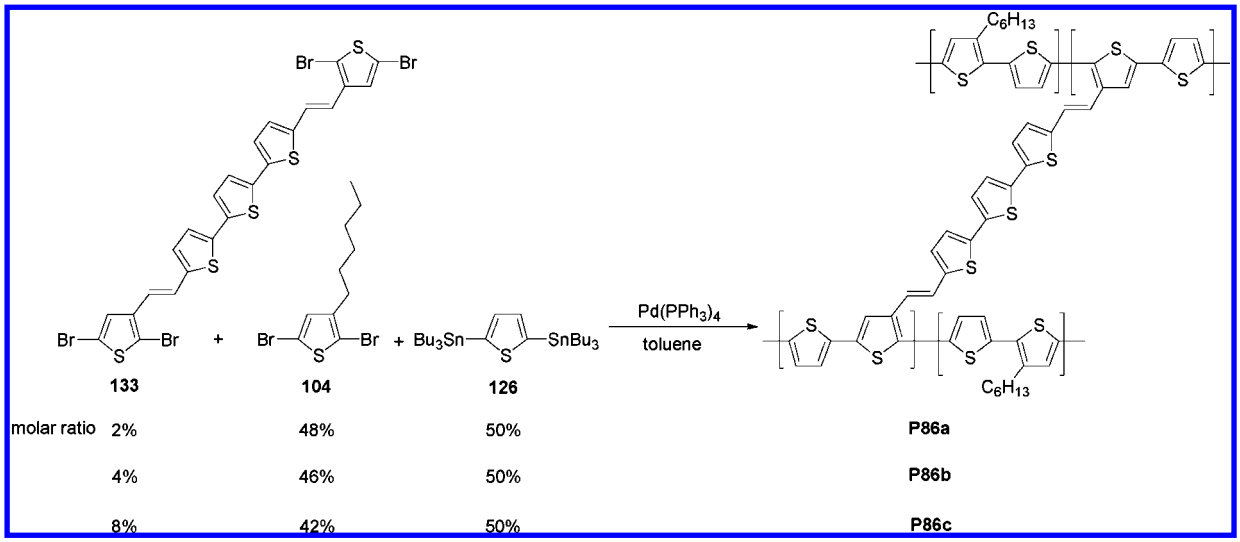


jugated vinylene−terthiophene−vinylene (VTTV) bridges (2% **P86a**, 4% **P86b**, 8% **P86c**), were synthesized by Li and co-workers via Stille coupling (Scheme 39).[221] These bridges connected and conjugated with the polythiophene main chains might provide an avenue to facilitate efficient charge transport from chain to chain in the network.[222−224] The hole mobilities of these polymers, determined according to the space-charge-limited current model, are $4.7 \times 10^{-3}$, $2.58 \times 10^{-3}$, and $9.48 \times 10^{-4}$ $cm^2/(V\ s)$ for **P86a**, **P86b**, and **P86c**, respectively. The value for **P86a** is about 3 times higher than that of the corresponding non-bridge-conjugated polymer. Notably, any further increase in the bridge content is accompanied by more steric distortion in the main chain as evidenced by the declining hole mobility and blue-shifted absorption spectra. A PCE of 1.72% for the solar cell device based on a 1:1 (w/w) blend of **P86a** and PCBM can be obtained.

In a similar approach to improving the charge mobility between conjugated polymers, Scherf et al. synthesized a series of modified polythiophenes **P87** by polymerizing 2,5-dibromo-3-hexylthiophene with a small amount of a tetrafunctional branching agent, 2,5,2′,5′-tetrabromo-3,3′-bithiophene, under McCullough-type Grignard metathesis conditions (Scheme 40).[225] It has been shown that systematically increasing the branching unit from 2% through 4% to 8% in the P3HT backbone leads to improved solubility, a blue-shifted absorption, and decreased hole mobility with concomitant reduced solar cell power conversion efficiency. These phenomena can certainly be attributed to the lower

**Scheme 40. Synthesis of P87 by Grignard Metathesis and a Kumada−Corriu Coupling Reaction**

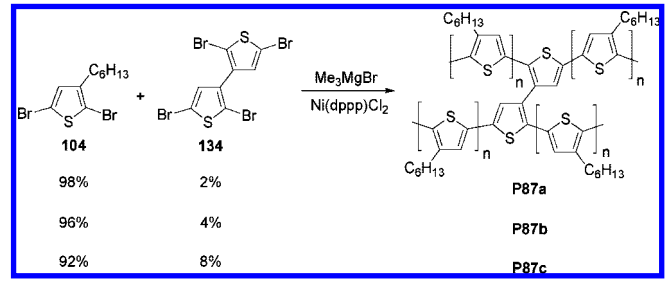

**Scheme 41. Synthesis of PITN (P88) by Electrochemical Polymerization and Its Mesomeric Structure**

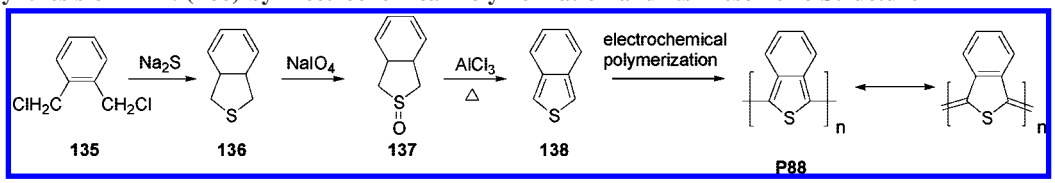


**Scheme 42. Synthesis of P89 by Thermal Polymerization of Dithiophthalide**

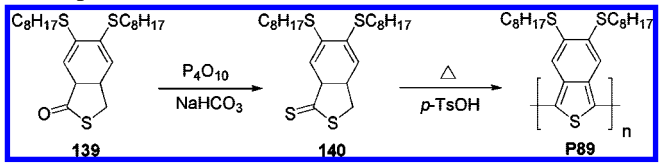


degree of solid-state ordering and packing caused by the severe interchain distortion of the backbone due to branching effects. The best PCE of 2% comes from a **P87a** /PCBM (1:1, w/w) BHJ solar cell, showing a moderate reduction in efficiency as compared to a P3HT-based device having a PCE of 3.5% under identical conditions. These results are also in good agreement with the fact that the degree of regioregularity impacts the backbone conformation of poly(3-alkylthiophene).

## 6.4. Isothianaphthene-Based Polymers

Polyisothianaphthene (PITN, **P88**) is a polythiophene derivative where all the thiophene rings are fused to a benzene ring at the 3,4-positions of thiophene. The first PITN was reported by Wudl et al. in 1984 and prepared by electrochemical polymerization (Scheme 41).[42] The PITN main chain tends to favor the quinoid form to preserve the benzene aromaticity at the expense of the thiophene aromaticity. As a consequence, PITN is the first conjugated polymer to have a band gap as low as 1 eV, which is 1 eV smaller than that of polythiophene. The monomer precursor isothianaphthene (ITN, **138**) was prepared by dehydration of the sulfoxide **137**, which was made by the $NaIO_4$ oxidation of **136** (Scheme 41).[226]

PITN syntheses have been described using various electrochemical or oxidative polymerizations of isothianaphthene. Straightforward chemical polymerization routes have also been developed to make substituted PITNs with sufficient solubilities and tunable band gaps. As shown in Scheme 42, the thermal polymerization of dithiophthalide **140**[227,228] in the presence of catalytic amounts of toluenesulfonic acid afforded poly(5,6-bis(octylmercapto)isothianaphthene) (**P89**). Its band gap of 1.16 eV is too low to obtain sufficient photovoltaic performance.[229]

Incorporation of different aromatic units into PITN allows greater structural versatility for the fine-tuning of the intrinsic properties. However, the use of these low band gap PITN derivatives for solar cell device applications encountered difficulties such as inefficient polymerization, low molecular weights, poor film-forming ability, and the unstable nature of both the isothianaphthene monomer and the polymer. Thiophene−isothianapthene copolymers **P90**, **P91**, and **P92,** synthesized by $FeCl_3$ oxidative polymerization (Scheme 43) with band gaps of 1.8, 1.5, and 1.4 eV, respectively, cannot form homogeneous pinhole-free thin films by spin-coating due to their low molecular weights, which is a result of an inefficient oxidative coupling reaction.[230,231]

In addition to PCBM and a donor polymer, poly(methyl methacrylate) (PMMA) was required to serve as the host

**Scheme 43. Synthesis of P90−P92 by $FeCl_3$ Oxidative Polymerization**

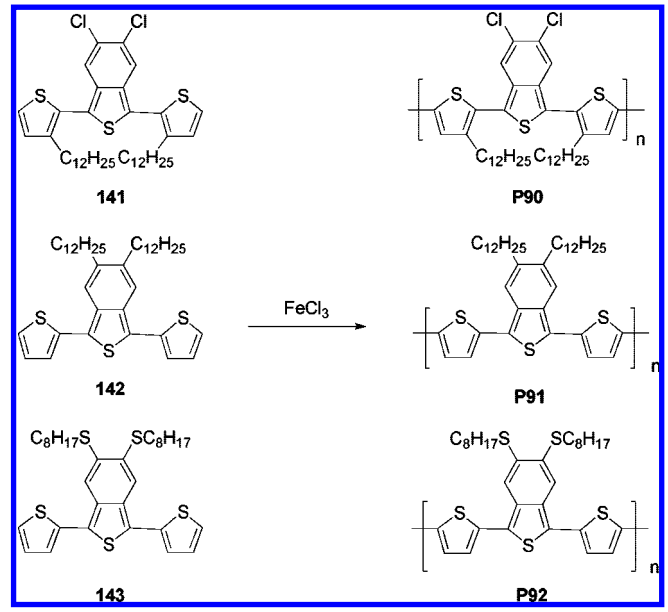


matrix in the active layer to improve the film-forming property. The PSC based on PMMA/**P90**/PCBM (1:2:6, w/w/w) showed the highest device characteristic with a PCE of 0.31%.[231]

Hillmyer and co-workers reported a new distannylisothianaphthene compound (**144**) which was synthesized by the *n*-BuLi lithiation of isothianaphthene (**138**) in tetramethylethylenediamine (TMEDA) and THF followed by reaction with trimethyltin chloride.[232] This molecule is chemically stable under an inert atmosphere at low temperatures and can be used as a useful building block to prepare the alternating ITN−fluorene copolymer **P93** or the ITN–thiophene copolymer **P94** by a Stille coupling with 9,9-dihexyl-2,7-dibromofluorene (**60**) or bis(bromothienyl)-isothianaphthene **145**, respectively (Scheme 44). It is particularly noteworthy that **145** can also be synthesized from **144** by a Stille coupling reaction with 2-bromo-3-decylthiophene (**146**) followed by NBS bromination. This is a more facile way for making dithienylisothianaphthene derivatives without using the traditional route, which requires harsh conditions involved with using Lawesson's reagent.[233,234] Although when blended with PCBM (1:4, w/w) **P93** has a larger band gap of 2.3 eV, it showed a higher PCE of 0.46% than **P94** (band gap 1.66 eV) with a PCE of 0.23% under the same testing conditions. This could be ascribed to its better film-forming properties.

## 6.5. Cyclopenta[2,1-*b*:3,4-*b*′]dithiophene-Based Polymers

Structurally analogous to fluorene, 4*H*-cyclopenta[2,1-*b*:3,4-*b*′]dithiophene (CPDT) derivatives, where two thiophene units are tied and rigidified by a covalent carbon, have attracted considerable research interest.[235] Due to its fully

**Scheme 44. Synthesis of P93 and P94 by a Stille Coupling Reaction**

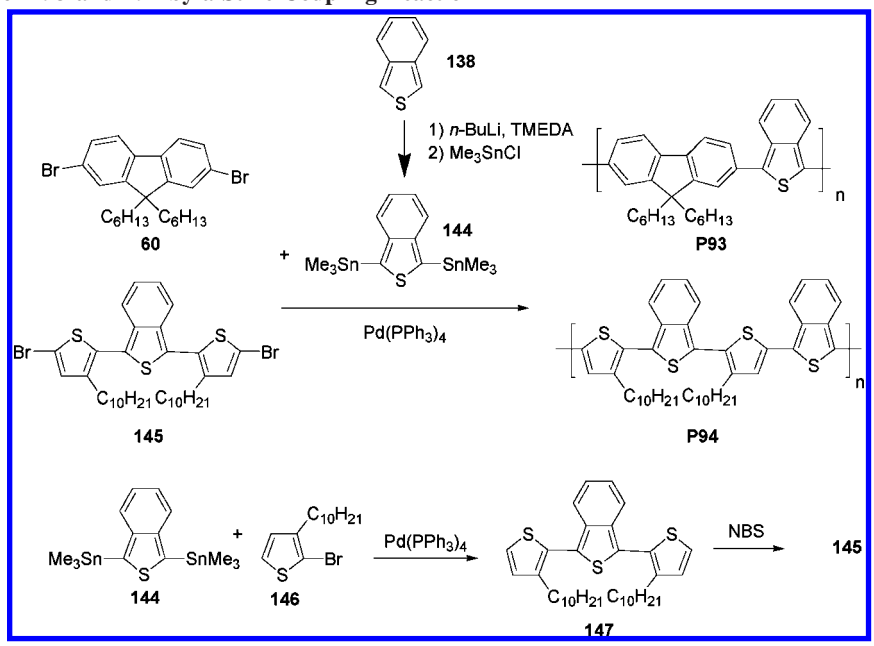


**Scheme 45. Synthesis of Homopolymers P95−P97**

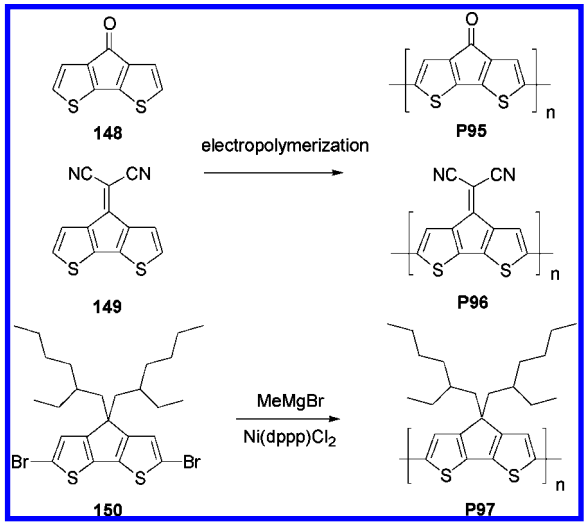


coplanar structure, many intrinsic properties based on bithiophene can be altered, leading to extended conjugation, lower HOMO−LUMO energy band gaps, and stronger intermolecular interactions. Furthermore, the option of functionalization at the bridging carbon allows greater structural variations for fine-tuning both the electronic and steric properties.

As reported by Ferraris and co-workers,[236,237] poly(cyclopenta[2,1-*b*:3,4-*b*′]dithiophen-4-one) (**P95**) or poly(4-(dicyanomethylene)-4*H*-cyclopenta[2,1-*b*:3,4-*b*′]dithiophene) (**P96**) were electropolymerized from their parent monomers **148** and **149**, respectively (Scheme 45). Owing to the electron-withdrawing effect of the ketone or dicyano groups for reducing the aromaticity of bithiophene and stabilizing the quinoid form, the band gaps of **P95** and **P96** can be markedly reduced to as low as 1.2 and 0.8 eV, respectively. To make solution-processable polymers, 2,6-dibromo-CPDT **150** with two 2-ethylhexyl side chains was homopolymerized by a Ni-catalyzed coupling reaction to afford **P97**.[238] The resulting polymer showed a much lower band gap of ca. 1.7−1.8 eV compared to its analogous poly(3-alkylthiophene) or polyfluorene. It should be noted that the absorption spectra of this polymer both in solution and in the solid state are essentially identical. This suggests that self-assembly of the interchain interactions in the solid state is not established.

To further decrease the band gap and improve the absorption coverage, poly[2,6-(4,4-bis(2-ethylhexyl)-4*H*-cyclopenta[2,1-*b*;3,4-*b*′]dithiophene)-*alt*-4,7-(2,1,3-benzothiadiazole)] (PCPDTBT) (**P98**) containing alternating CPDT units as the donor and benzothiadiazole units as the acceptor was developed and synthesized by Zhu and co-workers via a Stille coupling (Scheme 46).[239] With two ethylhexyl groups, PCPDTBT is very soluble in organic solvents and has good miscibility with PCBM, thus facilitating its processability. The HOMO and LUMO values, from electrochemical measurements, were calculated to be −5.3 and −3.57 eV, respectively. The optical band gap, from solid-state absorption, is approximately 1.4 eV, which is regarded as ideal for polymer−fullerene BHJ solar cells. Unlike the homopolymer of CPDT, PCPDTBT showed a much greater red shift in the absorption spectrum of the thin film than in solution. This indicates more interchain interactions when benzothiadiazole units are incorporated. When blended with $PC_{71}BM$, the BHJ device achieves a PCE of up to 3.5% with a $J_{sc}$ of 11.8 mA/cm$^2$ and a $V_{oc}$ of 0.65 V. This is together with an elevated EQE higher than 25% over the spectral range from 400 to 800 nm: the maximum of 38% is around 700 nm. Moreover, the photocurrent production is extended to wavelengths even longer than 900 nm.[240] The high performance of PCPDTBT can be attributed to its broad, strong absorption spectrum and high mobility of charge carriers. The planar structure facilitates carrier transport between the polymer chains, allowing its hole mobility to reach up to 1 $\times$ 10$^{-3}$ cm$^2$/(V s). By incorporating a small amount of 1,8-octanedithiols into the PCPDTBT/$PC_{71}BM$ solution prior to spin coating, the solar cell efficiency was further improved to 5.5% through the formation of an optimal bulk morphology which enhances both the photoconductivity and charge carrier lifetime.[241] Without the need for thermal annealing during fabrication, this approach offers easier control over tailoring the morphology and is especially applicable to the more amorphous p-type polymers with low degrees of crystallinity where thermal annealing is less effective.[242,243]

**Scheme 46. Synthesis of P98 by a Stille Coupling Reaction**

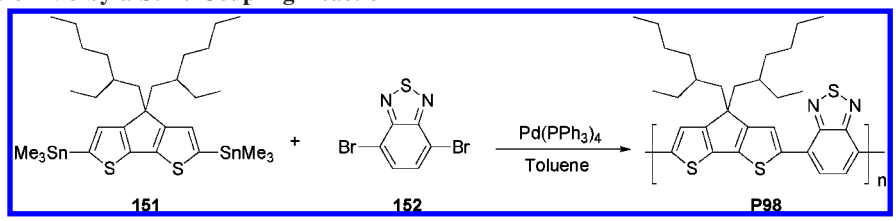


**Scheme 47. Synthesis of P99 by a Stille Coupling Reaction**

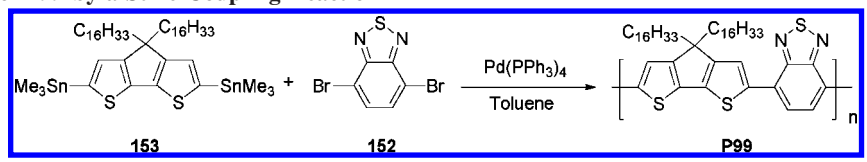


**Scheme 48. Synthesis of P100 by a Stille Coupling Reaction**

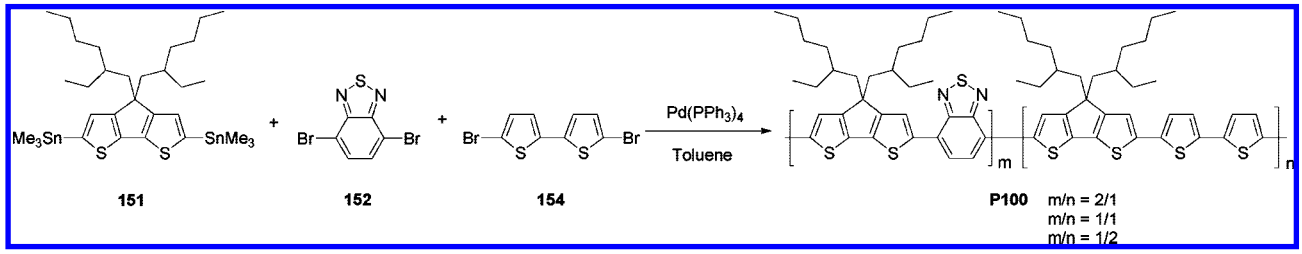


Heeger and co-workers also reported an efficient tandem cell with two active layers. This was aimed at maximizing the sunlight harvesting by smartly integrating a complementary pair comprised of P3HT with the wider band gap and PCPDTBT with the smaller band gap. The result led to the realization of a record-high PCE of over 6%.[244] Because PCPDTBT is the first breakthrough on the way to developing efficient low band gap D−A polymers, extensive analysis of the physical behavior of PCPDTBT/PCBM blends was carried out, namely, in terms of photoconductivity,[245] electron transfer,[246] and charge transport.[247]

About the same time, Müllen and co-workers reported a polymer (**P99**) analogous to PCPDTBT (**P98**) but with 4,4-dihexyldecyl substituents instead of the ethylhexyl groups (Scheme 47). **P99** shows a markedly high hole mobility of 0.17 $cm^2/(V\ s)$ in FET. This can be attributed to the enhanced packing order as a result of the introduction of the straight side chains.[248]

By decreasing the content of the acceptor 4,7-(2,1,3-benzothiadiazole) molecule **152** and introducing 5,5′-[2,2′]bithiophene **154** as the donor, a series of random copolymers **P100** were also synthesized (Scheme 48).[239] Through adjusting the D:A ratio, the absorption characteristics can be tuned to cover the whole visible spectrum. Initial cell testing on **P100**/PCBM has already resulted in PCE values of up to 3% being attained.

Subsequently, CPDT was used as an electron-donating building block for the construction of a series of alternating D−A conjugated polymers. In addition to benzothiadiazole, other electron-accepting moieties such as quinoxaline and dithiophene-ylbenzothiadiazole were also copolymerized with CPDT to form **P101** and **P102**, respectively (Scheme 49).[249] By using a 19:1 (v/v) mixture of chlorobenzene and anisole as the solvent to cast the **P102**/PCBM film, the optimal morphology was attained and the corresponding PSC device reached a PCE of 2.1%.

4,7-Dibromo-2,1,3-benzoselenadiazole (BSe), which is similar to the benzothiadiazole unit, was also coupled with CPDT by a Stille coupling to make the polymer **P103**.[250] A PCE of 0.89% was recorded with a $J_{sc}$ of 5 $mA/cm^2$ and a $V_{oc}$ of 0.52 V. The poorer performance of **P103** compared to PCPDTBT is attributed to its weaker absorbance and an imbalance in the hole and electron transport of the active layer.

A number of synthetic routes directed toward the preparation of useful CPDT monomers require laborious multistep synthesis and purification.[251−254] Considerable interest in the preparation of the ketone **160** as a precursor for low band gap polymers led to a more efficient route developed by Brzezinski and Reynolds using only three steps from starting material **157** (Scheme 50).[255] The ketone **160** is further reduced to **161** by a hydrazine Wolff−Kishner reduction. The methylene proton in **161** is acidic enough to undergo a double alkylation in the presence of potassium hydroxide in dimethyl sulfoxide to yield **163**. Lithiation of **163** by *tert*-butyllithium and sequential quenching using trimethyltin chloride afforded the distannyl monomer **151** ready for polymerization.

## 6.6. Silafluorene- and Dithieno[3,2-*b*:2′,3′-*d*]silole-Based Polymers

Compared with many heterocyclic arenes such as thiophene, furan, or pyrrole, the silole (silacyclopentadiene) ring has the smallest HOMO−LUMO band gap and the lowest lying LUMO level due to the $\sigma^*-\pi^*$ conjugation between the $\pi$-symmetrical $\sigma^*$ orbital of two $\sigma$ exocyclic bonds on silicon and the $\pi^*$ orbital of the butadiene moiety.[256] As a result a variety of conjugated small molecules and polymers consisting of silole derivatives exhibit extraordinarily unique properties such as high fluorescence efficiency and electron affinity and excellent electron mobility.[257−260] Conjugated polymers containing alternating electron-rich pyrroles or thiophenes and silole units have shown considerably smaller band gaps, which is indicative of the electron-accepting ability of silole to induce intramolecular charge transfer.[261−263] It is envisioned that the silole unit can serve as a useful building block in the molecular design of new conjugated

**Scheme 49. Synthesis of P101−P103 by a Stille Coupling Reaction**

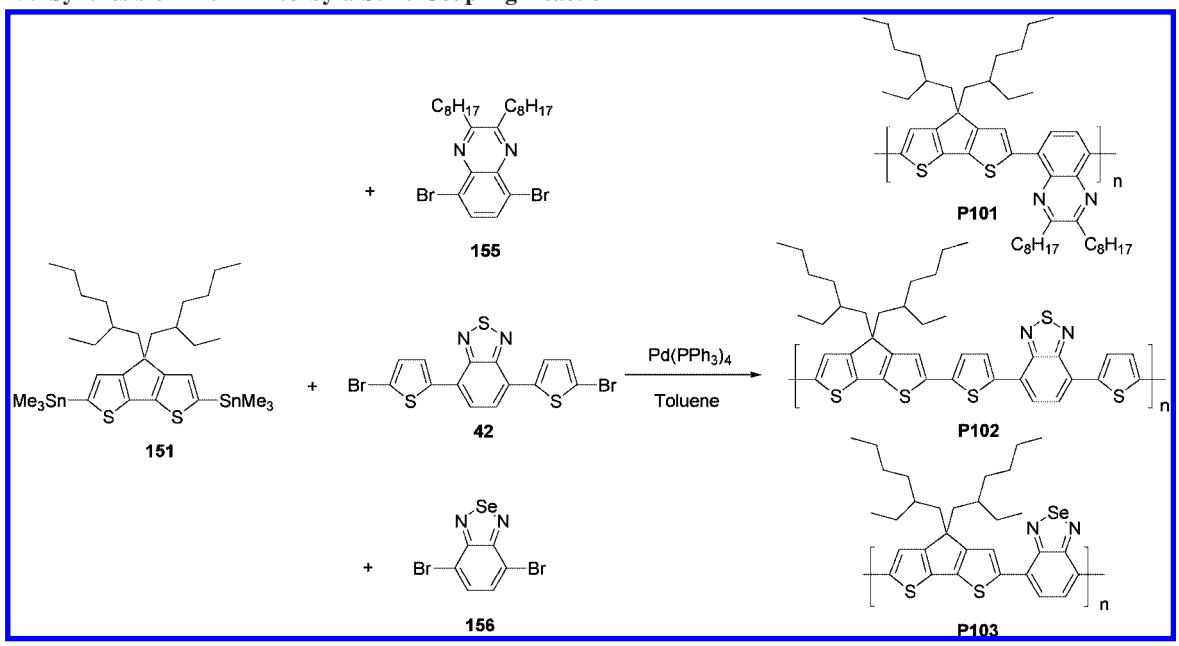


**Scheme 50. Synthetic Route toward Monomer 151**

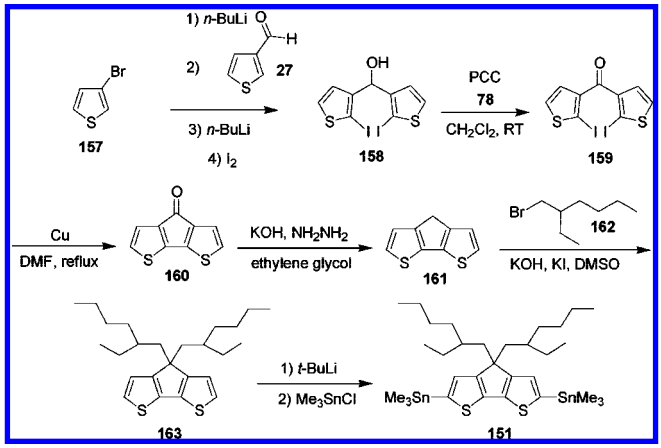


**Scheme 51. Synthesis of P104 by a Suzuki Coupling Reaction**

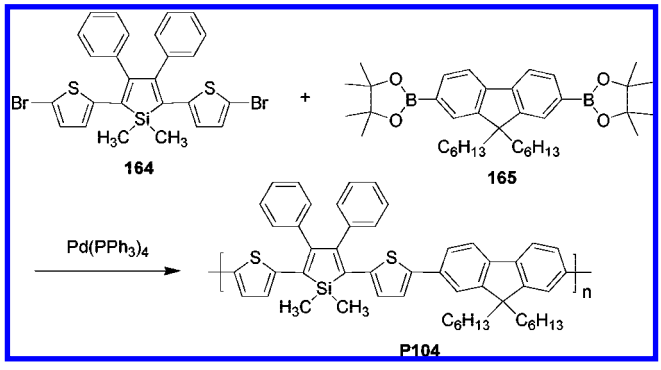


polymers for use in organic solar cell applications. An alternating copolymer **P104**, derived from 9,9-dihexylfluorene and the 1,1-dimethyl-3,4-diphenyl-2,5-bis(2′-thienyl)-silole unit, was synthesized by a Suzuki coupling (Scheme 51).[264] The HOMO and LUMO levels and the optical band gap of **P104** were determined to be −5.71, −3.6, and 2.08 eV, respectively. Blended with PCBM in the active layer of a bulk heterojunction device, **P104** achieved a promising PCE of 2.01%.

A facile synthesis aimed toward accessing 2,5-difunctional silole derivatives has been described by Tamao and co-workers (Scheme 52).[265] Upon treatment with lithium naphthalenide, bis(phenylethynyl)dimethylsilane (**167**) undergoes intramolecular reductive cyclization to form 2,5-dilithiosilole **168**, which was then transformed into 2,5-dizincated silole **169**. A Negishi Pd-catalyzed cross-coupling of this intermediate with 2-bromothiophene (**117**) afforded 2,5-bis(2′-thienyl)silole **170**, which was further brominated by NBS to furnish **164**.

The fluorene-containing D−A conjugated polymer **P44** and its derivatives have all been shown to have good photovoltaic properties as well as to deliver high PCEs over the 2−3% range. When the carbon atom on the 9-position of the fluorene unit is replaced with a silicon atom, a new type of building block, namely, silafluorene evolves. By fusing a silole ring between two phenyl rings, the silafluorene is expected to combine the advantages of both the silole and fluorene intrinsic properties. The tetravalence of the silicon atom in the silole ring opens up two additional substitution sides for the introduction of solubilizing groups. Cao and co-workers made the copolymer **P105**, which was synthesized by the Suzuki coupling[266] of 2,7-silafluorene **171** and dithienylbenzothiadiazole unit **42** (Scheme 53).

The solar cells made from a **P105**:PCBM (1:2, w/w) blend achieved a $V_{oc}$ of 0.9 V, a $J_{sc}$ of 9.5 mA/cm$^2$, an FF of 50.7%, and a PCE of up to 5.4%. The high $V_{oc}$ can be attributed to the low-lying HOMO of **P105**, which is −5.39 eV. From FET measurements, **P105** showed a hole mobility of $1 \times 10^{-3}$ cm$^2$/(V s), which is much higher than that of the PFO-DBT polymer ($3 \times 10^{-4}$ cm$^2$/(V s)). In addition, **P105** exhibits a lower optical band gap and a greater red-shifted absorption maximum compared to PFO-DBT **P45a** (1.82 vs 1.92 eV and 565 vs 544 nm, respectively). These enhanced properties contribute to improved hole transport and broader absorption, leading to a higher $J_{sc}$ and an acceptable FF. Around the same time, a parallel study using the same polymer was reported by Leclerc et al.[267]

The synthetic route for monomer **171** was developed by Holmes and co-workers (Scheme 54).[268] An Ullmann coupling of compound **172** gave the dimerization product **173**.

**Scheme 52. Synthetic Route toward Monomer 165**

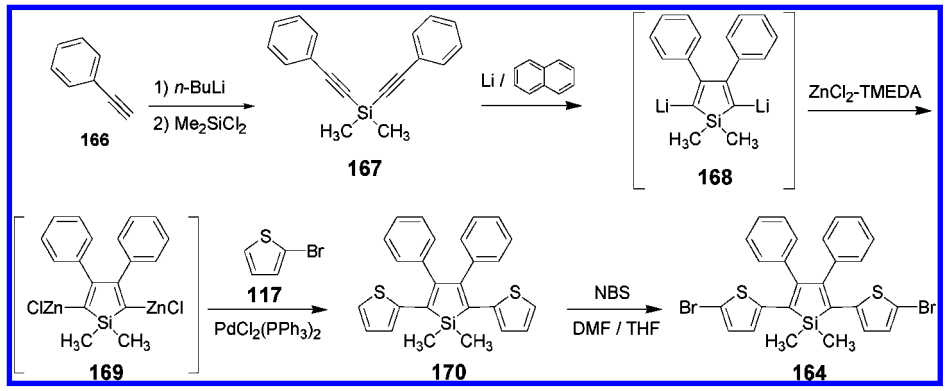


**Scheme 53. Synthesis of P105 by a Suzuki Coupling Reaction**

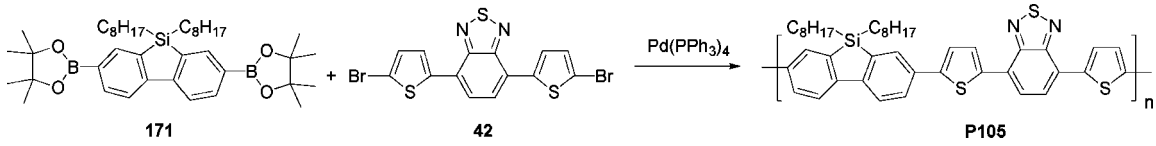


**Scheme 54. Synthetic Route toward Monomer 171**

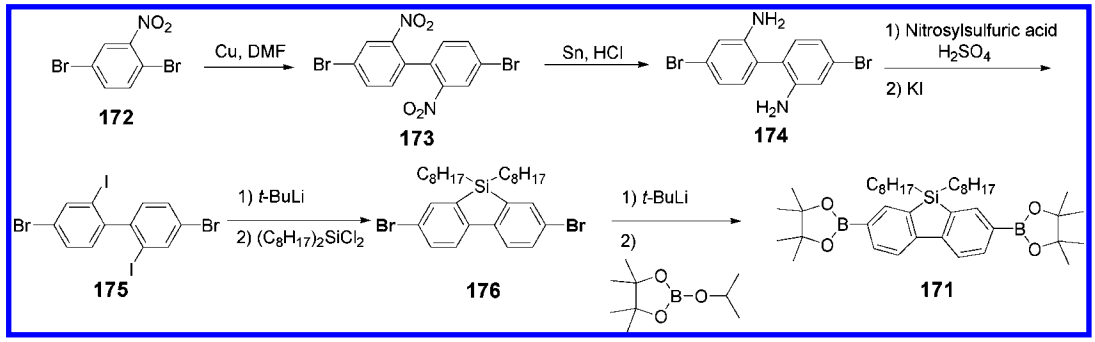


Reduction of the nitro groups in **173** yielded the amino compound **174**. This was followed by iodination via a diazonium pathway to generate **175**. Selective lithiation of the iodo groups of **175** by *tert*-butyllithium to react with dioctyldichlorosilane led to the formation of the central silole ring of **176**. Finally, the bromo groups in **176** can be easily transformed to the bis(boronic ester) **171**.

In view of the beneficial molecular design on going from fluorene to silafluorene, the exceptional cyclopentadithiophene system is further modified by substituting the carbon atom with a silicon bridge to generate a dithienosilole having a silole ring embedded in the center of dithiophene. A dithienosilole homopolymer (**P106**) and an alternating dithienosilole and dithienylbenzothiadiazole copolymer (**P107**) were reported and synthesized by Stille coupling reactions (Scheme 55).[269] Due to the incorporation of electron-accepting units, the copolymer **P107** has both a lower HOMO level, −5.13 eV, and a smaller band gap, 1.4 eV, than the homopolymer **P106** (−4.85 and 1.9 eV, respectively). The best photovoltaic performance after thermal annealing at 140 °C was based on **P107**/PCBM (1:1, w/w) and showed a $V_{oc}$ of 0.44 V, a $J_{sc}$ of 1.32 mA/cm$^2$, and a PCE of 0.18%.

Recently, Yang and co-workers reported another dithienosilole-containing copolymer (**P108**). Here benzothiadiazole is the acceptor and 2-ethylhexyls are the solublizing groups, which makes it structurally similar to PCPDTBT (Scheme 55).[270] The HOMO and LUMO of the polymer were estimated to be −5.05 and −3.27 eV, respectively. Although the optical band gap of 1.45 eV is very close to the polymer PCPDTBT, the substitution of the silicon atom significantly improved the hole-transport properties. The hole mobility of **P108** ($3 \times 10^{-3}$ cm$^2$/(V s)), determined by a field-effect transistor, is 3 times higher than that for PCPDTBT. The photovoltaic device with an active layer of **P108**/$PC_{71}BM$ (1:1, w/w) exhibited a $V_{oc}$ of 0.68 V, a $J_{sc}$ of 12.7 mA/cm$^2$, and a very impressive PCE of 5.1%. Notably, the EQE as a function of the wavelength showed a broad response ranging from 350 to 800 nm.

The synthesis of the distannyldithienosilole **179** is shown in Scheme 56. By a selective lithium−bromide exchange followed by nucleophilic substitution, the trimethylsilyl group was introduced into the 5,5′-positions of the bithiophene compound **181** to act as a protecting group. As a consequence, the subsequent lithiation in compound **181** only occurred at the 3,3′-positions of the bithiophene, which then underwent cyclization through double addition to dialkyldichlorosilane and gave **182**. NBS bromination via electrophilic aromatic substitution to replace the trimethylsilyl moiety resulted in the formation of compound **183**, which was then converted to the distannyl compound **179** by lithiation and final quenching with trimethyltin chloride.

## 6.7. Dithieno[3,2-*b*:2′,3′-*d*]pyrrole-Based Polymers

After the tricyclic cyclopentadithiophene and dithienosilole rings were shown to serve as excellent donor components with various acceptor units in low band gap polymers, dithieno[3,2-*b*:2′,3′-*d*]pyrrole attracted attention

**Scheme 55. Synthesis of P106−P108 by a Stille Coupling Reaction**

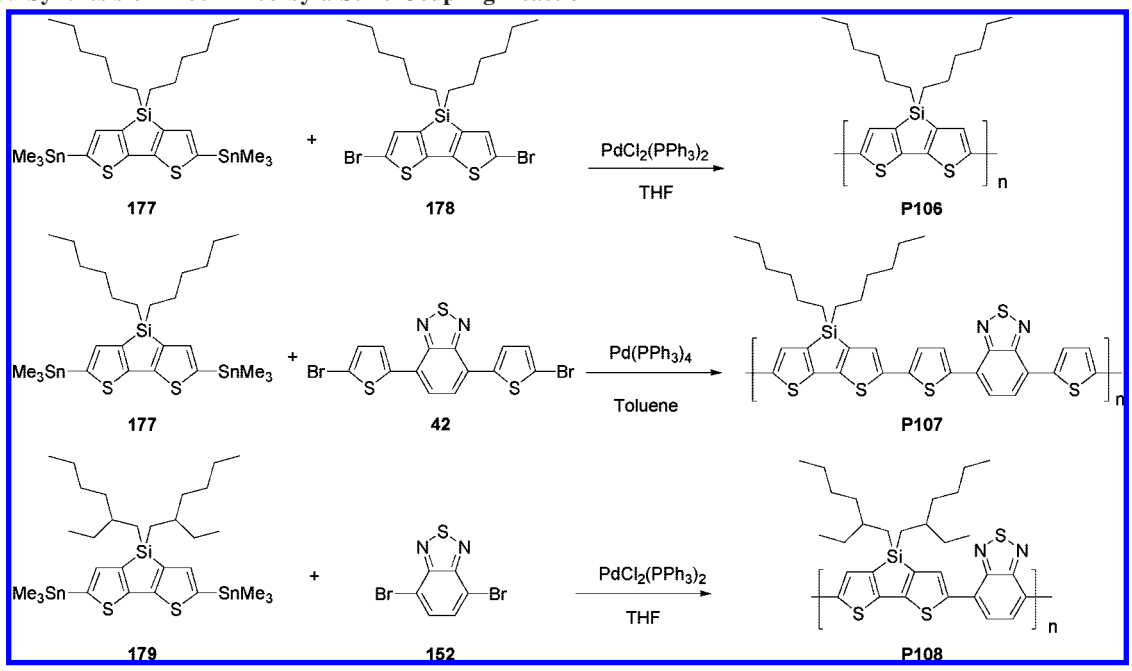


**Scheme 56. Synthetic Route toward Monomer 179**

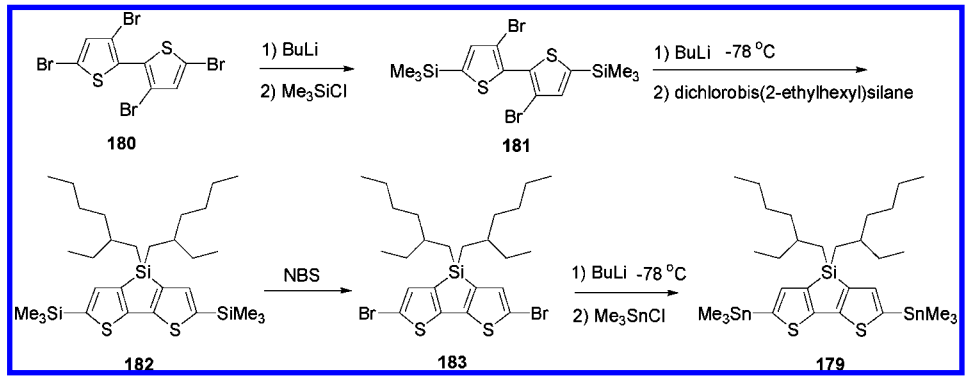


**Scheme 57. Synthesis of P109 by $FeCl_3$ Oxidative Polymerization and P110 by a Stille Coupling Reaction**

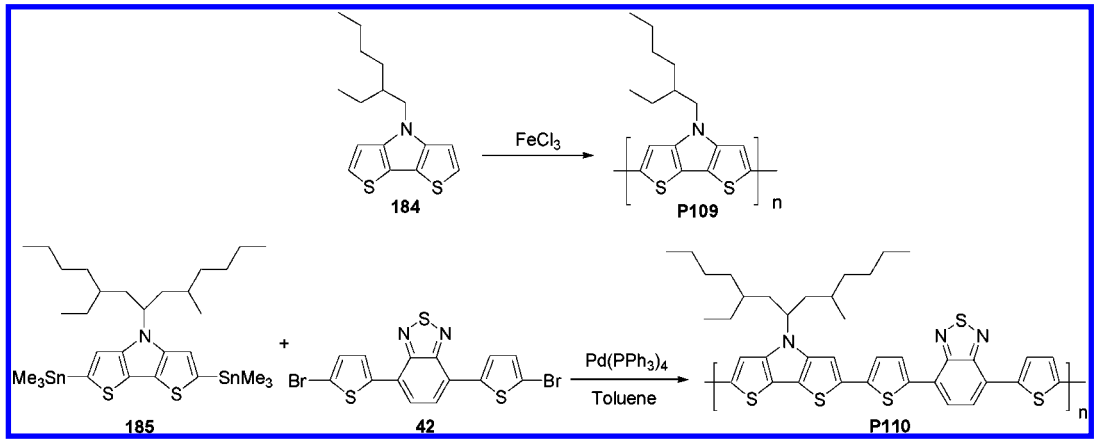


as another appealing fused bithiopene member with a bridged nitrogen having strong electron-donating ability. As reported by Rasmussen and synthesized by the oxidation polymerization of **184**, the homopolymer poly(dithieno[3,2-*b*:2′,3′-*d*]pyrrole) **P109** showed a reduced band gap of ca. 1.7 eV and a high red-emitting quantum efficiency.[271] Hashimoto and co-workers reported another D−A conjugated copolymer (**P110**) constituted of alternating dithienopyrrole and dithienylbenzothiadiazole units and synthesized by a Stille cross-coupling reaction (Scheme 57).[272] **P110** showed a greater red-shifted absorption maximum at 697 nm in a film than in solution at 671 nm. This indicates strong interchain interactions due to its coplanar structure. Compared with the homopolymer dithienopyrrole, **P110** also exhibited a more bathochromic shift in the absorption spectrum and a smaller optical band gap of 1.46 eV. Again this demonstrates efficient charge transfer between the donating dithienopyrrole and accepting benzothiadiazole units. The PSC based on **P110** as the donor and blended with PCBM (1:1, w:w) exhibited a PCE of 2.18%.

**Scheme 58. Synthetic Route toward Monomers 185 and 191**

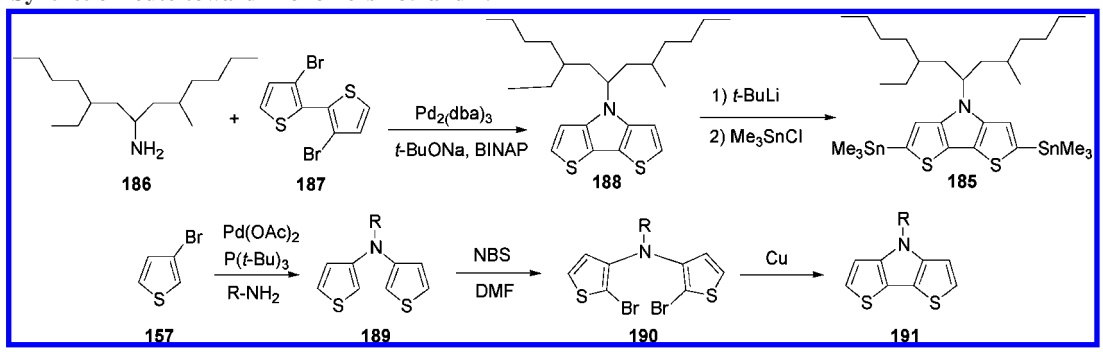


**Scheme 59. Dibromo and Distannyl Monomers for the Synthesis of Polymers P111−P117 by a Stille Coupling Using $Pd(PPh_3)_4$ as the Catalyst**

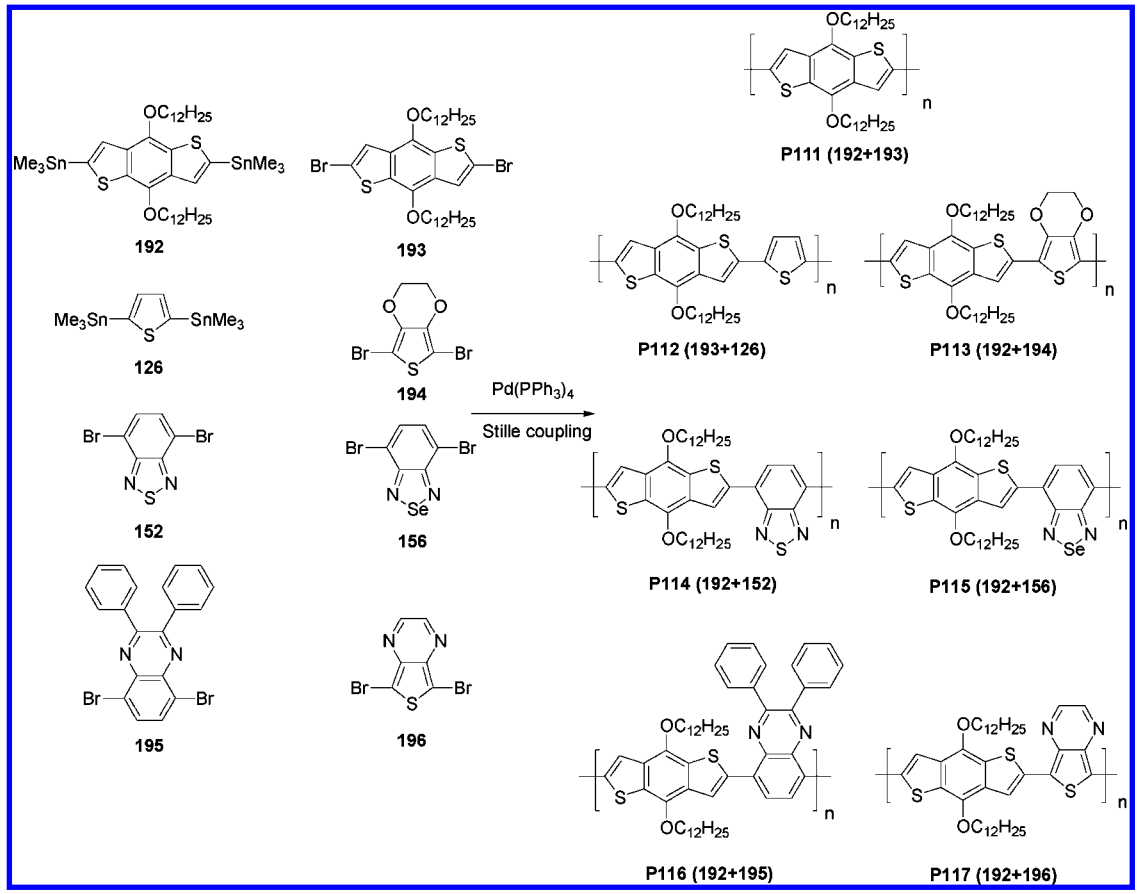


The dithieno[3,2-*b*:2′,3′-*d*]pyrrole ring of **188** was built up by a one-step cyclization through a double Pd-catalyzed amination of 3,3′-dibromobithiophene (**187**) with the primary amine **186** having a long aliphatic side chain (Scheme 58). Another efficient way to synthesize the dithieno[3,2-*b*:2′,3′-*d*]pyrrole ring involves the Pd-catalyzed amination of 3-bromothiophene (**157**) with a variety of primary amines to form **189**. This is followed by a one-pot NBS bromination and Cu cyclization to yield **191**(Scheme 58).[273]

## 6.8. Benzo[1,2-*b*:4,5-*b*′]dithiophene-Based Polymers

The benzo[1,2-*b*:4,5-*b*′]dithiophene (BDT) unit has emerged as an attractive building block for making conjugated polymers due to its large planar conjugated structure ideal for efficient $\pi-\pi$ packing. Alternating BDT and bithiophene copolymers exhibiting a high field-effect transistor mobility of 0.25 $cm^2/(V\ s)$ and enhanced stability has been reported.[274]

Yang and co-workers reported a series of BDT-based polymers, **P111−P117,** with different alternating units. They systematically investigated their structure−property relationships for PSC applications.[275] Using a Stille cross-coupling of the relevant monomers, 4,8-bisalkoxy-BDT was copolymerized with two types of electron-donating units, including thiophene and (ethylenedioxy)thiophene (EDOT), and four electron-deficient units, including thieno[3,4-*b*]pyrazine (TPZ), benzoselenadiazole (BSe), 2,3-diphenylquinoxaline (DPQ), and benzothiadiazole (BT) (Scheme 59). The absorption spectrum of the homopolymer **P111** showed a maximum wavelength at 495 nm. As the donating strength of the incorporated unit increases from thiophene in **P112** to EDOT in **P113**, the maximum absorption shifts to 511 and 532 nm, respectively. However, it was found that the electron-donating power of EDOT in **P113** also resulted in an increased HOMO level and a subsequent decrease in $V_{oc}$. On the other hand, the ability of the four electron-deficient

**Scheme 60. Synthetic Route toward Monomer 192**

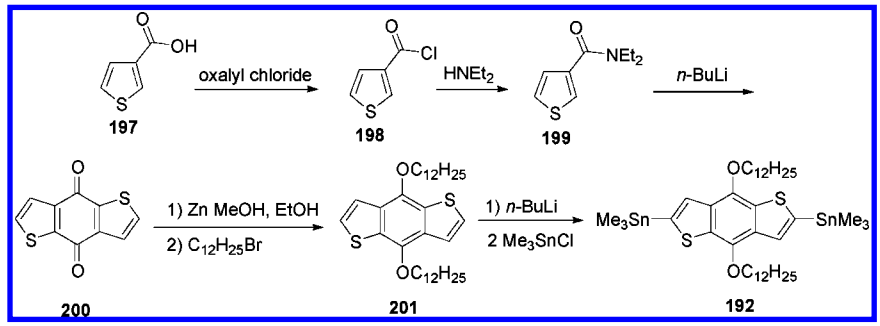


**Scheme 61. Synthesis of P118 by a Stille Coupling Reaction**

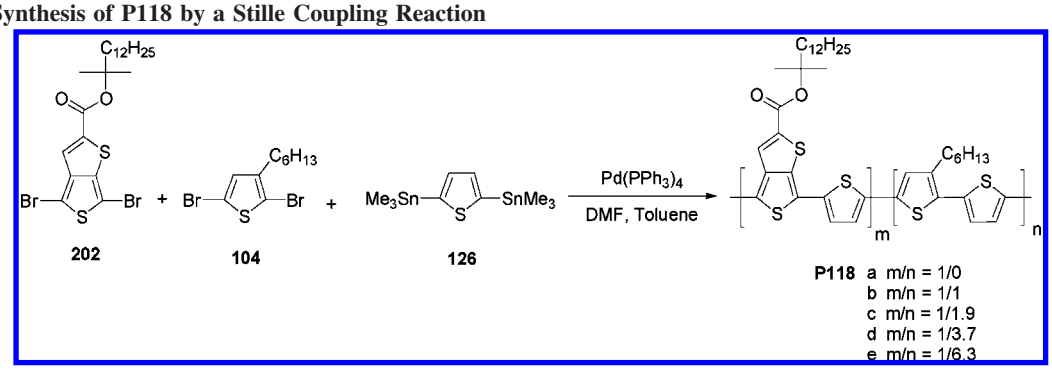


units to lower the band gap of the corresponding polymer is in the order TPZ (**P117**) > BSe (**P115**) > DPQ (**P116**) > BT (**P114**). This also reflects their electron-accepting strength as well as their capability to adopt the quinoid structure in the polymer. As a result, **P117** containing TPZ showed a very low band gap of 1.05 eV, which matchs the solar spectrum well. However, because of the fact that the HOMO level lies somewhat too high, the $V_{oc}$ of **P117** is only 0.21 V. One interesting observation is that, unlike the BSe analogue, the BT unit in the BDT-based polymer **P114** can narrow the band gap by depressing the LUMO level without elevating its HOMO level when compared to the standard homopolymer **P111**. This is reflected in an improved $V_{oc}$ of 0.68 V. When blended with PCBM (1:1, w/w), **P112** showed the highest PCE, 1.6%, with a $V_{oc}$ of 0.75 V, a $J_{sc}$ of 3.78 mA/cm$^2$, and an FF of 0.56.

The synthesis of the monomer 1,8-bis(dodecyloxy)-BDT **192** is shown in Scheme 60. Lithiation of *N*,*N*-diethylthiophene-3-carboxamide (**199**) with butyllithium, followed by nucleophilic addition to the amide group, afforded the cyclized dimerization product **200**. The central benzoquinone of **200** was reduced to a hydroquinone-type intermediate by treatment with zinc dust followed by *O*-alkylation to produce **201** in a one-pot reaction.[276] The resulting **201** can be directly lithiated by butyllithium and then quenched with trimethyltin chloride to obtain **192** without having to go through a bromination step.

## 6.9. Thieno[3,4-*b*]thiophene-Based Polymers

The low band gap strategy involving PITN derivatives led to interest in other fused ring systems as potential building blocks for p-type conjugated polymers. Like ITN with its thiophene-fused benzene ring, thieno[3,4-*b*]thiophene (TT) is thiophene fused with another thiophene ring at the 3,3′-thiophene positions. Polythieno[3,4-*b*]thiophene (PTT) is capable of stabilizing the quinoid form of the main chain, resulting in a very low band gap of 0.84 eV accompanied by good electrochemical stability.[277−279] However, such a low band gap polymer is not ideal for solar cell applications.

To dilute the thieno[3,4-*b*]thiophene content in the main chain with a view to adjusting the band gap, a series of copolymers **P118** consisting of thieno[3,4-*b*]thiophene and thiophene units were synthesized by Stille coupling reactions (Scheme 61).[280] By changing the ratio between thiophene and thieno[3,4-*b*]thiophene to fine-tune the degree of quinoid formation, the band gap and energy levels of the polymer could be controlled to optimal values. As expected, the band gap of the polymer decreases as the thieno[3,4-*b*]thiophene increases by compressing the HOMO and LUMO levels closer to each other. Importantly, **P118a** with the highest content of thieno[3,4-*b*]thiophene exhibits the greatest hole mobility, very comparable to that of P3HT, suggesting that the more the TT units induce the quinoid form the greater the planarity along the aromatic backbone to facilitate charge transport. In addition, when the TT ratio decreases in the copolymers, the 3-hexylthiophene units are irregularly attached to the backbone, which causes a twisting of the main chain and leads to decreased hole mobility. **P118d** with an *m*:*n* ratio of 1:3.7 has a more ideal optical band gap of 1.45 eV and more optimal HOMO/LUMO levels relative to the PCBM acceptor, achieving a highest $J_{sc}$ of 8.66 mA/cm$^2$ and a PCE of 1.93% among these polymers using the composite of polymer/PCBM (1:1, w/w) in BHJ solar cells. Although **P118a** showed only a PCE of 0.73% due to its band gap as low as 1.2 eV, which limits its application for the solar cell, its derivative with a different alkyl chain has been successfully used in a plastic near-infrared photodetector.[281]

A regioregular 3-hexylthiophene-conjugated oligomer (**203**) and its polymer analogue **P119** containing small amounts of thieno[3,4-*b*]thiophene were also synthesized (Scheme 62).[282] The perfluorohexyl substituent is used to stabilize the electron-rich thieno[3,4-*b*]thiophene and renders it more chemically stable. The optical band gap of **203** and **P119** determined to be ca. 1.6 eV is much lower than that of P3HT (1.9 eV) due to the effect of the introduced

**Scheme 62. Synthesis of P119 by a Stille Coupling Reaction and Chemical Structure of Oligomer 203**

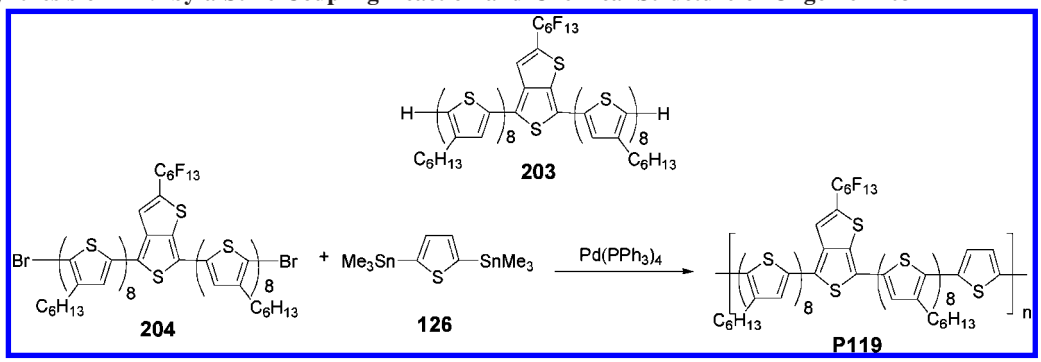


**Scheme 63. Synthesis of P120 by a Stille Coupling Reaction**

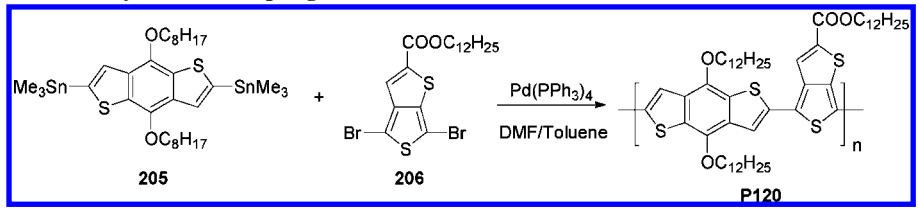


**Scheme 64. Synthetic Route toward Monomer 206**

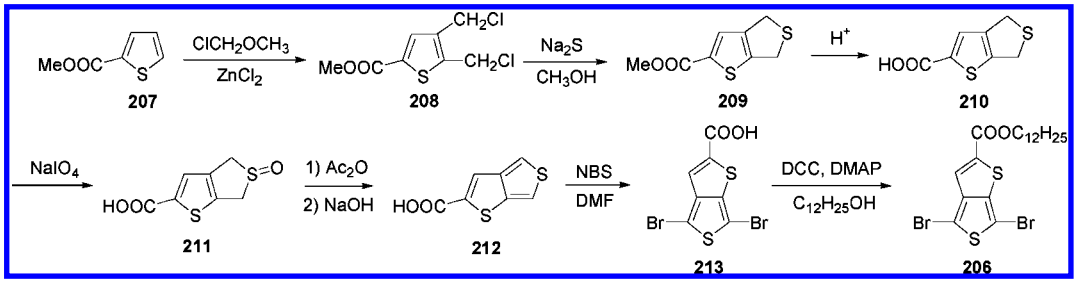


thienothiophene units. Although **203** and **P119** exhibited similar optical properties and HOMO energies due to the similarity of structure, **P119** having higher molecular weight showed better hole mobility due to the extension of the electron delocalization length in the polymer and better miscibility with PCBM to yield an optimal morphology of an interpenetrating nanofiber with a diameter ranging from 15 to 20 nm. In contrast, 30−40 nm fibers were found in the **203**/PCBM blend because of the more favorable phase separation. Therefore, the **P119**-based solar cell devices achieved a PCE of 2.38% and outperformed the 0.46% obtained from the oligomer **203**.

To take advantage of the BDT and thieno[3,4-*b*]thiophene units together, Yu and co-workers designed and synthesized the copolymer **P120**. Stille coupling produced a product comprised of alternating BDT and thieno[3,4-*b*]thiophene units (Scheme 63).[283] The ester-substituted thieno[3,4-*b*]thiophene in this polymer makes it both soluble and oxidatively stable. The optical band gap derived from the onset of the film absorption is 1.6 eV. The HOMO and LUMO were determined to be −4.9 and −3.2 eV, respectively. The BHJ solar cells were fabricated using a **P120**/PCBM composite (1:1, w/w), giving a $V_{oc}$ of 0.58 V, a $J_{sc}$ of 12.5 mA/cm$^2$, and a high power conversion efficiency of 4.76%. An improved conversion efficiency of up to 5.3% was achieved when the polymer was blended with $PC_{71}BM$. The thienothiophene unit tends to stabilize the quinoid structure in the polymer chain and thus enhances the planarity along the polymer backbone. The high power conversion efficiency can be attributed to the rigidity and planarity of the polymer backbone, leading to a high hole mobility of $4.5 \times 10^{-4}$ cm$^2$/V s as measured by the space charge limited current method. The synthesis of monomer **206** is shown in Scheme 64. Chloromethylation of **207** by using chloromethyl methyl ether with zinc chloride as a catalyst afforded the bis(chloromethyl) product **208**, which was cyclized by reacting with sodium sulfide to give compound **209**. After hydrolysis of **209** to give the carboxylic acid **210**, the sulfide was oxidized to the sulfoxide **211** by sodium metaperiodate.[284] Reacting with acetic anhydride followed by base-induced elimination, compound **211** was reduced to form a thiophene ring in compound **212**. Bromination followed by etherification led to the formation of the final product **206**.

## 6.10. Thieno[3,2-*b*]thiophene-Based Polymers

Another attractive example of the fused thiophene family is thieno[3,2-*b*]thiophene. The incorporation of linearly symmetrical and coplanar thieno[3,2-*b*]thiophene units in the conjugated polymer is predicted to facilitate the adoption of a low-energy backbone conformation, leading to strong interchain interactions for ordered packing. Unfortunately, polythieno[3,2-*b*]thiophene has very poor solubility, which limits its characterization and processability.[285,286] The introduction of alkyl chains into the $\beta$-position of the thieno[3,2-*b*]thiophene unit can improve the solubility, but the down side is that it also imposes a negative effect on the effective conjugation due to severe steric-hindrance-induced twisting between the neighboring units.[287,288] To reduce steric interactions and thereby restore planarity and conjugation, vinylene units serving as spacers were incorporated and copolymerized with either a 3-hexylthiophene or a thieno[3,2-

**Scheme 65. Synthesis of P121 and P122 by Stille Coupling Reactions**

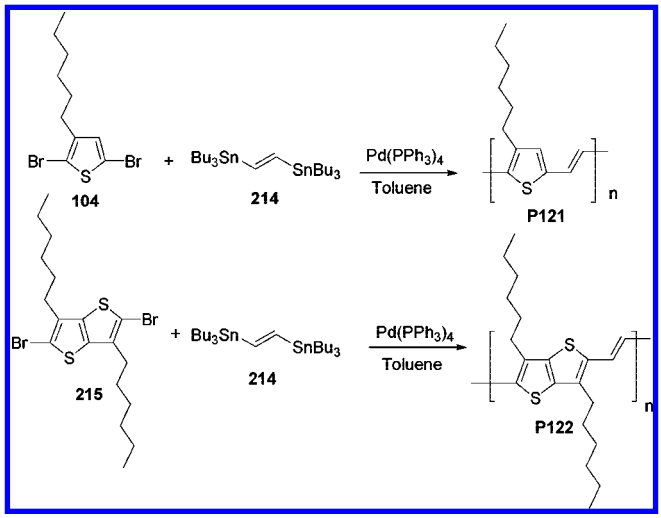


*b*]thiophene unit to prepare the copolymers **P121** and **P122**, respectively (Scheme 65).[289]

It was observed that the absorption maximum of **P122** in solution is at 538 nm, which is 18 nm hypsochromically shifted as compared with that of **P121**, implying that hexyl groups in the thienothiophene unit still cause distortion of the polymer backbone. It is noteworthy that, whereas no emission was observed for **P121**, **P122** exhibits strong photoluminescence in the wavelength range from 500 to 750 nm. From field-effect transistor studies, **P122** showed a hole mobility of $4.64 \times 10^{-4}$ cm$^2$/(V s). After thermal annealing at 180 °C for 30 min, the hole mobility dramatically increased to 0.019 cm$^2$/(V s). The morphology investigated by AFM indicated that, after annealing, crystalline domains were induced in the **P122** film from its original amorphous phase, leading to markedly improved mobility. On the contrary, the **P121** films exhibited only characteristic amorphous morphologies both with and without annealing. As a result, **P121** showed relatively low mobility on the order of $10^{-4}$ cm$^2$/(V s). Due to the higher mobility resulting from the thieno[3,2-*b*]thiophene units, the PCE of the PSCs based on **P122** reached 0.28%, which is superior to the 0.19% for the **P121** device.

Poly(2,5-bis(3-tetradecylthiophene-2-yl)thieno[3,2-*b*]thiophene (**P123**) containing no substituents on the thieno[3,2-*b*]thiophene units but with two long tetradecyl chains on the bithiophene unit was reported by McCulloch and co-workers (Scheme 66).[290] Two symmetrical monomers coupled by a Pd-catalyzed Stille reaction offer a regioregular arrangement of the polymer under formation. The tail-to-tail arrangement of the alkyl chains on the bithiophene units also minimizes the steric interactions between neighboring units, leading to coplanarity of the backbone and hence promoting self-organization. It was found that the hairy rigid-rod **P123** exhibits a liquid-crystalline phase and self-assembles into a highly crystalline domain with lamellar and $\pi$-stacked polymer chains.[291,292] The side chain attachment density in **P123** is sufficiently low to allow interdigitation, which provides a three-dimensional ordering.[293] Due to this enhanced structural order, a remarkably high field-effect hole mobility of 0.2−0.6 cm$^2$/(V s) was realized. This is even greater than that obtained in regioregular P3HT (0.1−0.2 cm$^2$/(V s)).[290] Its potential application in BHJ solar cells was therefore investigated.[294,295] The HOMO and LUMO levels of **P123** were estimated to be −5.1 and −3.1 eV, which are very close to those of P3HT. The PSCs fabricated from the active layer of **P123**/PC$_{71}$BM (1:4, w/w) achieved the maximum PCE of 2.3% with a $V_{oc}$ of 0.58 V, a $J_{sc}$ of 12.5 mA/cm$^2$, and an FF of 0.48. The synthesis of **216** is outlined in Scheme 67.[296] Deprotonation of 3-bromothiophene with lithium diisopropylamide (LDA) followed by quenching with *N*-formylpiperidine afforded **218**. The Michael addition of ethylmercaptoacetate to the 3-position of **218** followed by elimination of bromide and an Aldol condensation yielded **219.** This was then hydrolyzed to the corresponding carboxylic acid **220**. Decarboxylation by copper and quinoline led to the formation of thieno[3,2-*b*]thiophene **221**. Lithiation of **221** and quenching with trimethyltin chloride led to 2,5-bis-trimethylstannyl-thieno[3,2-*b*]thiophene **216**.

## 6.11. Other Fused Thiophene-Based Conjugated Polymers

Three bithiophene-based compounds planarized by bridging benzo, naphtho, and quinoxalino units were polymerized with the CDPT moiety **225** by Suzuki coupling to yield the corresponding polymers **P124**, **P125**, and **P126**, respectively (Scheme 68).[297] These fused five−six−five tricyclic conjugated segments are designed to enhance molecular planarity and $\pi$-electron delocalization. The optical band gap was estimated to be 2.00, 1.91, and 1.94 eV for **P124**, **P125**, and **P126**, respectively, very comparable to that of P3HT and larger than that of the CPDT homopolymer with a band gap of 1.7−1.8 eV. This result indicated that, although incorporation of a benzene ring fused into two thiophenes enhances the coplanarity, the formation of a 14-$\pi$-electron system with a higher degree of aromaticity may also reduce the quinoid formation in the polymer chain, resulting in a higher band gap. With additional benzene rings or pyrazine rings fused with this system, the delocalization decreases the aromaticity so that the band gap can be reduced to some extent. It is expected that lower polymer band gaps can be obtained if **221**−**224** are copolymerized with an electron-withdrawing acceptor instead of the electron-rich CPDT. Due to the presence of an electron-deficient pyrazine ring, −5.15 eV was the lowest HOMO for **P126**. BHJ photovoltaic devices made from **P126**/PCBM (1:1.6, w/w) exhibited an overall PCE of 1.14%.

The synthesis of the monomers **222**−**224** is depicted in Schemes 69−71. The Pd-catalyzed coupling reaction of 3,3′-diiodo-2,2′-bithiophene (**226**) and 9-octadecyne gave the cyclization product **227**, which was brominated to obtain the monomer **222** (Scheme 69).[298] The Suzuki coupling reaction of **228** with 3-thiopheneboronic acid gave the product **229**. Oxidative photocyclization of **229** by UV irradiation in the presence of a catalytic amount of iodine resulted in the formation of compound **230**, which was then brominated to obtain the final monomer **223** (Scheme 70). The condensation of the 1,2-diamine **231** with 1,2-diketone **232** directly furnished the dehydrogenated product **233**, which after NBS bromination gave the final monomer **224** (Scheme 71).

4,9-Dihydro-*s*-indaceno[1,2-*b*:5,6-*b*′]dithiophene-4,9-dione derivatives are pentacyclic systems consisting of a thiophene−1,4-phenylene−thiophene skeleton with two fused cyclopentadienone rings in between. This new conjugated diketone system has been shown to have unique optical and redox properties.[299] This pentacyclic component was copolymerized with different ratios of thiophene units to afford two new conjugated polymers (**P127a** (*m*:*n* = 1:5) and

**Scheme 66. Synthesis of P123 by a Stille Coupling Reaction**

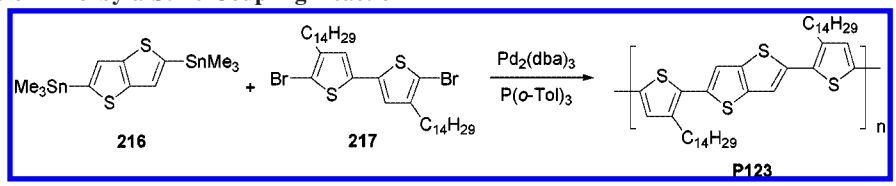


**Scheme 67. Synthetic Route toward Monomer 216**

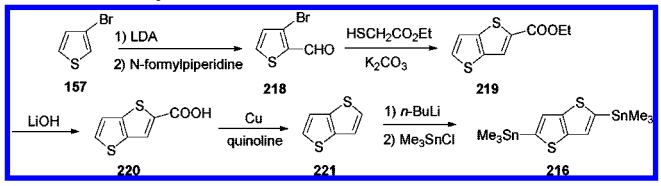


**P127b** (*m*:*n* = 1:2.5)) using a Stille cross-coupling reaction (Scheme 72).[300] When the diketone content is higher than that of **P127b**, the resulting polymer becomes insoluble. **P128** with a pure polythiophene main chain was also prepared for comparison. Besides the absorption at 300−600 nm which is observed in **P128**, **P127a** and **P127b** exhibited an additional broad absorption peak at 600−800 nm which is assigned to the $\pi-\pi$ transition of the diketone unit. However, both in solution and in the solid state, the absorption coefficient of the lower energy absorption band is much weaker than those in the 300−600 nm region. This prevents efficient light harvesting at longer wavelengths. As the diketone unit content increases, the oxidation potential of **P127b** becomes higher than those of **P128** and **P127a** due to the electron-withdrawing effect of the diketone units. These three polymers have very similar band gaps at ca. 2.3 eV as determined by cyclic voltammetry. The PCE values of solar cells using blends of these polymers with PCBM (1:3, w/w) were measured and found to be 0.33% for **P127a** and 0.26% for **P127b**, better than that of **P128**, which is 0.11%.

The synthesis of the monomer **234** is shown in Scheme 73.[299] Due to its decreasing solubility as a result of chain elongation, hexyl groups were introduced in each of the terminal thienyl units in **236**. Desilylation of the protecting trimethylsilyl groups in **236** with trifluoroacetic acid resulted in the formation of **237**. Saponification of the diesters **237** yielded the terephthalic acid **238**, which is readily converted into the corresponding acid dichloride **239**. A Lewis acid-promoted intramolecular Friedel−Crafts cyclization of **239** furnished the diketone **240**, which was easily brominated at the terminal thiophenes by NBS to give **234**.

Two new low band gap polymers based on the thiophene–phenylene–thiophene moiety (TPT) have been reported by Ko and co-workers.[301,302] As shown in Scheme 74, the synthesis involved a Pd-catalyzed Stille coupling under microwave-assisted conditions.[303] TPT and benzothiadiazole units were copolymerized with bithiophene or thiophene units to generate **P129** or **P130**, respectively. Two outer thiophenes are rigidified and held together using a central phenyl ring, which provides a coplanar conjugated backbone of pentacyclic fused aromatic rings. This planar structure provides effective conjugation and facilitates strong intermolecular interactions, leading to a low band gap of 1.76 eV for **P129** and 1.70 eV for **P130** and a high absorption coefficient for efficient light harvesting. Furthermore, a high hole mobility of $3.4 \times 10^{-3}$ cm$^2$/(V s) for **P130** was obtained in a field-effect transistor, allowing efficient charge extraction and a high fill factor. Blending **P130** with $PC_{71}BM$ in the active layer (1:3, w/w) gave the highest performance and delivered a PCE of 4.4%, a $V_{oc}$ of 0.8 V, a $J_{sc}$ of 10.1 mA/cm$^2$, and an FF of 0.53. The PCE is better than that of a cell based on P3HT (PCE = 3.9%) under the same conditions. **241** was prepared by following the procedure developed by Wong et al. (Scheme 75).[304] A double nucleophilic addition of (4-hexylphenyl)magnesium bromide (**243**) to the ester groups of **242** led to the formation of the benzylic alcohol **244**, which was then subjected to intramolecular annulation through acid-mediated Friedel−Crafts reaction to furnish **245**. The NBS bromination of **245** yielded the final monomer **241**.

## 6.12. Pyrrole-Containing Polymers

A pyrrole-containing polymer (**P131**) has been synthesized by the Stille coupling of 2,5-bis(5-(trimethylstannyl)-2-thienyl)-*N*-dodecylpyrrole (**246**) and 4,7-dibromo-2,1,3-benzothiadiazole (**152**) using $Pd(PPh_3)_2Cl_2$ as the catalyst (Scheme 76).[305,306] During the polycondensation, extensive destannylation of the distannyl monomer **246** occurred. This resulted in a low molecular weight polymer terminated with bromobenzothiadiazole end groups. Polymers with higher molecular weights can be obtained by adding excessive amounts of the distannyl monomer **246**. As a result of alternating electron-rich and electron-deficient units along the conjugated chain, this polymer shows a low band gap of 1.6 eV. Efficient photoinduced electron transfer from the donor **P131** to the acceptor PCBM, in the blending composite, has been demonstrated by photoinduced absorption and photoluminescence quenching of **P131**. The solar cell device based on **P131**/PCBM (1:1, w/w) showed a $V_{oc}$ of 0.67 V, a $J_{sc}$ of 0.8 mA/cm$^2$, an FF of 0.35, and a PCE of 0.34%. The efficiency has been further improved by up to 1% with a **P131**:PCBM ratio of 1:3. Despite the band gap of **P131** being significantly lower than that of MDMO-PPV, the $V_{oc}$ is decreased by only 0.1 V. Alternatively, **P131** can be utilized as an efficient near-infrared-emitting material in light-emitting diode applications since it shows an emission peak at 800 nm with a turn-on voltage below 4 V.[37]

## 6.13. Other Donor−Acceptor Conjugated Polymers

Diketopyrrolopyrrole-based (DPP) chromophores have been widely used as organic pigments in various applications such as paints and color inks.[307] In terms of planar conjugated bicyclic structures and the electron-withdrawing nature of the polar amide group, the diketopyrrolopyrrole unit can be exploited as a promising acceptor for p-type conjugated polymers. A semiconductor of a conjugated polymer containing the diketopyrrolopyrrole unit has shown ambipolar high electron and hole mobility both close to 0.1 cm$^2$/(V s) in an FET device.[308] Very recently, Janssen and co-workers reported a new conjugated polymer (**P132**) based on alternating electron-rich quaterthiophene and electron-deficient diketopyrrolopyrrole units.[309] The polymer synthesized by the Yamamoto coupling of **247** exhibits an ideal band gap of

**Scheme 68. Synthesis of P124−P126 by Stille Coupling Reactions**

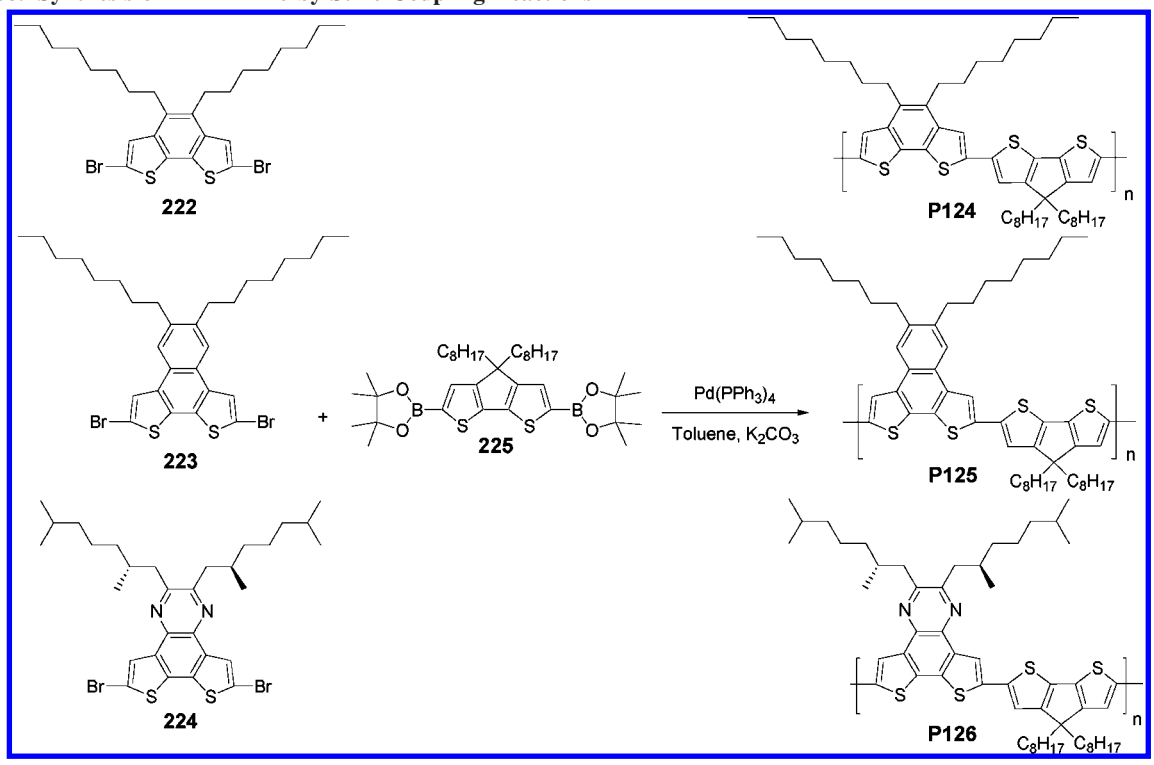


**Scheme 69. Synthetic Route toward Monomer 222**

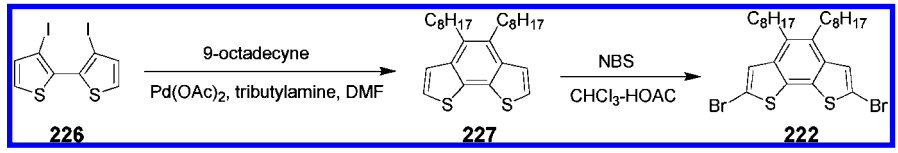


**Scheme 70. Synthetic Route toward Monomer 223**

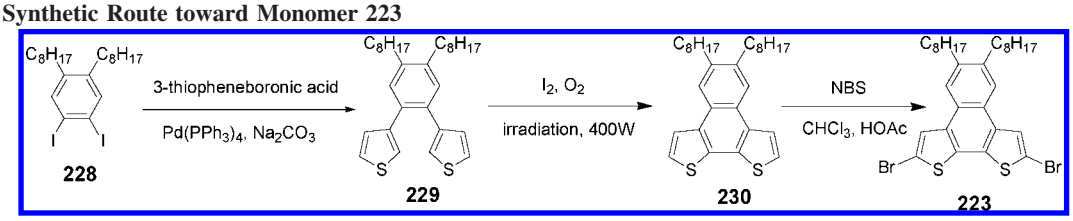


**Scheme 71. Synthetic Route toward Monomer 224**

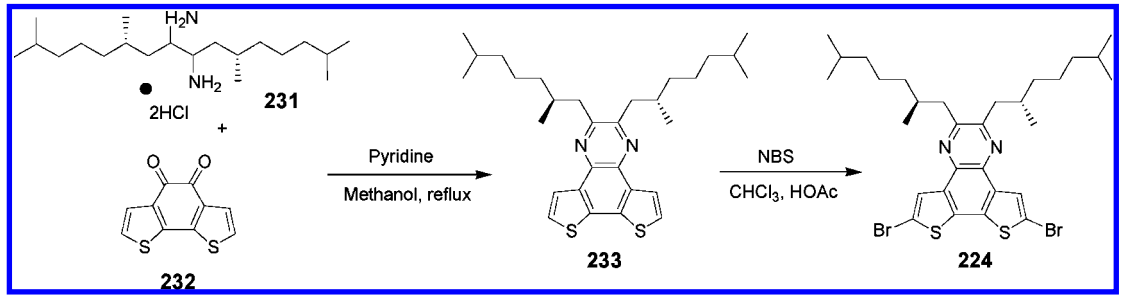


1.4 eV (Scheme 77). The absorption spectrum of **P132** in chloroform shows a $\lambda_{max}$ at 650 nm and an onset at 720 nm. However, an onset significantly red-shifted to 860 nm and vibronic fine structure were observed when **P132** was dissolved in *o*-dichlorobenzene (ODCB), which is indicative of strong intermolecular-interaction-induced semicrystalline aggregation. The film spin-cast from a chloroform solution of **P132**/PCBM showed amorphous polymer morphology due to the fast evaporation of the chloroform, which does not allow for the development of crystallinity. Therefore, the cell in which the active layer was processed from chloroform only exhibited a very low EQE of 0.13 at 680 nm. It was found that by using a chloroform/ODCB mixture (4:1) to process the active layer, a large degree of semicrystallinity could be formed. On the basis of these optimal processing conditions, the best device using **P132**/PCBM (1:2, w/w) gave a PCE of 3.2%. By utilizing $PC_{71}BM$ as the acceptor, the photovoltaic performance was further improved and showed a high PCE of 4.0%, an FF of 0.58, a $V_{oc}$ of 0.61 V, and a $J_{sc}$ of 11.3 mA/cm$^2$.

The synthesis of monomer **247** is shown in Scheme 78. Reaction of 2-thiophenecarbonitrile (**248**) with 0.5 equiv of

**Scheme 72. Synthesis of P127 and P128 by Stille Coupling Reactions**

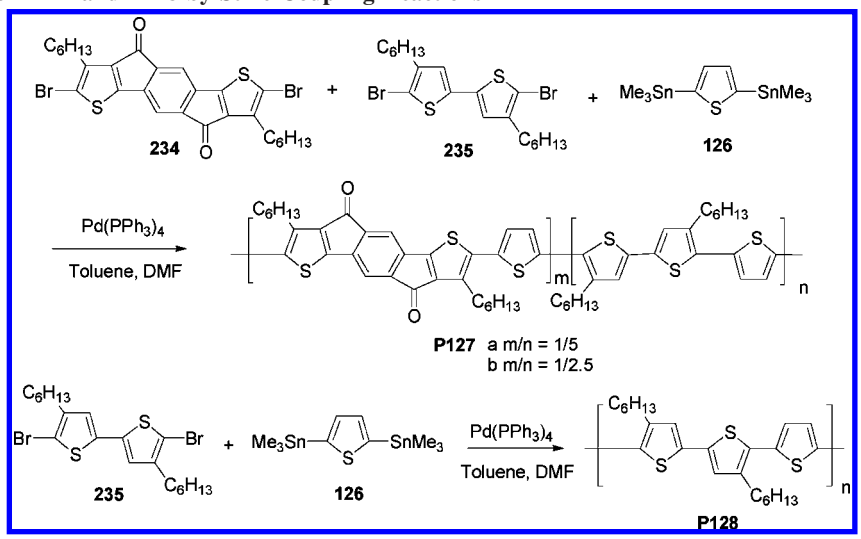


**Scheme 73. Synthetic Route toward Monomer 234**

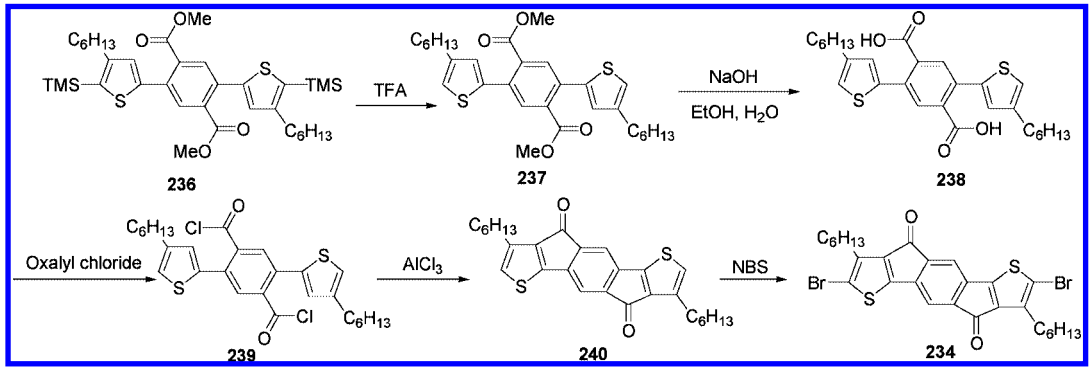


**Scheme 74. Synthesis of P129 and P130 by Stille Coupling Reactions**

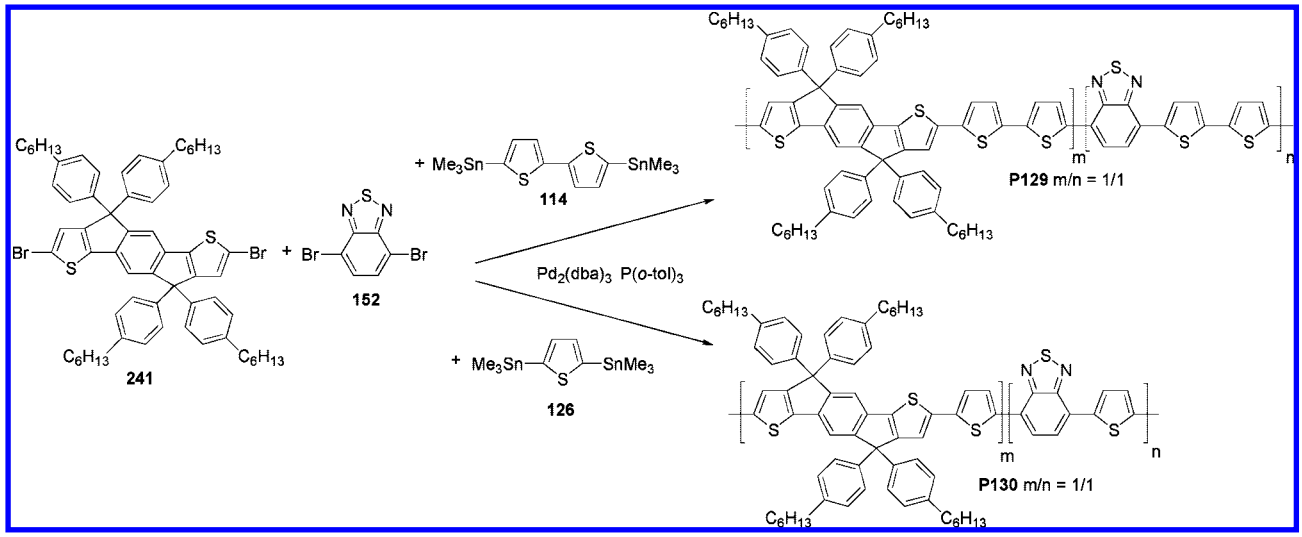


di-*n*-butyl succinate ester in *tert*-amyl alcohol under basic conditions afforded an insoluble dimerization product (**249**) which was allowed to undergo *N*-alkylation with **162** to give compound **250**. Bromination of **250** by NBS, followed by a Stille coupling and sequential bromination, produced the final monomer **247**.

Janssen and co-workers[310,311] reported a series of side chain substituted conjugated polymers (**P133**, **P134**, and **P135**) that consist of alternating electron-rich bithiophene and electron-deficient units including benzothiadiazole, thienopyrazine, and thiadiazoloquinoxaline, respectively. These polymers were synthesized from the corresponding dibromo monomers **254**−**257** via a Yamamoto reductive reaction using $Ni(COD)_2$ as the dehalogenating reagent (Scheme 79). The advantage of Yamamoto coupling is that only a single component of monomer can self-polymerize to afford the alternating D−A polymer with moderate to high molecular weight. These polymers are very soluble in common organic solvents with the help of the branched (2-ethylhexyl)oxy side chains. The absorption edges of **P133**, **P134**, and **P135** in solution are located at 720, 915, and 960 nm, respectively. In the solid state, the band edges are further red-shifted to

**Scheme 75. Synthetic Route toward Monomer 241**

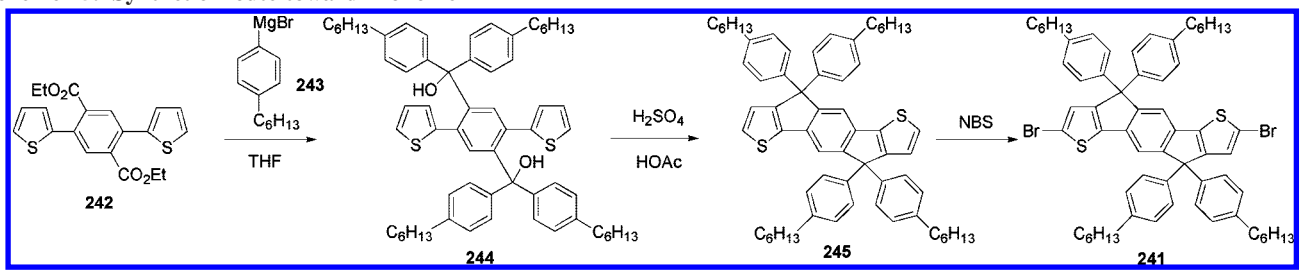


**Scheme 76. Synthesis of P131 by a Stille Coupling Reaction**

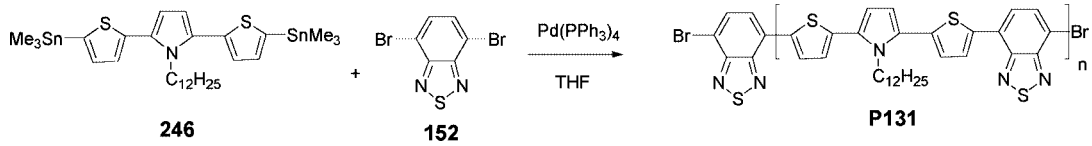


**Scheme 77. Synthesis of P132 by a Yamamoto Coupling Reaction**

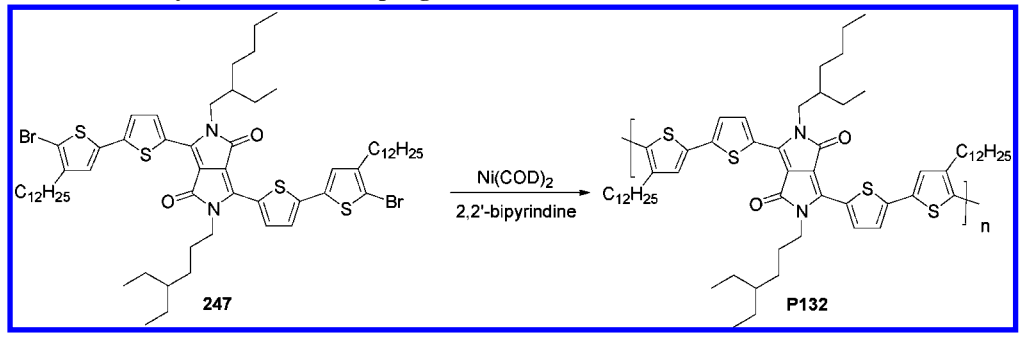


**Scheme 78. Synthetic Route toward Monomer 247**

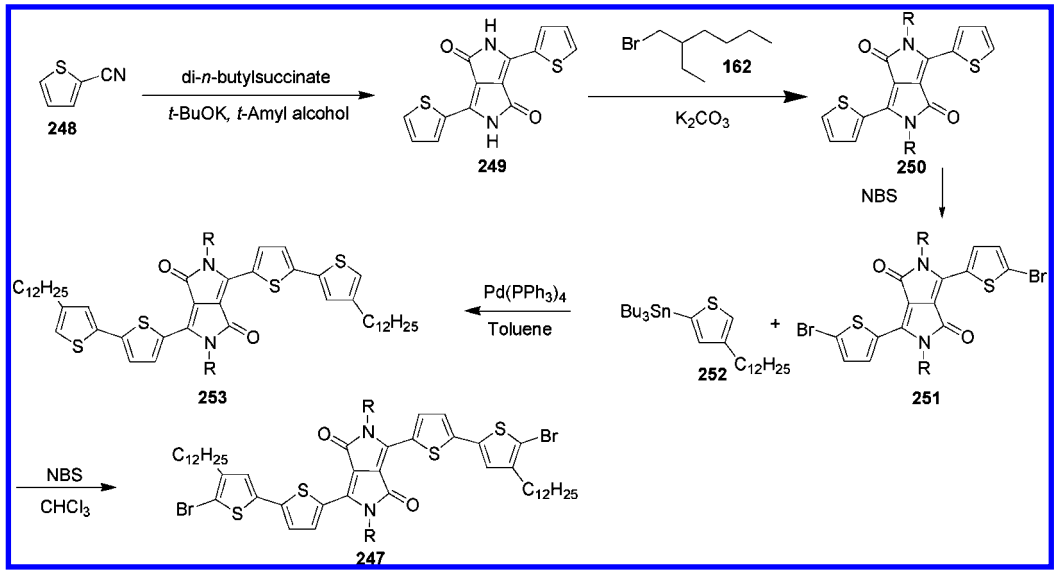


800, 965, and 1034 nm corresponding to optical band gaps of 1.55, 1.28, and 1.20 eV for **P133**, **P134**, and **P135**, respectively. Again, the thienopyrazine unit is more capable of forming quinoid main chains than benzothiadiazole, leading to a much lower band gap. The slightly red-shifted absorption and lower optical band gap of **P135** compared to **P134** indicate improved conjugation caused by a more coplanar structure of the main chain in **P135** due to the absence of bulky substituents, although **P134** has stronger donating alkoxythiophene and **P135** has a stronger acceptor due to the inductive effect of the alkoxy group in the *meta*-position of the phenyl ring. Therefore, in the present case, steric effects dominate over electronic effects. The electron-donating (2-ethylhexyl)oxy side chains attached to the **P134** backbone decrease the oxidation potential by 0.18 V compared to that of **P135**. The PSC device based on **P134**/PCBM (1:4, w/w) gave a $V_{oc}$ of 0.39 V, a $J_{sc}$ of 1.5 mA/cm$^2$, and a PCE of 0.29%. A similar device based on **P135** showed much improved performance with a $V_{oc}$ of 0.56 V, a $J_{sc}$ of 3.1 mA/cm$^2$, and a PCE of 1.1%. This is attributed to its lower HOMO and improved miscibility with PCBM compared to those of **P134**. On the other hand, a **P133**-based device reached a higher $V_{oc}$ of 0.77 V with a PCE of 0.9%. The electron-accepting strength of benzothiadiazole can be further enhanced by fusing another pyrazine ring into the vacant sites of the phenyl ring to form thiadiazoloquinoxa-

**Scheme 79. Synthesis of P133−P136 by Yamamoto Coupling Reactions from 254−257**

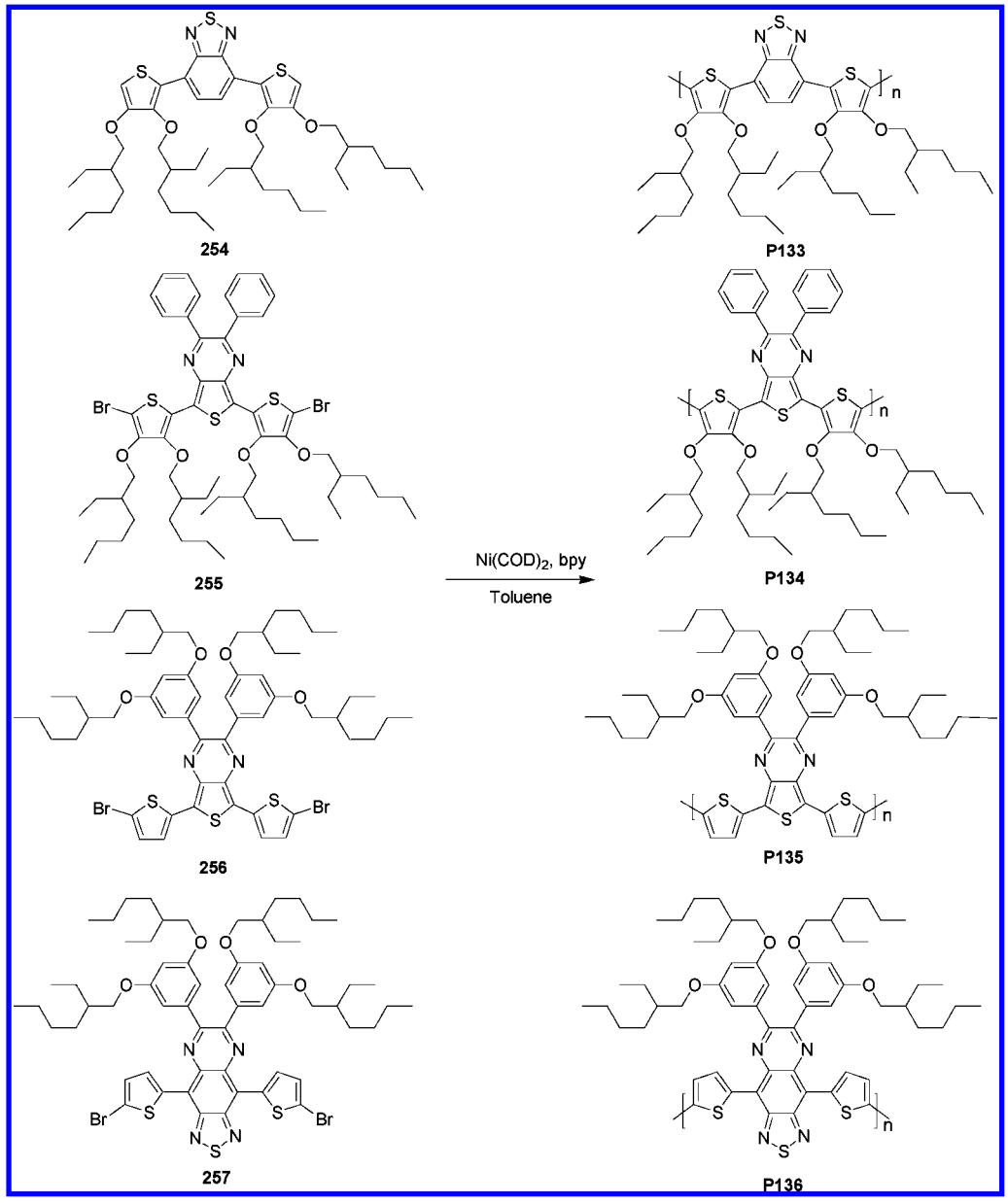


line. By arranging thiadiazoloquinoxaline and bithiophene in an alternating fashion, the polymer **P136** exhibits a strong absorption in the near-infrared region along with an ultrasmall band gap of 0.94 eV in solution.[312] The onsets of the oxidation and reduction waves of **P136** are at −0.09 and −1.06 eV vs $Fc/Fc^+$, respectively, and provide an electrochemical band gap of 0.97 eV. However, the high electron affinity of thiadiazoloquinoxaline also significantly lowers the LUMO, resulting in negligible offset between **P136** and PCBM and thus inefficient photoinduced electron transfer. $PC_{84}BM$ with an electron affinity larger by 0.35 V than PCBM was therefore used to increase the LUMO offset between donor and acceptor.[313] The device based on **P136**/$PC_{84}BM$ (1:4, w/w) showed a photoresponse up to about 1300 nm, which is one of furthest red shifts reported for a polymer BHJ solar cell. However, the overall device efficiency still remains low.

Benzobis(thiadiazole), derived from benzothiadiazole fused with another thiadiazole ring, is an extremely electron-deficient unit due to its high tendency for the formation of quinoid structures and the hypervalent sulfur atom (Chart 20).[314,315] A polymer (**P137**) containing quaterthiophene as the donor and benzobis(thiadiazole) as the acceptor was synthesized by Stille coupling (Scheme 80).[316] An analogous polymer (**P138**) using benzothiadiazole as the acceptor was also prepared for comparison. From the absorption spectra, **P137** shows an extremely low band gap of 0.67 eV, which is 1 eV lower than 1.65 eV for **P138** and even lower than that of polyisothianaphthene (1 eV). This result further demonstrates the exceptional electron-accepting power of the benzobis(thiadiazole) subunit. Solar cell devices with a large area (3 $cm^2$) based on a **P138**/PCBM (1:2, w/w) blend gave a photovoltaic response with a PCE of 0.62%.[317] However,

**Chart 20. Resonance Structure of Benzobis(thiadiazole) (258)**

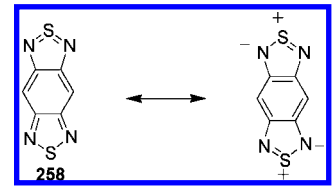

**Scheme 80. Synthesis of Benzobis(thiadiazole)-Containing P137 and P138 by a Stille Coupling Reaction**

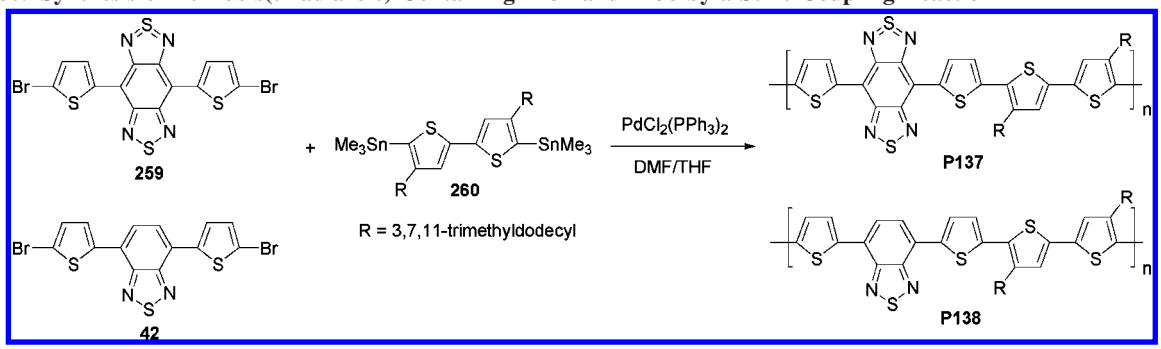


**Scheme 81. Synthesis of PYM-Containing P139 and P140 by Stille Coupling Reactions**

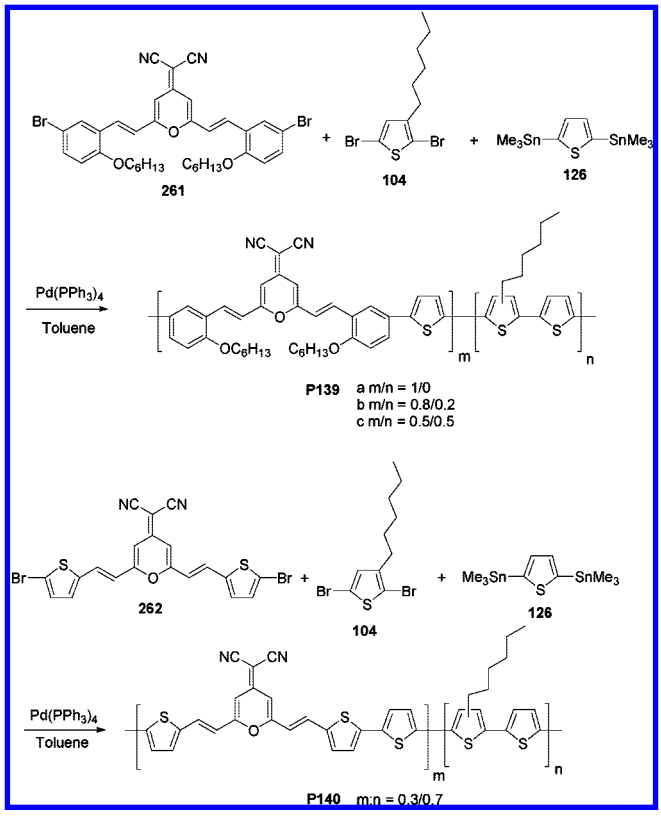


the devices produced with **P137** showed very low $V_{oc}$ and $J_{sc}$ values, which is ascribed to the mismatch of LUMO energy levels between **P137** and PCBM. This result again emphasizes the importance of controlling the band gap and corresponding energy levels of the polymer with respect to PCBM when the band gap starts to decrease.

2-Pyran-4-ylidenemalononitrile (PYM) is known to have strong electron-withdrawing abilities and has been intensively used as the electron acceptor part of red-emitting and nonlinear optical materials.[318,319] A series of copolymers utilizing the PYM unit as the electron acceptor were reported by Dai and co-workers.[320] Different amounts of PYM units were copolymerized with thiophene units to yield the D−A-type copolymers **P139** and **P140** (Scheme 81). It was found that the properties of the polymer can be controlled by varying the PYM content ratio and the thiophene units. Increasing the thiophenes from **P139a** through **P139b** to **P139c** results in red-shifted absorption spectra, gradually reduced band gaps (2.33, 2.21, and 1.99 eV), higher HOMO levels (−5.17, −5.10, and −5.01 eV), and relatively unchanged LUMO levels. As expected, the increasing trend in $V_{oc}$ values was observed on going from **P139c** to **P139b** to **P139a** in accordance with the HOMO levels. The solar cells using a polymer/PCBM (1:1, w/w) blend achieved PCEs of 0.08%, 0.2%, and 0.6% for **P139a**, **P139b**, and **P139c**, respectively. Because the thiophene unit and PYM are connected through the *meta*-position of a phenyl ring, the effective conjugation of the main chain is disrupted. Therefore, increasing the content of thiophene units leads to enhanced charge transport and hence improved $J_{sc}$ values and PCEs. When the phenyl group attached at the PYM moiety was replaced by a thiophene ring, **P140** showed an enhanced absorption and a higher PCE of 0.9%.

## 6.14. Poly(thienylvinylene)s (PTVs)

Poly(thienylvinylene)s are another class of polythiophene-based conjugated polymers. These polymers display high nonlinear optical responses, moderate charge mobilities, and good electroluminescent properties. By inserting a vinylene unit between every thiophene unit to planarize the main chain and reduce aromaticity, PTVs exhibit more effective conjugation and lower band gaps than polythiophenes. Much attention and effort has been paid to evaluate their potential for organic solar cell applications. Like the synthesis of PPV, there are two synthetic approaches used in the preparation of PTVs. One approach involves a straightforward polymerization reaction in a single step using the appropriate monomers to generate the conjugated polymer. Two typical transition-metal-catalyzed reactions can be used to synthesize PTV directly. A Stille coupling of 2,5-dibromo-3-dodecylthiophene (**263**) and 1,2-bis(tributylstannyl)ethylene (**214**) is expected to yield regiorandom PTV (Scheme 82). However, the resulting polymer with a regioregularity greater than 90% was found.[321] This is because the oxidative addition of the palladium catalyst takes place selectively at the less sterically hindered 5-position of thiophene, leading to the formation of the intermediate compound **264**, which continues to polymerize to afford regioregular **P141**.

Interestingly, the Heck reaction of the monomer **265** designed to prepare regioregular PTV turned out to form the regioirregular polymer **P142** due to 15% α-arylation occurring during the reaction (Scheme 82). The regioregular **P141** made by Stille coupling has a lower optical band gap, 1.6 eV, than regiorandom **P142** made by the Heck coupling where the band gap is 1.8 eV. When **P141** was blended with PCBM, an external quantum efficiency with a maximum response at 580 nm was detected. This is approximately 100 nm red-shifted compared to that of the device made from the MDMO-PPV/PCBM blend. The PSC device based on regioregular **P141**/PCBM (1:10, w/w) showed a moderate PCE of 0.24%.[322]

**Scheme 82. Synthesis of Regioregular P141 by a Stille Coupling Reaction and P142 with Defects by a Heck Coupling Reaction**

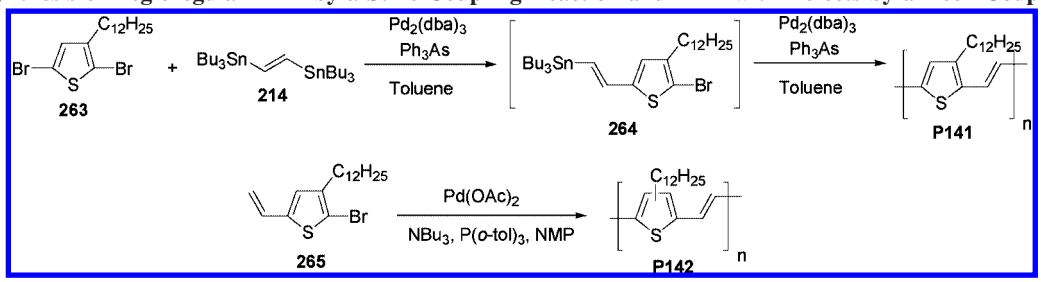


**Scheme 83. Synthesis of P143 with a Conjugated Side Chain by a Stille Coupling Reaction**

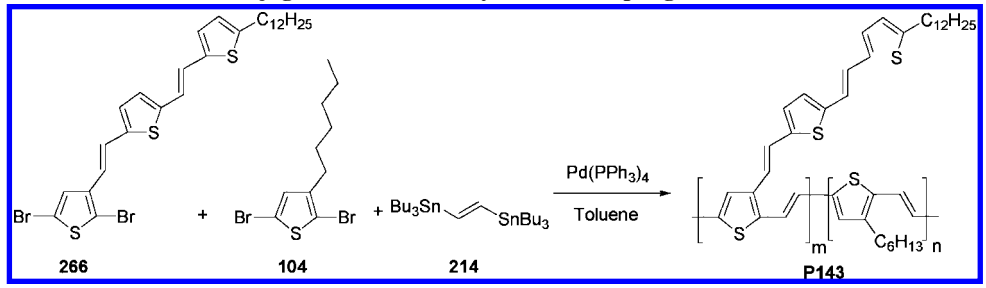


**Scheme 84. Synthesis of Poly(thienylenevinylene) P144**

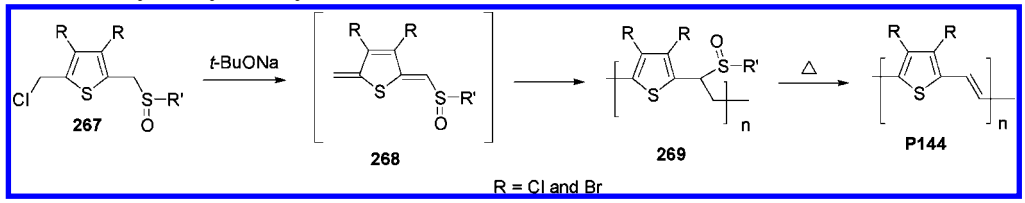


**Scheme 85. Synthesis of Poly(thienylenevinylene) P145**

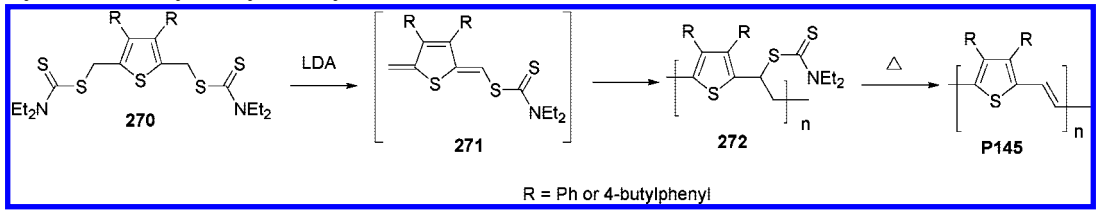


The strategy of using branched side chains conjugated to the main chain of polythiophene has also been applied to poly(thienylenevinylene)s. 2,5-Dibromothiophene **266** with a bis(thienylenevinylene) side chain was copolymerized with 2,5-dibromo-3-hexylthiophene (**104**) and 1,2-bis(tributylstannyl)ethylene (**214**) by a Stille coupling to form the bis(thienylenevinylene)-branched poly(thienylenevinylene) **P143** (Scheme 83).[323] With an *m*/*n* ratio of 0.35, this polymer shows a narrower band gap (1.57 eV) than poly((3-hexylthienylene)vinylene) (P3HTV) (1.62 eV) and a strong broad absorption band covering the whole visible region from 380 to 780 nm. The PCE of the PSC based on **P143**/PCBM (1:1, w/w) reached 0.32%, which is higher than 0.21% for P3HTV.

Another method is to prepare nonconjugated polymer precursors, which produce conjugated polymers in situ upon thermal or chemical treatment. This indirect approach is commonly applied to the synthesis of unsubstituted PTV to overcome the problematic processing resulting from the poor solubility of PTV. The sulfinyl route was developed by Vanderzande and co-workers to prepare the 3,4-dichloro- and 3,4-dibromo-PTV derivatives **P144** (Scheme 84).[324] In the presence of sodium *tert*-butoxide as the base, the sulfinyl monomer **267** was polymerized via the thiophene analogues of the *p*-quinodimethane intermediate **268** to obtain the polymer precursor **269**, which can readily undergo thermal elimination of the sulfinyl group to produce the 3,4-dihalo-substituted **P144** with a high molecular weight of >50000. Its optical band gap was estimated to be ca. 1.55 eV. The active layer of a solar cell device was made by spin-casting the polymer precursor **269**/PCBM (1:4, w/w) solution on top of the PEDOT substrate followed by thermally induced conversion at 70 °C to obtain the **P144** and PCBM composite. After postproduction thermal annealing, the device based on poly((3,4-dichlorothienylene)vinylene) gave a PCE of 0.18%. Following a similar mechanism, dithiocarbamate thiophene derivative **270** has also been developed to serve as a facile precursor for the synthesis of poly((3,4-diphenyl-2,5-thienylene)vinylene) (**P145**), which has enhanced thermal stability and a lower band gap of 1.7−1.8 eV (Scheme 85).[325,326]

## 7. Miscellaneous Conjugated Polymers

### 7.1. Poly(aryleneethynylene)s

Poly(aryleneethynylene)s are a class of conjugated polymers where aromatic or heteroaromatic groups are linked by acetylene units. The internal triplet bonds in the polymer main chain provide extended conjugation and rigidified

**Scheme 86. Synthesis of P146 and P147 by a Sonogashira Coupling Reaction**

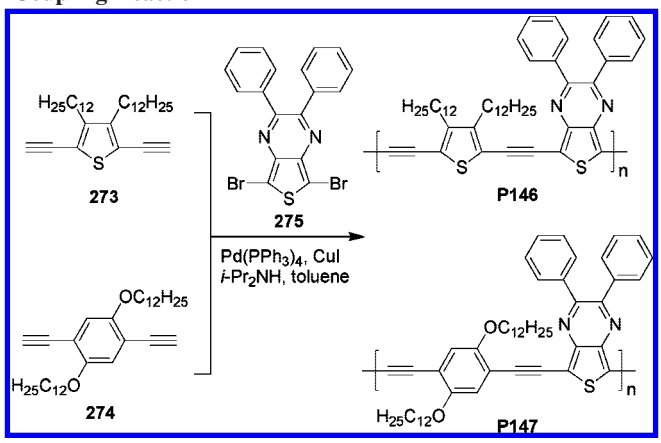


backbones for pronounced interchain interactions. To design low band gap polymers for solar cell applications, donor and acceptor moieties can be regioregularly separated by conjugated ethyne bridges. Scheme 86 shows the synthesis of two poly(heteroaryleneethynylene) derivatives containing thieno[3,4-*b*]pyrazine as the acceptor and thiophene (**P146**) or dialkoxyphenylene (**P147**) as the donor, respectively, via the palladium-catalyzed Sonogashira coupling reaction.[327] Both materials have wide absorption ranges from 390 to 800 nm and low optical band gaps of ca. 1.57 eV due to donor−acceptor push−pull effects through the conjugated triple bonds. A device based on **P146**:PCBM (1:1, w/w) showed a $J_{sc}$ of 10.72 mA/cm$^2$, a $V_{oc}$ of 0.67 V, and a PCE value of 2.37%. When using **P147**:PCBM (1:2, w/w) as the active layer, the device exhibited a $J_{sc}$ of 4.45 mA/cm$^2$, a $V_{oc}$ of 0.7 V, and a PCE value of 1.36%.

Scheme 87 shows the synthesis of a new poly(aryleneethynylene) copolymer (**P148**) grafted with tetrathiafulvalene (TTF) units via a Sonogashira coupling reaction between **278** and **279**.[328] This polymer has a conjugated main chain serving as the electron-deficient acceptor with an electron-rich TTF side chain as the electron donor, inducing intramolecular charge transfer between the TTF side chains and the benzothiadiazole-containing main chain. X-ray diffraction analysis suggests that strong self-assemby by $\pi-\pi$ stacking through interdigitation due to the coplanarity of the backbone leads to an optical band gap of 1.78 eV from its absorption edge. A polymer BHJ solar cell with the photoactive layer of **P148**:$C_{60}$ (2:1, w/w) showed a $J_{sc}$ of 2.47 mA/cm$^2$, a $V_{oc}$ of 0.42 V, an FF of 24.2%, and a PCE value of 0.25%.

## 7.2. Triarylamine-and Phenothiazine-Based Polymers

Triarylamine-based small molecules or polymers have been extensively utilized as hole-transporting materials for light-emitting diode applications due to their high hole mobility. It is envisaged that the introduction of electron-donating triarylamine segments into the polymer main chain in conjunction with an electron-deficient unit would form an alternating donor−acceptor arrangement. This should potentially afford a polymer with a lower band gap and improved intrinsic hole mobility. With this in mind, **P149**, which contains a triarylamine moiety in the main chain, and its PPV derivative **P150** were synthesized by a Heck coupling reaction (Scheme 88).[329] The optical band gap of **P150** is 1.76 eV, which is lower than that of **P149** with 1.86 eV. This can be rationalized by the fact that **P150** is a fully conjugated polymer whereas the conjugated length of **P149** is disrupted by the amino groups. In spite of a shorter conjugation length, **P149** still has a relatively low band gap due to efficient intramolecular charge transfer. The hole mobility, measured by a hole-only device based on the space charge limited current (SCLC), is determined to be $3.07 \times 10^{-5}$ and $4.58 \times 10^{-5}$ cm$^2$/(V s) for **P150** and **P149**, respectively. This indicates that incorporation of the triarylamine groups indeed improves the hole mobility. The high mobility for **P149** is translated to a higher $J_{sc}$ of 2.85 mA/cm$^2$ and a higher PCE of 0.52% compared to those of **P150** with a $J_{sc}$ of 2.16 mA/cm$^2$ and a PCE of 0.26%. It is also noteworthy that the nonplanar 3-dimensional structure of the triarylamine moiety makes the polymer more amorphous, which may exert a detrimental influence on the interchain charge carrier transport.

Scheme 89 depicts the Suzuki coupling synthesis of **P151** containing tricyclic phenothiazine units from **40** and **286**.[330] The phenothiazine moiety with its electron-rich sulfur and a nitrogen heteroatom incorporated into the polyfluorene skeleton can potentially serve as the donor segment in conjugated polymers and improve their hole-transporting abilities. In addition, attachment of two (phenylcyano)vinyl groups to the phenothiazine exerts an electron-withdrawing influence which reduces the band gap. The HOMO and LUMO of the resulting polymer **P151** are −5.26 and −3.12 eV, respectively. The band gap is 2.14 eV. This polymer's red-emitting luminescence in a thin film can be completely quenched in the presence of PCBM, implying efficient exciton dissociation. The best photovoltaic performance was obtained from a device which used **P151**:PCBM (1:3 in wt%) as the active layer; it showed a $J_{sc}$ of 2.38 mA/cm$^2$, a $V_{oc}$ of 0.78 V, and a PCE value of 0.53%.

Two other phenothiazine-based copolymers, comprising bithiophene (**P152**) and thieno[3,2-*b*]thiophene (**P153**) moieties, were also synthesized by Suzuki coupling reactions (Scheme 90).[331] The optical band gaps were calculated as 2.47 eV for **P152** and 2.54 eV for **P153**. A device based on **P152**/PCBM (1:1, w/w) demonstrated the best PCE of 0.24%. This is in contrast to the **P153**/PCBM device, which only showed a PCE of 0.1% albeit with a high $V_{oc}$ of 0.82 V. Because the absorption of these polymers only covers the 300−500 nm range, the relatively low device efficiencies are mainly due to the lack of sufficient absorption in the red and near-infrared regions.

## 7.3. Fluorenone-Based Polymers

Fluorenone-containing conjugated polymers have also attracted much interest for solar cell applications. It has been shown that the incorporation of rigid and planar fluorenone subunits into the conjugated polymer not only enhances the intermolecular self-organized packing, but also effectively prevents chain folding. The latter is one of the most likely limiting factors for efficient charge transport.[332] Furthermore, due to the electron-withdrawing effects of the ketone group, the fluorenone moiety exhibits a wider absorption band covering a large part of the visible spectrum. This effect can be more pronounced when fluorenone units are conjugated with electron-rich units in the polymer. Two regioregular copolymers (**P154**[333] and **P155**[334]) were synthesized by oxidative polymerization from the monomers **290** and **291**, respectively (Scheme 91). **P154** contains alternating fluorenone and tetrathienylenedivinylene

**Scheme 87. Synthesis of Poly(aryleneethynylene) Copolymer P148**

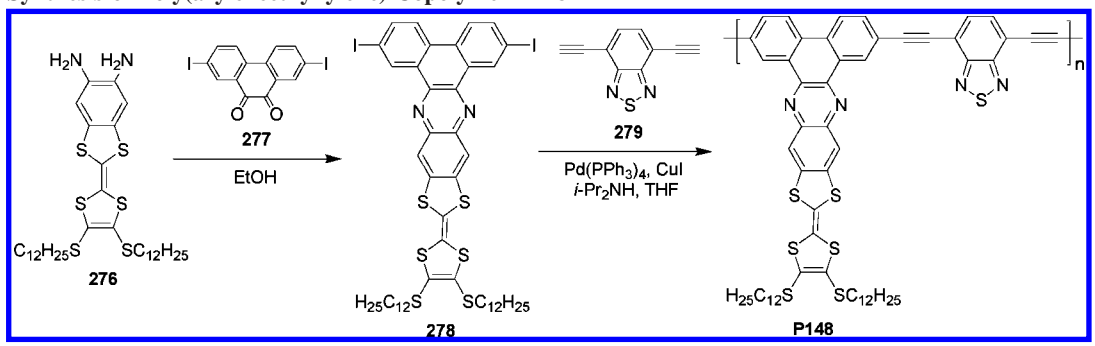


**Scheme 88. Synthesis of Triphenylamine-Containing Copolymer P149 and Its PPV Analogue P150**

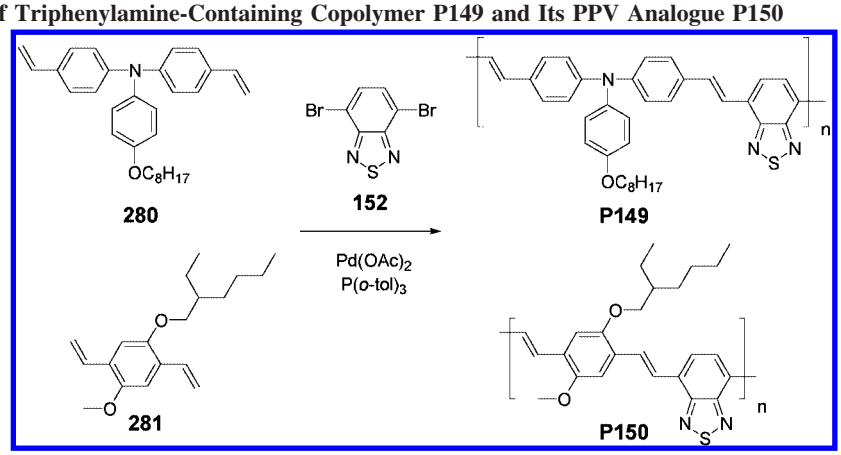


**Scheme 89. Synthetic Route toward Phenothiazine-Containing Copolymer P151**

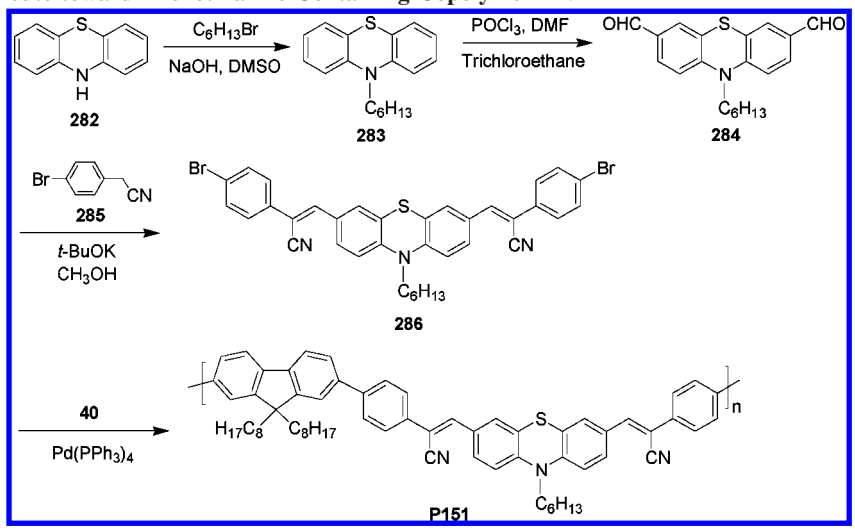


**Scheme 90. Synthetic Route toward Phenothiazine-Containing P152 and P153**

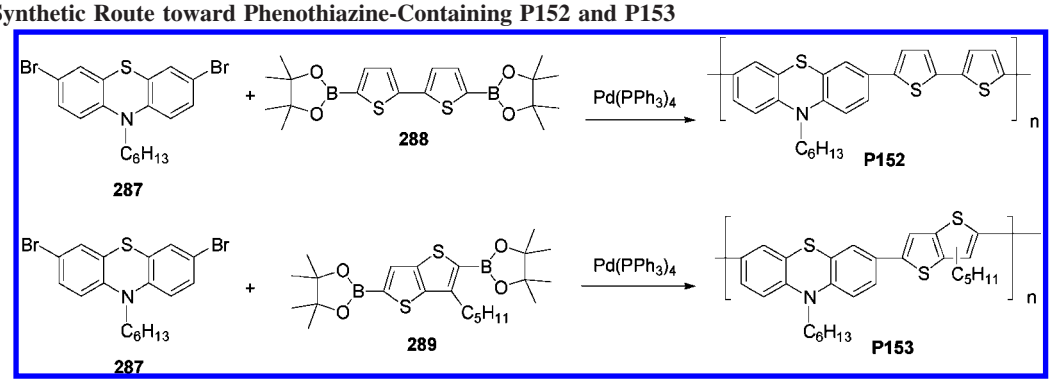


units, while **P155** consists of alternating fluorenone and tetrathiophene units. Compared to the solution state, significant bathochromic shifts and broadened spectra were observed for both **P154** and **P155** in the solid state. This is attributed to ordered interchain aggregation. The optical band gaps for **P154** and **P155** are 1.52 and 2.0 eV, respectively.

**Scheme 91. Synthetic Route toward Fluorenone-Containing P154 and P155**

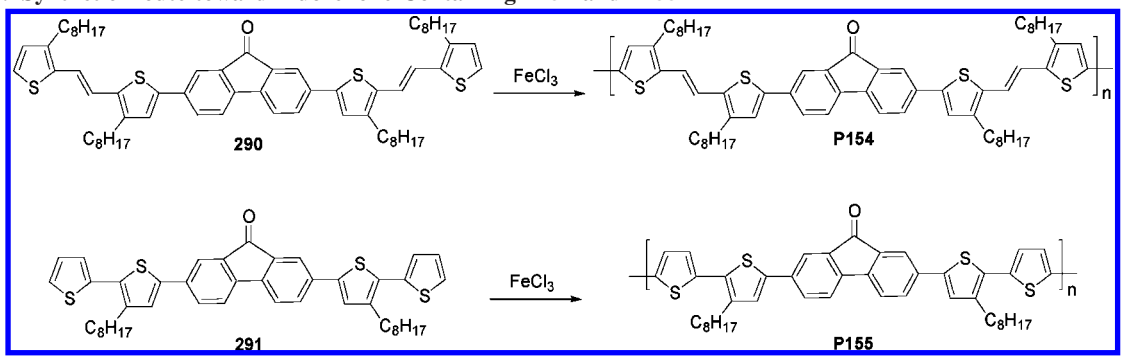


**Scheme 92. Synthesis of Porphyrin-Containing P156 by a Sonogashira Coupling Reaction**

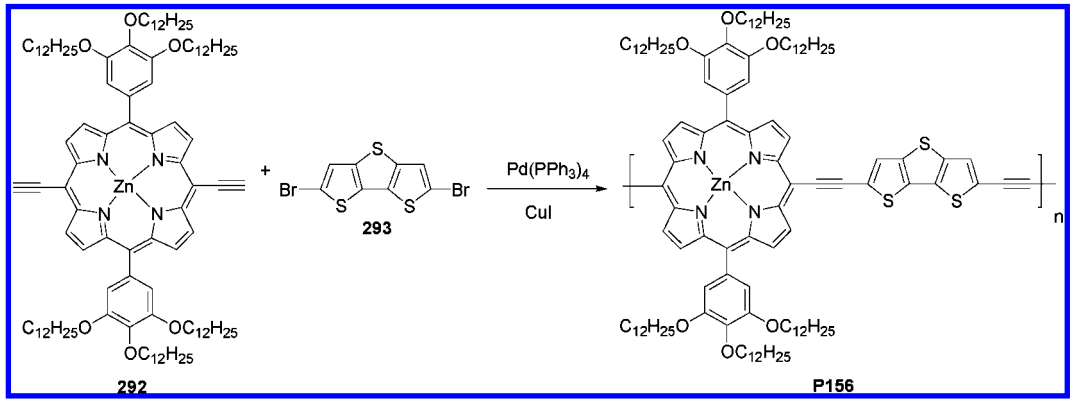


The best photovoltaic performance showed a PCE of 1.1% and 1.45% for the **P154**/PCBM- and **P155**/PCBM-based devices, respectively.

## 7.4. Porphyrin-Based Polymers

Porphyrin derivatives have attracted considerable attention as useful materials for organic photonic and electronic applications due to their large $\pi$-conjugation systems as well as their good photochemical and thermal stabilities. The involvement of porphyrin derivatives in many biological processes such as light harvesting and photoinduced electron transfer in the photosynthesis of plants strongly suggests that porphyrin molecules could serve as potential photosensitizers in dye-sensitized solar cells[335,336] as well as electron donors in BHJ solar cell application. Although organic solar cells utilizing porphyrin-containing polymers as active layers have been reported, only low power conversion efficiencies were obtained. This is presumably due to the limited light absorption of porphyrins insofar that the absorption spectra of porphyrin units exhibit narrow, strong Soret bands (410−430 nm) and weak Q-bands (530−540 nm) with nothing in between.[337] A soluble porphyrin−dithienothiophene copolymer (**P156**) was synthesized by a Sonogashira coupling reaction of **292** and **293** (Scheme 92).[338] Introduction of diethynyldithienothiophene into the porphyrin main chain is expected to reduce steric hindrance, extend conjugation, enhance absorption, and improve the charge-transport property. However, to ensure sufficient solubility of the porphyrin-containing polymer for solution processing, a large aliphatic chain insulating portion must be incorporated into the porphyrin unit, and this may have a negative effect on the charge transport. Although a rather small PCE of 0.3% was obtained for the PSC using **P156**/PCBM (1:3, w/w) as the active layer, this value is among the highest obtained so far for devices based on porphyrin-containing polymers.

**Scheme 93. Synthesis of P157**

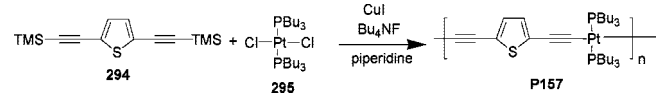


## 7.5. Platinum Metallopolyyne-Based Polymers

In addition to general strategies using organic donor and acceptor segments in the main chain, platinum alkyne organometallic units have attracted a great deal of interest. They can be incorporated into the conjugated polymers as a result of the fact that the d-orbital of the Pt can overlap with the p-orbital of the alkyne unit, leading to an enhancement in $\pi$-electron conjugation and delocalization along the polymer chain.[339] Moreover, due to strong spin−orbital coupling, efficient intersystem crossing in such organometallic species facilitates the formation of triplet excited states which have longer lifetimes and thus allow extended exciton diffusion lengths. Electron transfer from this triplet-spin donor to the acceptor produces a geminate ion−radical pair which also retains the triplet character, so that charge recombination is spin-forbidden and the probability of efficient charge separation is enhanced compared with those of the system involving only singlet exciton electron transfer. On the basis of these considerations, Schanze and Reynolds reported a polymer (**P157**) containing alternate platinum acetylide and thiophene units.[340] The trimethylsilyl protecting groups in **294** were in situ cleaved by tetrabutylammonium fluoride, and the intermediate was coupled with $Pt(PBu_3)_2Cl_2$ (**295**) in the presence of CuI to yield **P157** (Scheme 93).[341] The phosphorescence of this polymer has a maximum at 609 nm and was quenched upon the addition of PCBM. This is indicative of efficient electron transfer via the triplet excited state of the organometallic polymer. A photovoltaic device made from the 1:4 (w/w) blend of **P157** and PCBM gave a PCE of 0.27% with a $V_{oc}$ of 0.6−0.7 V. Due to the high

**Scheme 94. Synthesis of P158−P161**

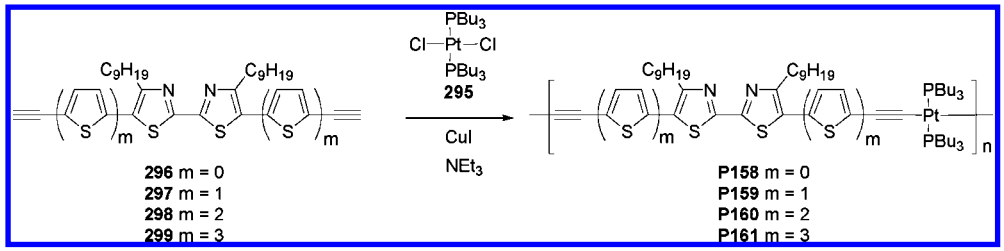


**Scheme 95. Synthesis of P162**

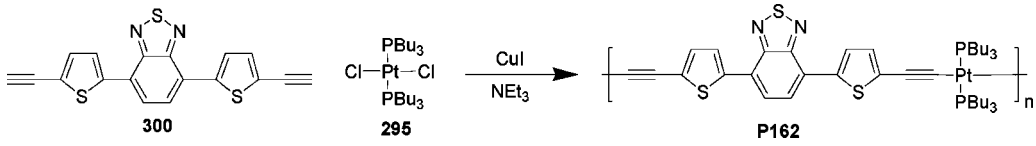


**Chart 21. Chemical Structures of P163−P166**

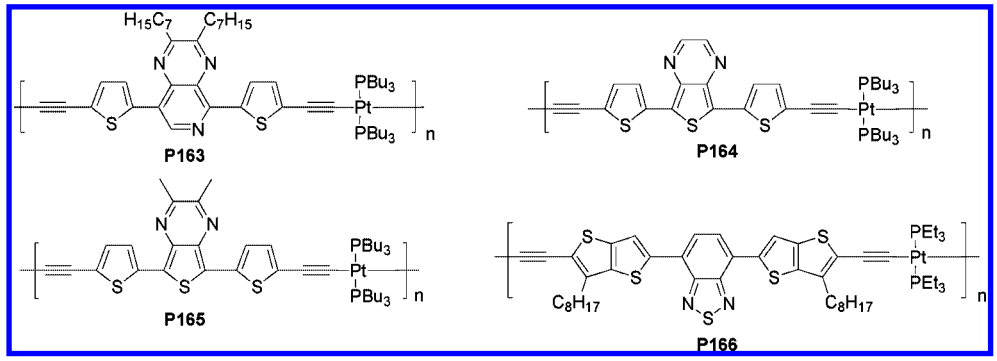


band gap of **P157**, the low efficiency is mainly due to its low coverage of the solar spectrum.

A series of platinum diacetylene-based polymers (**P158**−**P161**) containing electron-accepting bithiazole rings with different numbers of electron-donating thiophene units have been synthesized (Scheme 94) from their corresponding monomers **296**−**299**.[342] As the number of thiophene units increases, the band gap of the polymer decreases from 2.4 to 2.0 eV, due to the extended $\pi$-electron delocalization through D−A intramolecular charge transfer. It was also found from emission lifetime measurements that when the content of the heteroaryl units increases to dilute the organometallic influence, these low band gap polymers only exhibit singlet emission instead of triplet-excited-state phosphorescence. As a result, unlike Pt−monothiophene **P157** blends where charge separation occurs via the triplet state of the polymer, it is a charge-transfer excited state which is responsible for the photoinduced charge separation. The photovoltaic performance based on a polymer/PCBM (1:4, w/w) showed an increasing trend for PCE values from 0.21% to 0.76% to 2.14% to 2.5% for **P158** to **P161**, respectively. This is due to the increasing optical absorbance and hole mobility.

Wong and co-workers reported a thermally stable and air-stable compound (**P162**) which contains a platinum metallopolyyne as the donor and BT units as the acceptor to afford a narrow band gap of 1.85 eV (Scheme 95).[343] In a similar fashion, the polymer **P162** was synthesized simply by reacting a platinum dichloride (**295**) with a diacetylene moiety (**300**) under Sonogashira-type dehydrohalogenation conditions in the presence of a catalytic amount of copper iodide. Due to its lower HOMO level of −5.37 eV, the $V_{oc}$ obtained for the best cell was 0.82 eV with a very high $J_{sc}$ of 15.43 mA/cm$^2$. This resulted in a high PCE of 4.93% based on a 1:4 (w/w) blend of polymer/PCBM in the active layer. One noteworthy feature is that such a high performance was obtained without thermal annealing, which is needed to achieve a high efficiency for the P3HT−fullerene composite. Right after this report, Janssen et al. commented on the occurrence of such a high efficiency for **P162** as reported by Wong et al. and created a controversy.[344] It was argued that, on the basis of the optical data and the 70 nm film thickness of the active layer as reported in the paper, the highest PCE should not exceed 2.2%.

The potential of metalated conjugated polymers for use in PSCs continues to generate research where various platinum polyyne-based conjugated polymers with different donor−acceptor arrangements are used.[345−348] Very recently, Jenekhe and co-workers further synthesized a series of platinum diethylene-containing polymers in combination with different electron-accepting units. These included pyrido[3,4-*b*]pyrazine and thieno[3,4-*b*]pyrazine units (Chart 21).[345] In addition, a polymer exactly the same as **P162** using benzothiadiazole as the acceptor was also prepared. The device based on **P162** reached a PCE of 1.4% when blended with PCBM and a PCE of 2.41% when blended with $PC_{71}BM$. This value is more consistent with the calculated 2.2% than with the prior experimental data. Moreover, BHJ solar cells based on other polymers blended with $PC_{71}BM$ (1:4, w/w) gave lower PCE values, 0.68%, 0.36%, and 0.32% for **P163**, **P164**, and **P165**, respectively.

Using a similar strategy, Jen et al. made a Pt-metalated conjugated polymer (**P166**) using thieno[3,2-*b*]thiophene-connected benzothiadiazole as the core (Chart 21).[348] Despite this polymer being highly amorphous, a high hole mobility of $1\times 10^{-2}$ cm$^2$/(V s) (in the field-effect transistor) was achieved due to the more rigid structure enhancing the electron coupling between the donor and acceptor units along

**Scheme 96. Synthesis of a P167-Derivatized Double-Cable Fullerene Using a Sonogashira Coupling Reaction**

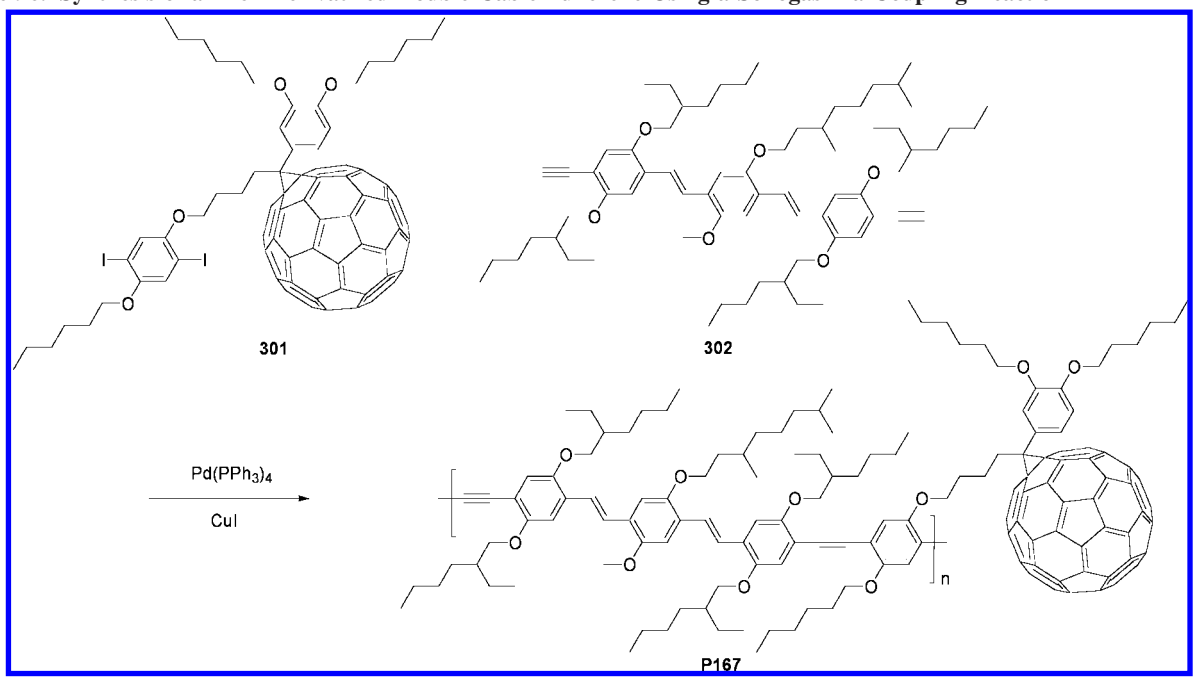


**Scheme 97. Synthesis of a P169-Derivatized Double-Cable Fullerene by Postfunctionalization**

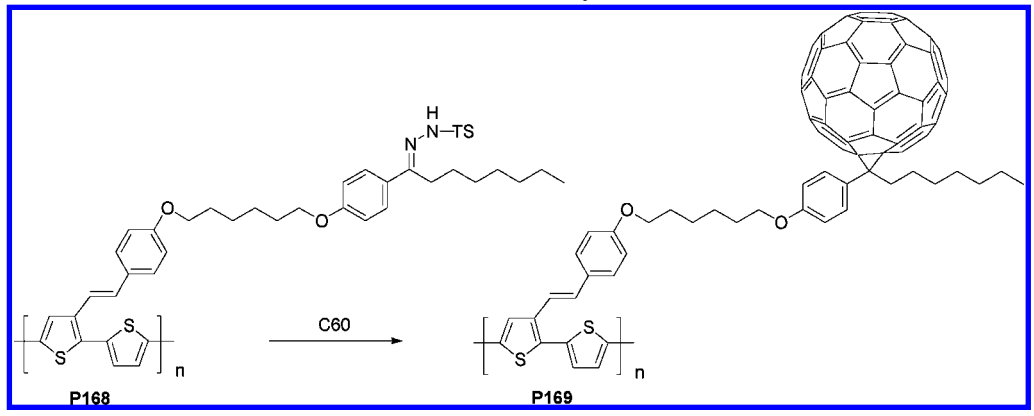


the polymer backbone. The best performance of solar cell devices based on **P166** and $PC_{71}BM$ (1:4, w/w) resulted in a high PCE of 4.3% without the need of post thermal annealing.

## 7.6. Double-Cable Fullerene-Derivatized Polymers

The most critical challenge in bulk heterojunction solar cells is that tremendous work is required to fine-tune the complicated physical interactions between electron donor–donor, acceptor−acceptor, and donor−acceptor units to obtain an optimal morphology with a well-defined nanostructure. Different combinations of polymer−fullerene blends led to completely different optimal conditions. Excessive thermal annealing can eventually lead to undesirable severe phase segregation. One promising way to solve this problem is to covalently attach fullerene to a conjugated polymer to form a so-called "double-cable fullerene-derivatized polymer", which can be regarded as a molecular heterojunction.[349−353] Such polymer structures ensure that donor and acceptor units are held in intimate proximity to facilitate exciton dissociation and furnish homogeneous distribution to prevent potential phase separation. After photoinduced electron transfer, the double cable creates two ideal channels for both hole transportation in the conjugated main chain and electron hopping between neighboring attached fullerenes. The first double-cable polymer (**P167**) used in PSCs was reported by Janssen et al. and synthesized by a Sonogashira reaction of diiodobenzene **301** having a pendent methanofullerene and oligo(*p*-phenylenevinylene)-diacetylene **302** (Scheme 96).[352] Photoluminescence quenching was observed in a thin film of **P167**, which indicates efficient photoinduced electron transfer. Further evidence of efficient electron transfer is found in the photoinduced absorption spectra, which show a characteristic band at 1.2 eV due to the methanofullerene radical anion and two distinctive bands at 0.62 and 1.53 eV assigned to cation radicals of the conjugated polymer. A PSC based on a double-cable polymer as the single component in the active layer (no additional fullerene derivative blended) exhibited a $J_{sc}$ of 0.42 mA/cm$^2$, a $V_{oc}$ of 0.83 V, and an FF of 0.29. The low efficiency of the device based on this double-cable polymer possibly results from the low content of fullerene relative to conjugated polymer, which limits the electron transportation. **P169,** another double-cable polymer, was synthesized by postfunctionalization of a thiophene-based conjugated polymer (**P168**) with $C_{60}$ (Scheme 97).[353] The phenylenevinylene side chain is used to increase the conjugation of the polymer. The role of the long aliphatic spacer

**Scheme 98. Synthesis of n-Type Copolymer P170 by Stille Coupling Reactions**

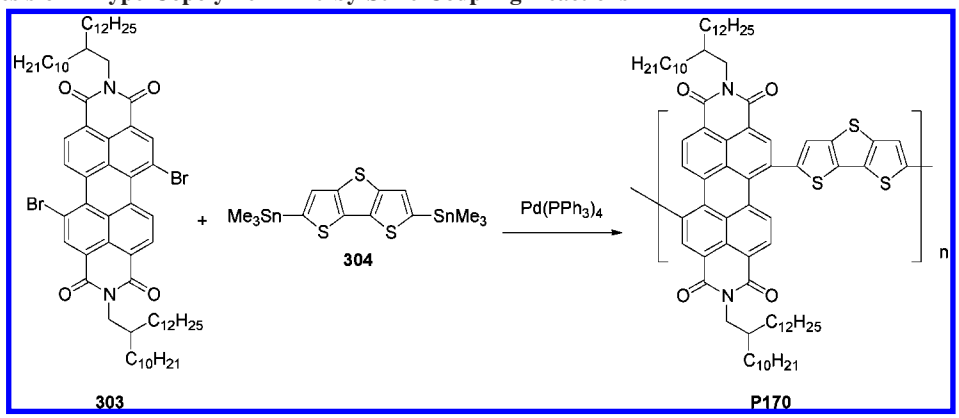


**Scheme 99. Synthetic Route toward Monomers 293 and 304**

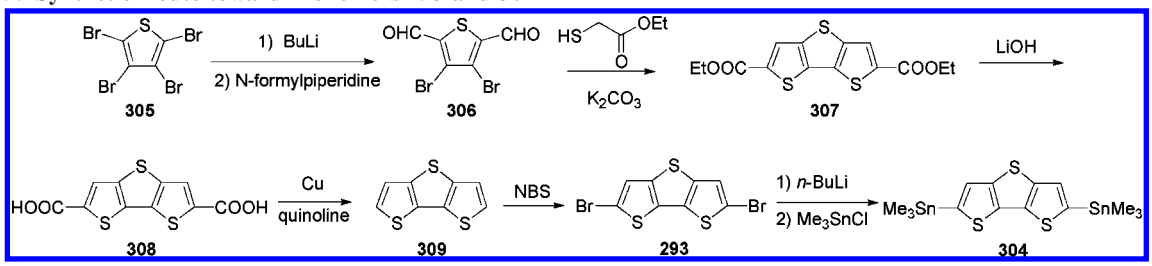


linking the backbone and $C_{60}$ is to improve solubility and simultaneously prevent donor−acceptor interaction in the ground state. The surface morphology as studied by AFM showed that the **P169** film is very smooth with an rms roughness of 1.4 nm, whereas the blend film of PCBM and reference polymer **P168** without the attached pendent $C_{60}$ showed a roughness of 3.2 nm. These results indicate that the interpenetrating network in **P169** is possibly improved as a result of the larger interfacial donor−acceptor area at the molecular level. The maximum power conversion efficiency of the PSC based on this polymer reached 0.52%, which is the best value for a double-cable polymer ever reported. The fast recombination and inefficient hopping electron transport probably accounts for the poorer results of double-cable polymers compared to blended BHJ solar cells.

## 7.7. n-Type Conjugated Polymers

While considerable efforts have been devoted to the design and synthesis of new conjugated polymers with ideal p-type semiconducting properties for BHJ solar cells, n-type materials are still dominated by the fullerene family because of their outstanding electron-accepting and -transporting properties, in particular a soluble member known as PCBM. However, the major drawback of fullerene derivatives is their weak absorption in the visible and near-infrared regions. The employment of another complementary conjugated polymer in a polymer/polymer bulk heterojunction is an effective approach for enhancing the light absorption ability of n-type materials. However, the search for an n-type conjugated polymer with improved light absorption and n-type properties comparable to those of PCBM is far more challenging because the phase separation between two different conjugated polymers is more severe. Marder and co-workers reported a new conjugated polymer (**P170**) bearing alternating electron-rich dithienothiophene and electron-deficient perylenediimine (PDI) units (Scheme 98).[354] The donor–acceptor arrangement of the main chain induces a strong intramolecular charge transfer, which leads to an increased coverage of the solar spectrum. Electron mobility of this polymer measured by FET reached as high as $1.3 \times 10^{-2}$ $cm^2/(V\ s)$ thanks to the high electron affinity and mobility of the PDI units as well as the planar structure of the fused terthiophene. An all-polymer PSC was fabricated by blending **P170** as the electron acceptor with **P84** as the donor in the active layer (1:1, w/w). The average PCE was found to be over 1%, which so far is among the highest reported in all-polymer blend PSCs.

The synthesis of dithieno[3,2-*b*:2′,2′-*d*]thiophene developed by Holmes and Frey is outlined in Scheme 99.[355] The dilithiation of tetrabromothiophene (**305**) followed by quenching with 1-formylpiperidine afforded compound **306**. In the presence of base in DMF, cyclization between the dialdehyde **306** and ethyl mercaptoacetate gave compound **307** via a thiolate addition, bromo elimination, and sequential Aldol condensation to form the two outer thiophene rings. Hydrolysis of compound **307** gave the dicarboxylic acid **308**, which underwent decaboxylation with copper in quinoline to yield **309**.

Alternatively, another n-type conjugated polymer (**P171**) containing alternating PDI units and CPDT units was synthesized by the Stille coupling of **310** and **151** (Scheme 100).[356] The HOMO and LUMO levels of **P171** were determined to be −4.02 and −5.52 eV. Having such a low-lying LUMO makes it a good candidate of n-type material. Moreover, **P171** showed reversible n-doping/dedoping and p-doping/dedoping in electrochemical processes. A PSC device using **P171** as the electron acceptor and **P108** as the electron donor in the active layer was fabricated and showed a PCE of 0.43% with a $V_{oc}$ of 0.68 V and a $J_{sc}$ of 1.4 mA/cm.[2]

## 8. Conclusions and Future Prospects

With extensive research and accumulated practical experience that we have outlined in this review, the guidelines to pursuing and developing p-type conjugated polymers be-

**Scheme 100. Synthesis of n-Type Copolymer P171 by a Stille Coupling Reaction**

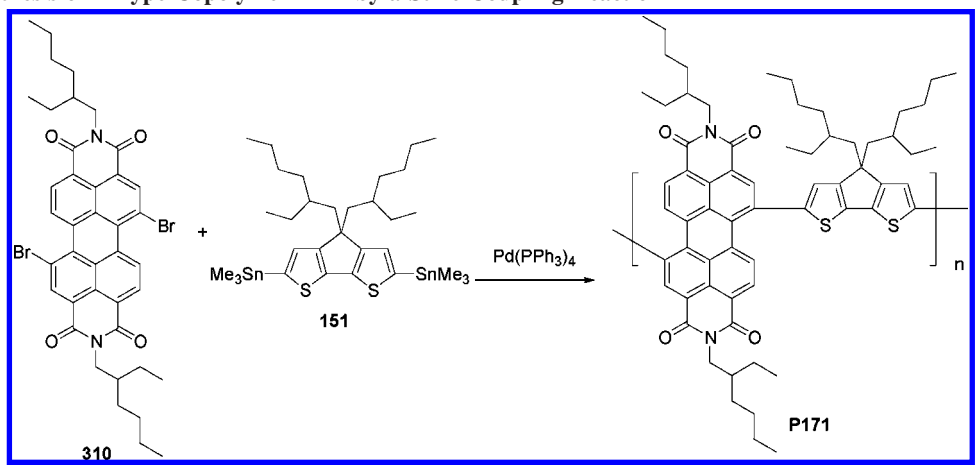


comes evident. The requirements of specific intrinsic properties necessary for an ideal donor material include (1) sufficient solubility to guarantee solution-processability as well as miscibility with n-type materials, (2) a low optical band gap for a strong and broad absorption spectrum to capture more solar energy, and 3) high hole mobility for accelerating charge transport, which in turn allows a thicker active layer required for increased light harvesting as well as reduced charge recombination and series resistance. In combination with a fixed electron acceptor, specific characteristics between a D−A pair are required: these include (1) appropriate HOMO and LUMO energies to ensure a large $V_{oc}$ and a downhill energy offset for exciton dissociation and (2) formation of an interpenetrating network with the optimum morphology for creating two distinct bicontinuous highways for transporting free charge carriers. In addition to the choice of viable molecular designs already in the "toolbox" such as chemical planarization, quinoidiation, and D−A arrangement, a new influx of molecular designs and synthetic endeavors has led to a range of novel p-type conjugated polymers. These advances have ensured an important step toward a better understanding of structure−property relationships. Structural analysis of the current successful low band gap conjugated polymers reveals that an alternating D−A arrangement is essential and must be combined with the necessary newly designed donor segments composed of multicyclic aromatic rings with enforced planarity. In accordance with these guidelines, the further development of promising donors might be fortuitously directed toward hybridizing different electron-rich aromatic units into mutually fused structures in the anticipation of benefiting from the individual intrinsic advantages. This will require more elegant designs and challenging synthesis. With respect to the development of acceptor units, the electron-withdrawing ability of an acceptor in a conjugated polymer needs to be carefully tweaked to ensure both efficient ICT transition and electron transfer. A too strong electron affinity will cause the formation of electron traps with deep-lying LUMO levels, resulting in poor electron transfer to the n-type material and hence low hole mobility. Among the wide range of acceptor units containing heteroaromatic rings with different electron affinities and resonance structures, the benzothiadiazole unit appears to be the most promising acceptor with the potential of achieving superior results. This reflects its more balanced electronic properties and simple planar structure. A general feature of the existing acceptor units is that the additional fused rings are extended in the axis perpendicular to the conjugated main chain. A range of more diversified structures outside this category is certainly desirable to fulfill the goal of creating the next generation of electron acceptors with prominent electronic and stereochemical properties. Although absorption abilities have been substantially enhanced as a result of the benefits of band gap engineering, a large number of newly produced low band gap polymers with suitable energy levels still exhibited inferior device performance compared to that of P3HT. Bulk morphological factors which are closely related to charge dissociation and transport are mainly responsible for this discrepancy. With more complex D−A conjugated polymer structures, the degree of stereoregularity is decreased to some extent. Furthermore, branched solubilizing groups introduced into the polymers to ensure solubility sometimes turn out to be able to attenuate intermolecular interactions in the solid state. As a result, the polymers generally have more amorphous character, which usually results in poorer charge-transporting properties. Without optimal control of the morphology on the nanoscale, it becomes difficult to translate the microscopic intrinsic properties of the conjugated polymer into macroscopic device performance. The development of amorphous-oriented conjugated polymers exhibiting high hole mobility might be an alternative way to overcome this problem and potentially eliminate the need of post-treatment to induce polymer crystallinity.

Beyond external treatments such as thermal or solvent annealing, bulk morphological engineering involving the tailoring of interactions between D and D, A and A, and D and A at the molecular level may emerge as an attractive solution and initiate a new explorative direction. The utilization of auxiliary supramolecular self-assembly between conjugated polymers and fullerene derivatives provides a broad window of interaction for the control of charge separation and transport within a well-defined morphology.[357] The formation of self-organized double-cable conjugated polymers can be realized by careful controlled molecular manipulation. Such a self-assembly-assisted arrangement can be permanently locked by smartly controlled lattice hardening to improve the long-term thermal stability of the morphology. Reactions triggered by light or heat for cross-linking the molecular system would be an ideal strategy.[358]

It is well-known that functional block copolymers are capable of forming nanoscale phase separations with cylindrical, lamellar, spherical, and bicontinuous morphologies.[359] It is of great interest that p-type- and n-type-containing block copolymers have the potential to be used to precisely control the nanostructure of the bulk heterojunction for improving the charge-separation at the p−n interface.

Compared with p-type conjugated polymers, current research energy devoted to the development of n-type polymers is relatively weak. This is presumably because of their low electron mobility and poor stability. However, there still holds great promise and opportunity to realize a high-performance all-polymer BHJ solar cell if an n-type conjugated polymer with electronic properties comparable to and optical properties superior to those of $C_{60}$ derivatives can be realized. The characteristic criteria of n-type semiconductors, developed for organic thin-film transistors, are also applicable to BHJ solar cells.[360−362] Future developments of n-type conjugated polymers should be directed toward achieving the following critical characteristics: (1) solubility for solution-processability and good film-forming properties, (2) miscibility and compatibility with a given p-type material in the bulk to form an optimal morphology, (3) a broad absorption spectrum, complementary to that of a p-type material, to maximizeits light-harvesting ability, (4) a high electron affinity with a low-lying LUMO energy level to facilitate efficient electron transfer and high electron mobility, (5) improved air stability of the transporting radical anion toward oxygen and water because they are notoriously responsible for electron trapping. The general guidelines of molecular design for electron-deficient n-type conjugated polymers is the introduction of electron-withdrawing moieties such as cyano, fluoro, perfluoroalkyl, perfluoroaryl, boron, and diimide into highly conjugated planar systems. Azaheteroaromatic-containing skeletons are particularly suitable.

It should be emphasized that the power conversion efficiency is more a device parameter than an intrinsic material parameter. This is because too many factors can affect the performance: blending ratios with the acceptor, solvent, annealing time and temperature, thickness of each layer, device layout, and conductivity of PEDOT related to the edge effect.[363] High efficiency of a device is a combination of material properties with judicious and careful optimization of the various fabrication conditions. One should not judge and determine a particular material's performance solely by the device value.

To produce BHJ photovoltaic devices with PCEs exceeding 10% will certainly require efforts of an interdisciplinary approach. By integrating new advanced device concepts and the nanostructure engineering of the morphology,[364] the future development of functional conjugated polymers will ensure their key role in bringing high-efficiency and low-cost plastic solar cells one step closer to successful commercialization. This review attempts to review the important and growing research field covering the synthesis and development of custom-tailored polymers for use in the increasingly relevant application of high-performance solar cells. We hope that this overview will stimulate further important research in this exciting field.

## 9. Acknowledgments

We thank Dr. Martin Dubosc, Dr. Yong-Ming Liao, and Mr. Chao-Hsiang Hsieh for their help in preparing this manuscript. We thank the National Science Council of the Republic of China for financial support.

## 10. References

(1) Brabec, C. J.; Sariciftci, N. S.; Hummelen, J. C. *Adv. Funct. Mater.* **2001**, *11*, 15.
(2) Günes, S.; Neugebauer, H.; Sariciftci, N. S. *Chem. Rev.* **2007**, *107*, 1324.
(3) Wöhrle, D.; Meissner, D. *Adv. Mater.* **1991**, *3*, 129.
(4) Tang, C. W. *Appl. Phys. Lett.* **1986**, *48*, 183.
(5) Halls, J. J. M.; Pichler, K.; Friend, R. H.; Moratti, S. C.; Holmes, A. B. *Appl. Phys. Lett.* **1996**, *68*, 3120.
(6) Theander, M.; Yartsev, A.; Zigmantas, D.; Sundström, V.; Mammo, W.; Andersson, M. R.; Inganäs, O. *Phys. Rev. B* **2000**, *61*, 12957.
(7) Haugeneder, A.; Neges, M.; Kallinger, C.; Spirkl, W.; Lemmer, U.; Feldmann, J.; Scherf, U.; Harth, E.; Gügel, A.; Müllen, K. *Phys. Rev. B* **1999**, *59*, 15346.
(8) Stübinger, T.; Brütting, W. *J. Appl. Phys.* **2001**, *90*, 3632.
(9) Markov, D. E.; Amsterdam, E.; Blom, P. W. M.; Sieval, A. B.; Hummelen, J. C. *J. Phys. Chem. A* **2005**, *109*, 5266.
(10) Yu, G.; Gao, J.; Hummelen, J. C.; Wudl, F.; Heeger, A. J. *Science* **1995**, *270*, 1789.
(11) Sariciftci, N. S.; Smilowitz, L.; Heeger, A. J.; Wudl, F. *Science* **1992**, *258*, 1474.
(12) Allemond, P. M.; Koch, A.; Wudl, F.; Rubin, Y.; Diederich, F.; Alvarez, M. M.; Anz, S. J.; Whetten, R. L. *J. Am. Chem. Soc.* **1991**, *113*, 1050.
(13) Brabec, C. J.; Zerza, G.; Cerullo, G.; Silvestri, S. D.; Luzatti, S.; Hummelen, J. C.; Sariciftci, S. *Chem. Phys. Lett.* **2001**, *340*, 232.
(14) Neugebauer, H.; Brabec, C. J.; Hummelen, J. C.; Janssen, R. A. J.; Sariciftci, N. S. *Synth. Met.* **1999**, *102*, 1002.
(15) Neugebauer, H.; Brabec, C. J.; Hummelen, J. C.; Sariciftci, N. S. *Sol. Energy Mater. Sol. Cells* **2000**, *61*, 35.
(16) Singh, T. B.; Marjanović, N.; Matt, G. J.; Günes, S.; Sariciftci, N. S.; Ramil, A. M.; Andreev, A.; Sitter, H.; Schwödiauer, R.; Bauer, S. *Org. Electron.* **2005**, *6*, 105.
(17) Becker, S. A.; Sivula, K.; Kavulak, D. F.; Fréchet, J. M. J. *Chem. Mater.* **2007**, *19*, 2927.
(18) Riedel, I.; von Hauff, E.; Parisi, J.; Martín, N.; Giacalone, F.; Dyakonov, V. *Adv. Funct. Mater.* **2005**, *15*, 1979.
(19) Popescu, L. M.; van't Hof, P.; Sieval, A. B.; Jonkman, H. T.; Hummelen, J. C. *Appl. Phys. Lett.* **2006**, *89*, 213507.
(20) Xu, Z.; Chen, L.-M.; Yang, G.; Huang, C.-H.; Hou, J.; Wu, Y.; Li, G.; Hsu, C.-S.; Yang, Y. *Adv. Funct. Mater.* **2009**, *19*, 1.
(21) Hummelen, J. C.; Knight, B. W.; LePeg, F.; Wudl, F. *J. Org. Chem.* **1995**, *60*, 532.
(22) Wienk, M. M.; Kroon, J. M.; Verhees, W. J. H.; Knol, J.; Hummelen, J. C.; van Hal, P. A.; Janssen, R. A. J. *Angew. Chem., Int. Ed.* **2003**, *42*, 3371.
(23) Yao, Y.; Shi, C.; Li, G.; Shrotriya, V.; Pei, Z.; Yang, Y. *Appl. Phys. Lett.* **2006**, *89*, 153507.
(24) Arbogast, J. W.; Foote, C. S. *J. Am. Chem. Soc.* **1991**, *113*, 8886.
(25) Scharber, M. C.; Mühlbacher, D.; Koppe, M.; Denk, P.; Waldauf, C.; Heeger, A. J.; Brabec, C. J. *Adv. Mater.* **2006**, *18*, 789.
(26) Coakley, K. M.; McGehee, M. D. *Chem. Mater.* **2004**, *16*, 4533.
(27) Koster, L. J. A.; Mihailetchi, V. D.; Blom, P. W. M. *Appl. Phys. Lett.* **2006**, *88*, 093511.
(28) Winder, C.; Sariciftci, N. S. *J. Mater. Chem.* **2004**, *14*, 1077.
(29) Bundgaard, E.; Krebs, F. C. *Sol. Energy Mater. Sol. Cells* **2007**, *91*, 954.
(30) Kroon, R.; Lenes, M.; Hummelen, J. C.; Blom, P. W. M.; de Boer, B. *Polym. Rev.* **2008**, *48*, 531.
(31) Thompson, B. C.; Fréchet, J. M. J. *Angew. Chem., Int. Ed.* **2008**, *47*, 58.
(32) Mayer, A. C.; Scully, S. R.; Hardin, B. E.; Rowell, M. W.; McGehee, M. D. *Mater. Today* **2007**, *10*, 28.
(33) Roncali, J. *Chem. Rev.* **1997**, *97*, 173.
(34) Brabec, C. J.; Cravino, A.; Meissner, D.; Sariciftci, N. S.; Fromherz, T.; Rispens, M. T.; Sanchez, L.; Hummelen, J. C. *Adv. Funct. Mater.* **2001**, *11*, 374.
(35) Lenes, M.; Wetzelaer, G.-J. A. H.; Kooistra, F. B.; Veenstra, S. C.; Hummelen, J. C.; Blom, P. W. M. *Adv. Mater.* **2008**, *20*, 2116.
(36) Kooistra, F. B.; Knol, J.; Kastenberg, F.; Popescu, L. M.; Verhees, W. J. H.; Kroon, J. M.; Hummelen, J. C. *Org. Lett.* **2007**, *9*, 551.
(37) Brabec, C. J.; Winder, C.; Sariciftic, N. S.; Hummelen, J. C.; Dhanabalan, A.; van Hal, P. A.; Janssen, R. A. J. *Adv. Funct. Mater.* **2002**, *12*, 709.
(38) Halls, J. J. M.; Cornil, J.; dos Santos, D. A.; Silbey, R.; Hwang, D.-H.; Holmes, A. B.; Brédas, J. L.; Friend, R. H. *Phys. Rev. B* **1999**, *60*, 5721.
(39) van Mullekom, H. A. M.; Vekemans, J. A. J. M.; Havinga, E. E.; Meijer, E. W. *Mater. Sci. Eng., R* **2001**, *32*, 1.
(40) Roncali, J. *Macromol. Rapid Commun.* **2007**, *28*, 1761.
(41) Brédas, J. L. *J. Chem. Phys.* **1985**, *82*, 3808.
(42) Wudl, F.; Kobayashi, M.; Heeger, A. J. *J. Org. Chem.* **1984**, *49*, 3382.
(43) Brédas, J. L.; Heeger, A. J.; Wudl, F. *J. Phys. Chem.* **1986**, *85*, 4673.
(44) Hoogmartens, I.; Adriaensens, P.; Vanderzande, D.; Gelan, J.; Quattrocchi, C.; Lazzaroni, R.; Brédas, J. L. *Macromolecules* **1992**, *25*, 7347.

(45) Pomerantz, M.; Chaloner-Gill, B.; Harding, L. O.; Tseng, J. J.; Pomerantz, W. J. *Synth. Mater.* **1993**, *55*, 960.
(46) Pomerantz, M.; Gu, X. *Synth. Mater.* **1997**, *84*, 243.
(47) Brisset, H.; Thobie-Gautier, C.; Gorgues, A.; Jubault, M.; Roncali, J. *J. Chem. Soc., Chem. Commum.* **1994**, 1305.
(48) Orti, E.; Sanchis, M. J.; Viruela, P. M.; Vituela, R. *Synth. Met.* **1999**, *101*, 602.
(49) Roncali, J.; Thobie-Gautier, C. *Adv. Mater.* **1994**, *6*, 846.
(50) Pei, Q.; Zuccarello, G.; Ahlskog, M.; Inganäs, O. *Polymer* **1994**, *35*, 1347.
(51) Zhang, Q. T.; Tour, J. M. *J. Am. Chem. Soc.* **1998**, *120*, 5355.
(52) Kitamura, C.; Tanaka, S.; Yamashita, Y. *Chem. Mater.* **1996**, *8*, 570.
(53) Brocks, G.; Tol, A. *J. Phys. Chem.* **1996**, *100*, 1838.
(54) Yamamoto, T.; Zhou, Z.-H.; Kanbara, T.; Shimura, M.; Kizu, K.; Maruyama, T.; Nakamura, Y.; Fukuda, T.; Lee, B.-L.; Ooba, N.; Tomaru, S.; Kurihara, T.; Kaino, T.; Kubota, K.; Sasaki, S. *J. Am. Chem. Soc.* **1996**, *118*, 10389.
(55) van Mullekom, H. A. M.; Vekemans, J. A. J. M.; Meijer, E. W. *Chem. Commun.* **1996**, 2163.
(56) Pivrikas, A.; Sariciftci, N. S.; Juška, G.; Österbacka, R. *Prog. Photovoltaics* **2007**, *15*, 677.
(57) Facchetti, A. *Mater. Today* **2007**, *10*, 28.
(58) Shirota, Y.; Kageyama, H. *Chem. Rev.* **2007**, *107*, 953.
(59) Sadki, S.; Schottland, P.; Brodie, N.; Sabouraud, G. *Chem. Soc. Rev.* **2000**, *29*, 283.
(60) Roncali, J. *Chem. Rev.* **1992**, *92*, 711.
(61) Waltman, R. J.; Bargon, J. *Can. J. Chem.* **1986**, *64*, 76.
(62) Toshima, N.; Hara, S. *Prog. Polym. Sci.* **1995**, *20*, 155.
(63) Cheng, Y.-J.; Luh, T.-Y. *J. Organomet. Chem.* **2004**, *689*, 4137.
(64) Tamao, K.; Sumitani, K.; Kumda, M. *J. Am. Chem. Soc.* **1972**, *94*, 4374.
(65) Stille, J. K. *Angew. Chem., Int. Ed.* **1986**, *25*, 508.
(66) Miyaura, N.; Suzuki, A. *Chem. Rev.* **1995**, *95*, 2457.
(67) Sonogashira, K. *J. Organomet. Chem.* **2002**, *653*, 46.
(68) Bao, Z.; Chan, W. K.; Yu, L. *J. Am. Chem. Soc.* **1995**, *117*, 12426.
(69) Yamamoto, T.; Morita, A.; Miyazaki, Y.; Maruyama, T.; Wakayama, H.; Zhou, Z.-H.; Nakamura, Y.; Kanbara, T.; Sasaki, S.; Kubota, K. *Macromolecules* **1992**, *25*, 1214.
(70) Burroughes, J. H.; Bradley, D. D. C.; Brown, A. R.; Marks, R. N.; Mackay, K.; Friend, R. H.; Burns, P. L.; Holmes, A. B. *Nature* **1990**, *347*, 539.
(71) McDonald, R. N.; Campbell, T. W. *J. Am. Chem. Soc.* **1960**, *82*, 4669.
(72) Wessling, R. A.; Zimmerman, R. G. U.S. Patent 3401152, 1968.
(73) Wessling, R. A. *J. Polym. Sci., Polym. Symp.* **1985**, *72*, 55.
(74) Burn, P. L.; Kraft, A.; Baigent, D. R.; Bradley, D. D. C.; Brown, A. R.; Friend, R. H.; Gymer, R. W.; Holmes, A. B.; Jackson, R. W. *J. Am. Chem. Soc.* **1993**, *115*, 10117.
(75) Padmanaban, G.; Ramakrishnan, S. *J. Am. Chem. Soc.* **2000**, *122*, 2244.
(76) Louwet, F.; Vanderzande, D.; Gelan, J.; Mullens, J. *Macromolecules* **1995**, *28*, 1330.
(77) Lutsen, L.; Adriaensens, P.; Becker, H.; Van Breemen, A. J.; Vanderzande, D.; Gelan, J. *Macromolecules* **1999**, *32*, 6517.
(78) Son, S.; Dodabalapur, A.; Lovinger, A. J.; Galvin, M. E. *Science* **1995**, *269*, 376.
(79) Papadimitrakopoulos, F.; Konstadinidis, K.; Miller, T. M.; Opila, R.; Chandross, E. A.; Galvin, M. E. *Chem. Mater.* **1994**, *6*, 1563.
(80) Braun, D.; Heeger, A. J. *Appl. Phys. Lett.* **1991**, *58*, 1982.
(81) Gilch, H. G.; Wheelwright, W. L. *J. Polym. Sci., Part A: Polym. Chem.* **1966**, *4*, 1337.
(82) Wan, W. C.; Antoniadis, H.; Choong, V. E.; Razafitrimo, H.; Gao, Y.; Feld, W. A.; Hsieh, B. R. *Macromolecules* **1997**, *30*, 6567.
(83) Neef, C. J.; Ferraris, J. P. *Macromolecules* **2000**, *33*, 2311.
(84) Denton, F. R.; Lahti, P. M.; Karasz, F. E. *J. Polym. Sci., Part A: Polym. Chem.* **1992**, *30*, 2223.
(85) Issaris, A.; Vanderzande, D.; Gelan, J. *Polymer* **1997**, *38*, 2571.
(86) Cho, B. R.; Han, M. S.; Suh, Y. S.; Oh, K. J.; Jeon, S. J. *J. Chem. Soc., Chem. Commun.* **1993**, 564.
(87) Hsieh, B. R.; Yu, Y.; forsythe, E. W.; Schaaf, G. M.; Feld, W. A. *J. Am. Chem. Soc.* **1998**, *120*, 231.
(88) Hsieh, B. R.; Yu, Y.; VanLaeken, A. C.; Lee, H. *Macromolecules* **1997**, *30*, 8094.
(89) Becker, H.; Spreitzer, H.; Kreuder, W.; Kluge, E.; Schenk, H.; Parker, I.; Cao, Y. *Adv. Mater.* **2000**, *12*, 42.
(90) Becker, H.; Spreitzer, H.; Ibrom, K.; Kreuder, W. *Macromolecules* **1999**, *32*, 4925.
(91) Chen, Z.-K.; Lee, N. H. S.; Huang, W.; Xu, Y.-S.; Cao, Y. *Macromolecules* **2003**, *36*, 1009.
(92) Liao, L.; Pang, Y.; Ding, L.; Karasz, F. E. *Macromolecules* **2001**, *34*, 6756.
(93) Moratti, S. C.; Cervini, R.; Holmes, A. B.; Baigent, D. R.; Friend, R. H.; Greenham, N. C.; Grüner, J.; Hamer, P. J. *Synth. Met.* **1995**, *71*, 2117.
(94) Bao, Z.; Chen, Y.; Cai, R.; Yu, L. *Macromolecules* **1993**, *26*, 5281.
(95) Alam, M. M.; Jenekhe, S. A. *Chem. Mater.* **2002**, *14*, 4775.
(96) Alam, M. M.; Jenekhe, S. A. *Chem. Mater.* **2004**, *16*, 4647.
(97) Zhang, F.; Johansson, M.; Andersson, M. R.; Hummelen, J. C.; Inganäs, O. *Adv. Mater.* **2002**, *14*, 662.
(98) Shrotriya, V.; Wu, E. H.-E.; Li, G.; Yao, Y.; Yang, Y. *Appl. Phys. Lett.* **2006**, *88*, 064104.
(99) Li, J.; Sun, N.; Guo, Z. X.; Li, C.; Li, Y.; Dai, L.; Zhu, D.; Sun, D.; Cao, Y.; Fan, L. *J. Phys. Chem. B* **2002**, *106*, 11509.
(100) Breeze, A. J.; Schlesinger, Z.; Carter, S. A.; Brock, P. J. *Phys. Rev. B* **2001**, *64*, 125205.
(101) Song, M. Y.; Kim, K. J.; Kim, D. Y. *Sol. Energy Mater. Sol. Cells* **2005**, *85*, 31.
(102) Wei, Q.; Hirota, K.; Tajima, K.; Hashimoto, K. *Chem. Mater.* **2006**, *18*, 5080.
(103) Neyshtadt, S.; Kalina, M.; Frey, G. L. *Adv. Mater.* **2008**, *20*, 2541.
(104) Shim, H. S.; Na, S. I.; Nam, S. H.; Ahn, H.-J.; Kim, H. J.; Kim, D.-Y.; Kim, W. B. *Appl. Phys. Lett.* **2008**, *92*, 183107.
(105) Shaheen, S. E.; Brabec, C. J.; Sariciftci, N. S.; Padinger, F.; Fromherz, T.; Hunnelen, J. C. *Appl. Phys. Lett.* **2001**, *78*, 841.
(106) Tajima, K.; Suzuki, Y.; Hashimoto, K. *J. Phys. Chem. C* **2008**, *112*, 8507.
(107) Pacios, R.; Chatten, A. J.; Kawano, K.; Durrant, J. R.; Bradley, D. D. C.; Nelson, J. *Adv. Funct. Mater.* **2006**, *16*, 2117.
(108) Kawano, K.; Ito, N.; Nishimori, T.; Sakai, J. *Appl. Phys. Lett.* **2006**, *88*, 073514.
(109) Lenes, M.; Koster, L. J. A.; Mihailetchi, V. D.; Blom, P. W. M. *Appl. Phys. Lett.* **2006**, *88*, 243502.
(110) Mens, R.; Adriaensens, P.; Lutsen, L.; Swinnen, A.; Bertho, S.; Ruttens, B.; D'Haen, J.; Manca, J.; Cleij, T.; Vanderzande, D.; Gelan, J. *J. Polym. Sci., Part A: Polym. Chem.* **2008**, *46*, 138.
(111) Park, J.; Han, S. H.; Senthilarasu, S.; Lee, S.-H. *Sol. Energy Mater. Sol. Cells* **2007**, *91*, 751.
(112) van Hal, P. A.; Wienk, M. M.; Kroon, J. M.; Verhees, W. J. H.; Slooff, L. H.; van Gennip, W. J. H.; Jonkheijm, P.; Janssen, R. A. J. *Adv. Mater.* **2003**, *15*, 118.
(113) Beek, W. J. E.; Wienk, M. M.; Kemerink, M.; Yang, X.; Janssen, R. A. J. *J. Phys. Chem. B* **2005**, *109*, 9505.
(114) Bouclé, J.; Ravirajan, P.; Nelson, J. *J. Mater. Chem.* **2007**, *17*, 3141.
(115) Sun, B.; Marx, E.; Greenham, N. C. *Nano Lett.* **2003**, *3*, 961.
(116) Tan, Z.; Tang, R.; Zhou, E.; He, Y.; Yang, C.; Xi, F.; Li, Y. *J. Appl. Polym. Sci.* **2008**, *107*, 514.
(117) Wen, S.; Pei, J.; Zhou, Y.; Xue, L.; Xu, B.; Li, Y.; Tian, W. *J. Polym. Sci., Part A: Polym. Chem.* **2009**, *47*, 1003.
(118) Shen, P.; Sang, G.; Lu, J.; Zhao, B.; Wan, M.; Zou, Y.; Li, Y.; Tan, S. *Macromolecules* **2008**, *41*, 5716.
(119) Granström, M.; Petritsch, K.; Arias, A. C.; Lux, A.; Andersson, M. R.; Friend, R. H. *Nature* **1998**, *395*, 257.
(120) Halls, J. J. M.; Walsh, C. A.; Greenham, N. C.; Marseglia, E. A.; Friend, R. H.; Moratti, S. C.; Homles, A. B. *Nature* **1995**, *376*, 498.
(121) Gupta, D.; Kabra, D.; Kolishetti, N.; Ramakrishnan, S.; Narayan, K. S. *Adv. Funct. Mater.* **2007**, *17*, 226.
(122) Dam, N.; Scurlock, R. D.; Wang, B.; Ma, L.; Sundahl, M.; Ogilby, P. R. *Chem. Mater.* **1999**, *11*, 1302.
(123) Colladet, K.; Fourier, S.; Cleij, T. J.; Lusten, L.; Gelan, J.; Vanderzande, D.; Nguyen, L. H.; Neugebauer, H.; Sariciftci, S.; Aguirre, A.; Janssen, G.; Goovaerts, E. *Macromolecules* **2007**, *40*, 65.
(124) Thompson, B. C.; Kim, Y. G.; Reynolds, J. R. *Macromolecules* **2005**, *38*, 5359.
(125) Thompson, B. C.; Kim, Y. G.; McCarley, T. D.; Reynolds, J. R. *J. Am. Chem. Soc.* **2006**, *128*, 12714.
(126) Hoppe, H.; Egbe, D. A. M.; Mühlbacher, D.; Sariciftci, N. S. *J. Mater. Chem.* **2004**, *14*, 3462.
(127) Egbe, D. A. M.; Nguyen, L. H.; Schmidtke, K.; Wild, A.; Sieber, C.; Guenes, S.; Sariciftci, N. S. *J. Polym. Sci., Part A: Polym. Chem.* **2007**, *45*, 1619.
(128) Egbe, D. A. M.; Nguyen, L. H.; Hoppe, H.; Mühlbacher, D.; Sariciftci, N. S. *Macromol. Rapid Commun.* **2005**, *26*, 1389.
(129) Scherf, U.; List, E. J. W. *Adv. Mater.* **2002**, *14*, 477.
(130) Bernius, M. T.; Inbasekaran, M.; O'Brien, J.; Wu, W. *Adv. Mater.* **2000**, *12*, 1737.
(131) Schulz, G. L.; Chen, X.; Holdcroft, S. *Appl. Phys. Lett.* **2009**, *94*, 023302.
(132) Tang, W.; Ke, L.; Tan, L.; Lin, T.; Kietzke, T.; Chen, Z. K. *Macromolecules* **2007**, *40*, 6164.
(133) Anthony, J. E. *Chem. Rev.* **2006**, *106*, 5028.
(134) Okamoto, T.; Bao, Z. *J. Am. Chem. Soc.* **2007**, *129*, 10308.

(135) Lloyd, M. T.; Mayer, A. C.; Subramanian, S.; Mourey, D. A.; Herman, D. J.; Bapat, A. V.; Anthony, J. E.; Malliaras, G. G. *J. Am. Chem. Soc.* **2007**, *129*, 9144.
(136) Okamoto, T.; Jiang, Y.; Qu, F.; Mayer, A. C.; Parmer, J. E.; McGehee, M. D.; Bao, Z. *Macromolecules* **2008**, *41*, 6977.
(137) Payne, M. M.; Odom, S. A.; Parkin, S. R.; Anthony, J. E. *Org. Lett.* **2004**, *6*, 3325.
(138) Herguth, P.; Jiang, X.; Liu, M. S.; Jen, A. K.-Y. *Macromolecules* **2002**, *35*, 6094.
(139) Campbell, A. J.; Bradley, D. D. C.; Antoniadis, H. *Appl. Phys. Lett.* **2001**, *79*, 2133.
(140) Arias, A. C.; MacKenzie, J. D.; Stevenson, R.; Halls, J. J.; Inbasekaran, M.; Woo, E. P.; Richards, D.; Friend, R. H. *Macromolecules* **2001**, *34*, 6005.
(141) Arias, A. C.; Corcoran, N.; Banach, M.; Friend, R. H.; MacKenzie, J. D. *Appl. Phys. Lett.* **2002**, *80*, 1695.
(142) Snaith, H. J.; Greenham, N. C.; Friend, R. H. *Adv. Mater.* **2004**, *16*, 1640.
(143) Kim, H.; Shin, M.; Kim, Y. *J. Phys. Chem. C* **2009**, *113*, 1620.
(144) McNeill, C. R.; Halls, J. J. M.; Wilson, R.; Whiting, G. L.; Berkebile, S.; Ramsey, M. G.; Friend, R. H.; Greenham, N. C. *Adv. Funct. Mater.* **2008**, *18*, 2309.
(145) Svensson, M.; Zhang, F.; Veenstra, S. C.; Verhees, W. J. H.; Hummelen, J. C.; Kroon, J. M.; Inganäs, O.; Andersson, M. R. *Adv. Mater.* **2003**, *15*, 988.
(146) Zhou, Q.; Hou, Q.; Zheng, L.; Deng, X.; Yu, G.; Cao, Y. *Appl. Phys. Lett.* **2004**, *84*, 1653.
(147) Hou, Q.; Xu, Y.; Yang, W.; Yuan, M.; Peng, J.; Cao, Y. *J. Mater. Chem.* **2002**, *12*, 2887.
(148) Zhang, F.; Jespersen, K. G.; Björström, C.; Svensson, M.; Andersson, M. R.; Sundström, V.; Magnusson, K.; Moons, E.; Yartsev, A.; Inganäs, O. *Adv. Funct. Mater.* **2006**, *16*, 667.
(149) Wang, P.; Abrusci, A.; Wong, H. M. P.; Svensson, M.; Andersson, M. R.; Greenham, N. C. *Nano Lett.* **2006**, *6*, 1789.
(150) Slooff, L. H.; Veenstra, S. C.; Kroon, J. M.; Moet, D. J. D.; Sweelssen, J.; Koetse, M. M. *Appl. Phys. Lett.* **2007**, *90*, 143506.
(151) Shi, C.; Yao, Y.; Yang, Y.; Pei, Q. *J. Am. Chem. Soc.* **2006**, *114*, 8980.
(152) Hou, Q.; Zhou, Q.; Zhang, Y.; Yang, W.; Yang, R.; Cao, Y. *Macromolecules* **2004**, *37*, 6299.
(153) Yang, R.; Tian, R.; Hou, Q.; Yang, W.; Cao, Y. *Macromolecules* **2003**, *36*, 7453.
(154) Yang, R.; Tian, R.; Yan, J.; Zhang, Y.; Yang, J.; Hou, Q.; Yang, W.; Zhang, C.; Cao, Y. *Macromolecules* **2005**, *38*, 244.
(155) Zhang, F.; Perzon, E.; Wang, X.; Mammo, W.; Andersson, M. R.; Inganäs, O. *Adv. Funct. Mater.* **2005**, *15*, 745.
(156) Perzon, E.; Wang, X.; Zhang, F.; Mammo, W.; Delgado, J. L.; de la Cruz, P.; Inganäs, O.; Langa, F.; Andersson, M. R. *Synth. Met.* **2005**, *154*, 53.
(157) Zhang, F.; Mammo, W.; Andersson, L. M.; Admassie, S.; Andersson, M. R.; Inganäs, O. *Adv. Mater.* **2006**, *18*, 2169.
(158) Delgado, J. L.; de la Cruz, P.; López-Arza, V.; Langa, F. *Tetrahedron Lett.* **2004**, *45*, 1651.
(159) Wang, X.; Perzon, E.; Delgado, J. L.; de la Cruzm, P.; Zhang, F.; Langa, F.; Andersson, M.; Inganäs, O. *Appl. Phys. Lett.* **2004**, *85*, 5081.
(160) Zhang, F.; Bijleveld, J.; Perzon, E.; Tvingstedt, K.; Barrau, S.; Inganäs, O.; Andersson, M. R. *J. Mater. Chem.* **2008**, *18*, 5468.
(161) Schulz, G. L.; Holdcroft, S. *Chem. Mater.* **2008**, *20*, 5351.
(162) Grazulevicius, J. V.; Strohriegl, P.; Pielichowski, J.; Pielichowsk, K. *Prog. Polym. Sci.* **2003**, *28*, 1297.
(163) Solomeshch, O.; Yu, Y.-J.; Medvedev, V.; Razin, A.; Blumer-Ganon, B.; Eichen, Y.; Jin, J.-I.; Tessler, N. *Synth. Met.* **2007**, *157*, 841.
(164) Ohmori, Y.; Kajii, H.; Sawatani, T.; Ueta, H.; Yoshino, K. *Thin Solid Films* **2001**, *393*, 407.
(165) Drolet, N.; Morin, J.-F.; Leclerc, N.; Wakim, S.; Tao, Y.; Leclerc, M. *Adv. Funct. Mater.* **2005**, *15*, 1671.
(166) Wakim, S.; Aich, B.-R.; Tao, Y.; Leclerc, M. *Polym. Rev.* **2008**, *48*, 432.
(167) Iraqi, A.; Wataru, I. *Chem. Mater.* **2004**, *16*, 442.
(168) Zhang, Z.-B.; Fujiki, M.; Tang, H.-Z.; Motonaga, M.; Torimistu, K. *Macromolecues* **2002**, *35*, 1988.
(169) Morin, J.-F.; Leclerc, M. *Macromolecules* **2001**, *34*, 4680.
(170) Dierschke, F.; Grimsdale, A. C.; Mullen, K. *Synthesis* **2003**, *16*, 2470.
(171) Cadogan, J. I. G.; Cameron-Wood, M.; Mackie, R. K.; Searle, R. J. G. *J. Chem. Soc.* **1965**, 4831.
(172) Li, J.; Dierschke, F.; Wu, J.; Grimsdale, A. C.; Müllen, K. *J. Mater. Chem.* **2006**, *16*, 96.
(173) Blouin, N.; Michaud, A.; Leclerc, M. *Adv. Mater.* **2007**, *19*, 2295.
(174) Blouin, N.; Michaud, A.; Gendron, D.; Wakim, S.; Blair, E.; Neagu-Plesu, R.; Belletête, M.; Durocher, G.; Tao, Y.; Leclerc, M. *J. Am. Chem. Soc.* **2008**, *130*, 732.
(175) Leclerc, N.; Michaud, A.; Sirois, K.; Morin, J. F.; Leclerc, M. *Adv. Funct. Mater.* **2006**, *16*, 1694.
(176) Barbarella, G.; Favaretto, L.; Sotgiu, G.; Zambianchi, M.; Arbizzani, C.; Bongini, A.; Mastragostino, M. *Chem. Mater.* **1999**, *11*, 2533.
(177) Li, Y.; Wu, Y.; Ong, B. S. *Macromolecules* **2006**, *39*, 6521.
(178) Boudreault, P.-L. T.; Wakim, S.; Blouin, N.; Simard, M.; Tessier, C.; Tao, Y.; Leclerc, M. *J. Am. Chem. Soc.* **2007**, *129*, 9125.
(179) Lu, J.; Liang, F.; Drolet, N.; Ding, J.; Tao, Y.; Movileanu, R. *Chem. Commun.* **2008**, 5315.
(180) Yudina, L. N.; Bergman, J. *Tetrahedron* **2003**, *59*, 1265.
(181) Tsai, J.-H.; Chueh, C.-C.; Lai, M.-H.; Wang, C.-F.; Chen, W.-C.; Ko, B.-T.; Ting, C. *Macromolecules* **2009**, *42*, 1897.
(182) Wei, Y.; Chan, C.-C.; Tian, J.; Jang, G.-W.; Hsueh, K. F. *Chem. Mater.* **1991**, *3*, 888.
(183) Souto Maior, R. M.; Hinkelmann, K.; Eckert, H.; Wudl, F. *Macromolecules* **1990**, *23*, 1268.
(184) Sato, M.-a.; Morii, H. *Macromolecules* **1991**, *24*, 1196.
(185) McCullough, R. D.; Lowe, R. D. *J. Chem. Soc., Chem. Commun.* **1992**, 70.
(186) McCullough, R. D.; Lowe, R. D.; Jayaraman, M.; Anderson, D. L. *J. Org. Chem.* **1993**, *58*, 904.
(187) Chen, T.-A.; Rieke, R. D. *J. Am. Chem. Soc.* **1992**, *114*, 10087.
(188) Chen, T.-A.; Wu, X.; Rieke, R. D. *J. Am. Chem. Soc.* **1995**, *117*, 233.
(189) Loewe, R. S.; Khersonsky, S. M.; McCullough, R. D. *Adv. Mater.* **1999**, *3*, 250.
(190) Loewe, R. S.; Ewbank, P. C.; Liu, J.; Zhai, L.; McCullough, R. D. *Macromolecules* **2001**, *34*, 4324.
(191) Sheina, E. E.; Liu, J.; Iovu, M. C.; Laird, D. W.; McCullough, R. D. *Macromolecules* **2004**, *37*, 3526.
(192) Iovu, M. C.; Sheina, E.; Gil, R. R.; Laird, D. W.; McCullough, R. D. *Macromolecules* **2005**, *38*, 8649.
(193) Yokoyama, A.; Miyakoshi, R.; Yokozawa, T. *Macromolecules* **2004**, *37*, 1169.
(194) Miyakoshi, R.; Yokoyama, A.; Yokozawa, T. *J. Am. Chem. Soc.* **2005**, *127*, 17542.
(195) Kim, Y. K.; Cook, S.; Tuladhar, S. M.; Choulis, S. A.; Nelson, J.; Durrant, J. R.; Bradley, D. D. C.; Giles, M.; McCulloch, I.; Ha, C.-S.; Ree, M. *Nat. Mater.* **2006**, *5*, 197.
(196) Moulé, A. J.; Meerholz, K. *Adv. Mater.* **2008**, *20*, 240.
(197) Li, G.; Shrotriya, V.; Huang, J.; Yao, Y.; Moriarty, T.; Emery, K.; Yang, Y. *Nat. Mater.* **2005**, *4*, 864.
(198) Chu, C.-W.; Yang, H.; Hou, W. J.; Huang, J.; Li, G.; Yang, Y. *Appl. Phys. Lett.* **2008**, *92*, 103306.
(199) Miller, S.; Fanchini, G.; Lin, Y.-Y.; Li, C.; Chen, C.-W.; Su, W.-F.; Chhowalla, M. *J. Mater. Chem.* **2008**, *18*, 306.
(200) Ma, W.; Yong, C.; Gong, X.; Lee, K.; Heeger, A. J. *Adv. Funct. Mater.* **2005**, *15*, 1617.
(201) Ayzner, A. L.; Wanger, D. D.; Tassone, C. J.; Tolbert, S. H.; Schwartz, B. J. *J. Phys. Chem. C* **2008**, *112*, 18711.
(202) Erb, T.; Zhokhavets, U.; Gobsch, G.; Raleva, S.; Stühn, B.; Schilinsky, P.; Waldauf, C.; Brabec, C. J. *Adv. Funct. Mater.* **2005**, *15*, 1193.
(203) Berson, S.; de Bettignies, R.; Bailly, S.; Guillerez, S. *Adv. Funct. Mater.* **2007**, *17*, 1377.
(204) Ma, W.; Gopinathan, A.; Heeger, A. J. *Adv. Mater.* **2007**, *19*, 3656.
(205) Sivula, K.; Luscombe, C. K.; Thompson, B. C.; Fréchet, J. M. J. *J. Am. Chem. Soc.* **2006**, *128*, 13988.
(206) Woo, C. H.; Thompson, B. C.; Kim, B. J.; Toney, M. F.; Fréchet, J. M. J. *J. Am. Chem. Soc.* **2008**, *130*, 16324.
(207) Thompson, B. C.; Kim, B. J.; Kavulak, D. F.; Sivula, K.; Mauldin, C.; Fréchet, J. M. J. *Macromolecules* **2007**, *40*, 7425.
(208) Ong, B. S.; Wu, Y.; Liu, P.; Gardner, S. *J. Am. Chem. Soc.* **2004**, *126*, 3378.
(209) Gurau, M. C.; Delongchamp, D. M.; Vogel, B. M.; Lin, E. K.; Fischer, D. A.; Sambasivan, S.; Richter, L. J. *Langmuir* **2007**, *23*, 834.
(210) Nguyen, L. H.; Hoppe, H.; Erb, T.; Günes, S.; Gobsch, G.; Sariciftci, N. S. *Adv. Funct. Mater.* **2007**, *17*, 1071.
(211) Schilinsky, P.; Asawapirom, U.; Scherf, U.; Biele, M.; Brabec, C. J. *Chem. Mater.* **2005**, *17*, 2175.
(212) Ma, Wanli, Kim, J. Y.; Lee, K.; Heeger, A. J. *Macromol. Rapid Commun.* **2007**, *28*, 1776.
(213) Zen, A.; Pflaum, J.; Hirschmann, S.; Zhuang, W.; Jaiser, F.; Asawapirom, U.; Rabe, J. P.; Scherf, U.; Neher, D. *Adv. Funct. Mater.* **2004**, *14*, 757.
(214) Hiorns, R. C.; de Bettignies, R.; Leroy, J.; Bailly, S.; Firon, M.; Sentein, C.; Khoukh, A.; Preud'homme, H.; Dagron-Lartigau, C. *Adv. Funct. Mater.* **2006**, *16*, 2263.
(215) Sheina, E. E.; Khersonsky, S. M.; Jones, E. G.; McCullough, R. D. *Chem. Mater.* **2005**, *17*, 3317.
(216) Heeney, M.; Zhang, W.; Crouch, D. J.; Chabinyc, M. L.; Gordeyev, S.; Hamilton, R.; Higgins, S. J.; McCulloch, I.; Skabara, P. J.; Sparrowe, D.; Tierney, S. *Chem. Commun.* **2007**, 5061.

(217) Ballantyne, A. M.; Chen, L.; Nelson, J.; Bradley, D. D. C.; Astuti, Y.; Maurano, A.; Shuttle, C. G.; Durrant, J. R.; Heeney, M.; Duffy, W.; McCulloch, I. *Adv. Mater.* **2007**, *19*, 4544.
(218) Hou, J.; Tan, Z.; Yan, Y.; He, Y.; Yang, C.; Li, Y. *J. Am. Chem. Soc.* **2006**, *128*, 4911.
(219) Li, Y.; Zou, Y. *Adv. Mater.* **2008**, *20*, 2952.
(220) Chang, Y.-T.; Hsu, S.-L.; Chen, G.-Y.; Su, M.-H.; Singh, T. A.; Diau, E. W.-G.; Wei, K.-H. *Adv. Funct. Mater.* **2008**, *18*, 2356.
(221) Zhou, E.; Tan, Z.; Yang, Y.; Huo, L.; Zou, Y.; Yang, C.; Li, Y. *Macromolecules* **2007**, *40*, 1831.
(222) Hittinger, E.; Kokil, A.; Weder, C. *Angew. Chem., Int. Ed.* **2004**, *43*, 1808.
(223) Weder, C. *Chem. Commun.* **2005**, 5378.
(224) Zhou, E.; Tan, Z.; Yang, C.; Li, Y. *Macromol. Rapid Commun.* **2006**, *27*, 793.
(225) Tu, G.; Bilge, A.; Adamczyk, S.; Forster, M.; Heiderhoff, R.; Balk, L. J.; Mühlbacher, D.; Morana, M.; Koppe, M.; Scharber, M. C.; Choulis, S. A.; Brabec, C. J.; Scherf, U. *Macromol. Rapid Commun.* **2007**, *28*, 1781.
(226) Cava, M. P.; Pollack, N. M.; Mamer, O. A.; Mitchell, M. J. *J. Org. Chem.* **1971**, *36*, 3932.
(227) van Asselt, R.; Vanderzande, D.; Gelan, J.; Froehling, P. E.; Aagaard, O. *Synth. Met.* **2000**, *110*, 25.
(228) Polec, I.; Henckens, A.; Goris, L.; Nicolas, M.; Loi, M. A.; Adriaensens, P. J.; Lutsen, L.; Manca, J. V.; Vanderzande, D.; Sariciftci, N. S. *J. Polym. Sci., Part A: Polym. Chem.* **2002**, *41*, 1034.
(229) Goris, L.; Loi, M. A.; Cravino, A.; Neugebauer, H.; Sariciftci, N. S.; Polec, I.; Lutsen, L.; Andries, E.; Manca, J.; de Schepper, L.; Vanderzande, D. *Synth. Met.* **2003**, *138*, 249.
(230) Shaheen, S. E.; Vangeneugden, D.; Kiebooms, R.; Vanderzande, D.; Fromherz, T.; Padinger, F.; Brabec, P. C. J.; Sariciftci, N. S. *Synth. Met.* **2001**, *121*, 1583.
(231) Vangeneugden, D. L.; Vanderzande, D. J. M.; Salbeck, J.; van Hal, P. A.; Janssen, R. A. J.; Hummelen, J. C.; Brabec, C. J.; Shaheen, S. E.; Sariciftci, N. S. *J. Phys. Chem. B* **2001**, *105*, 11106.
(232) Qin, Y.; Kim, J. Y.; Frisbie, C. D.; Hillmyer, M. A. *Macromolecules* **2008**, *41*, 5563.
(233) Mohanakrishnan, A. K.; Lakshmikantham, M. V.; McDougal, C.; Cava, M. P.; Baldwin, J. W.; Metzger, R. M. *J. Org. Chem.* **1998**, *63*, 3105.
(234) Vangeneugden, D. L.; Kiebooms, R. H. L.; Vanderzande, D. J. M.; Gelan, J. M. J. V. *Synth. Met.* **1999**, *101*, 120.
(235) Coppo, P.; Turner, M. L. *J. Mater. Chem.* **2005**, *15*, 1123.
(236) Lambert, T. L.; Ferraris, J. P. *J. Chem. Soc., Chem. Commun.* **1991**, 752.
(237) Ferraris, J. P.; Lambert, T. L. *J. Chem. Soc., Chem. Commun.* **1991**, 1268.
(238) Coppo, P.; Cupertino, D. C.; Yeates, S. G.; Turner, M. L. *Macromolecules* **2003**, *36*, 2705.
(239) Zhu, Z.; Waller, D.; Gaudiana, R.; Morana, M.; Mühlbacher, D.; Scharber, M.; Brabec, C. *Macromolecules* **2007**, *40*, 1981.
(240) Mühlbacher, D.; Scharber, M.; Zhengguo, M. M.; Zhu, M. M. Z.; Waller, D.; Gaudiana, R.; Brabec, C. *Adv. Mater.* **2006**, *18*, 2884.
(241) Peet, J.; Kim, J. Y.; Coates, N. E.; Ma, W. L.; Moses, D.; Heeger, A. J.; Bazan, G. C. *Nat. Mater.* **2007**, *6*, 497.
(242) Peet, J.; Soci, C.; Coffin, R. C.; Nguyen, T.-Q.; Mikhailovsky, A.; Moses, D.; Bazan, G. C. *Appl. Phys. Lett.* **2006**, *89*, 252105.
(243) Dante, M.; Garcia, A.; Nguyen, T.-Q. *J. Phys. Chem. C* **2009**, *113*, 1596.
(244) Kim, J. Y.; Lee, K.; Coates, N. E.; Moses, D.; Nguyen, T.-Q.; Dante, M.; Heeger, A. J. *Science* **2007**, *317*, 222.
(245) Soci, C.; Hwang, I.-W.; Moses, D.; Zhu, Z.; Waller, D.; Gaudiana, R.; Brabec, C. J.; Heeger, A. J. *Adv. Funct. Mater.* **2007**, *17*, 632.
(246) Hwang, I.-W.; Soci, C.; Moses, D.; Zhu, Z.; Waller, D.; Gaudiana, R.; Brabec, C. J.; Heeger, A. J. *Adv. Mater.* **2007**, *19*, 2307.
(247) Morana, M.; Wegscheider, M.; Bonanni, A.; Kopidakis, N.; Shaheen, S.; Scharber, M.; Zhu, Z.; Waller, D.; Gaudiana, R.; Brabec, C. *Adv. Funct. Mater.* **2008**, *18*, 1757.
(248) Zhang, M.; Tsao, H. N.; Pisula, W.; Yang, C.; Mishra, A. K.; Müllen, K. *J. Am. Chem. Soc.* **2007**, *129*, 3472.
(249) Moulé, A. J.; Tsami, A.; Bünnagel, T. W.; Forster, M.; Kronenberg, N. M.; Scharber, M.; Koppe, M.; Morana, M.; Brabec, C. J.; Meerholz, K.; Scherf, U. *Chem. Mater.* **2008**, *20*, 4045.
(250) Hou, J.; Chen, T. L.; Zhang, S.; Chen, H.-Y.; Yang, Y. *J. Phys. Chem. C.* **2009**, *113*, 1601.
(251) Lucas, P.; Mehdi, N. E.; Ho, H. A.; Bélanger, D.; Breau, L. *Synthesis* **2000**, *9*, 1253.
(252) Beyer, R.; Kalaji, M.; Kingscote-Burton, G.; Murphy, P. J.; Pereira, V. M. S. C.; Taylor, D. M.; Williams, G. O. *Synth. Mater.* **1998**, *92*, 95.
(253) Jeffries, A. T.; Moore, K. C.; Ondeyka, D. M.; Springsteen, A. W.; MacDowell, D. W. H. *J. Org. Chem.* **1981**, *46*, 2885.
(254) Kraak, A.; Wiersema, A. K.; Jordens, P.; Wynberg, H. *Tetrahedron* **1968**, *24*, 3381.
(255) Brzeziński, J. Z.; Reynolds, J. R. *Synthesis* **2002**, *8*, 1053.
(256) Yamaguchi, S.; Tamao, K. *Bull. Chem. Soc. Jpn.* **1996**, *69*, 2327.
(257) Tamao, K.; Uchida, M.; Izumizawa, T.; Furukawa, K.; Yamaguchi, S. *J. Am. Chem. Soc.* **1996**, *118*, 11974.
(258) Liu, M. S.; Luo, J.; Jen, A. K.-Y. *Chem. Mater.* **2003**, *15*, 3496.
(259) Luo, J.; Xie, Z.; Lam, J. W. Y.; Cheng, L.; Chen, H.; Qiu, C.; Kwok, H. S.; Zhan, X.; Liu, Y.; Zhu, D.; Tang, B. Z. *Chem. Commun.* **2001**, 1740.
(260) Chen, J.; Cao, Y. *Macromol. Rapid Commun.* **2007**, *28*, 1714.
(261) Tamao, K.; Ohno, S.; Yamaguchi, S. *Chem. Commun.* **1996**, 1873.
(262) Tamao, K.; Yamaguchi, S.; Shiozaki, M.; Nakagawa, Y.; Ito, Y. *J. Am. Chem. Soc.* **1992**, *114*, 5867.
(263) Yamaguchi, S.; Goto, T.; Tamao, K. *Angew. Chem., Int. Ed.* **2000**, *39*, 1695.
(264) Wang, F.; Luo, J.; Yang, K.; Chen, J.; Huang, F.; Cao, Y. *Macromolecules* **2005**, *38*, 2253.
(265) Tamao, K.; Yamaguchi, S.; Shiro, M. *J. Am. Chem. Soc.* **1994**, *116*, 11715.
(266) Wang, E.; Wang, L.; Lan, L.; Luo, C.; Zhuang, W.; Peng, J.; Cao, Y. *Appl. Phys. Lett.* **2008**, *92*, 033307.
(267) Boudreault, P.-L. T.; Michaud, A.; Leclerc, M. *Macromol. Rapid Commun.* **2007**, *28*, 2176.
(268) Chan, K. L.; McKiernan, M. J.; Towns, C. R.; Holmes, A. B. *J. Am. Chem. Soc.* **2005**, *127*, 7662.
(269) Liao, L.; Dai, L.; Smith, A.; Durstock, M.; Lu, J.; Ding, J.; Tao, Y. *Macromolecules* **2007**, *40*, 9406.
(270) Hou, J.; Chen, H. Y.; Zhang, S.; Li, G.; Yang, Y. *J. Am. Chem. Soc.* **2008**, *130*, 16144.
(271) Ogawa, K.; Rasmussen, S. C. *Macromolecules* **2006**, *39*, 1771.
(272) Zhou, E.; Nakamura, M.; Nishizawa, T.; Zhang, Y.; Wei, Q.; Tajima, K.; Yang, C.; Hashimoto, K. *Macromolecules* **2008**, *41*, 8302.
(273) Ogawa, K.; Rasmussen, S. C. *J. Org. Chem.* **2003**, *68*, 2921.
(274) Pan, H.; Li, Y.; Wu, Y.; Liu, P.; Ong, B. S.; Zhu, S.; Xu, G. *J. Am. Chem. Soc.* **2007**, *129*, 4112.
(275) Hou, J.; Park, M. H.; Zhang, S.; Yao, Y.; Chen, L. M.; Li, J. H.; Yang, Y. *Macromolecules* **2008**, *41*, 6012.
(276) Beimling, P.; Kossmehl, G. *Chem. Ber.* **1986**, *119*, 3198.
(277) Lee, K.; Sotzing, G. A. *Macromolecules* **2001**, *34*, 5746.
(278) Sotzing, G. A.; Lee, K. *Macromolecules* **2002**, *35*, 7281.
(279) Lee, B.; Yavuz, M. S.; Sotzing, G. A. *Macromolecules* **2006**, *39*, 3118.
(280) Liang, Y.; Xiao, S.; Feng, D.; Yu, L. *J. Phys. Chem. C* **2008**, *112*, 7866.
(281) Yao, Y.; Liang, Y.; Shrotriya, V.; Xiao, S.; Yu, L.; Yang, Y. *Adv. Mater.* **2007**, *19*, 3979.
(282) Liang, Y.; Feng, D.; Guo, J.; Szarko, J. M.; Ray, C.; Chen, L. X.; Yu, L. *Macromolecules* **2009**, *42*, 1091.
(283) Liang, Y.; Wu, Y.; Feng, D.; Tsai, S.-T.; Son, H.-J.; Li, G.; Yu, L. *J. Am. Chem. Soc.* **2009**, *131*, 56.
(284) Zwanenburg, D. J.; de Haan, H.; Wynberg, H. *J. Org. Chem.* **1966**, *31*, 3363.
(285) Rutherford, D. R.; Stille, J. K.; Elliott, C. M.; Reichert, V. R. *Macromolecules* **1992**, *25*, 2294.
(286) Danieli, R.; Taliani, C.; Zamboni, R.; Giro, G.; Biserni, M.; Masragostino, M.; Testoni, A. *Synth. Met.* **1986**, *13*, 325.
(287) Miguel, L. S.; Matzger, A. J. *Macromolecules* **2007**, *40*, 9233.
(288) Zhang, X.; Köhler, M.; Matzger, A. J. *Macromolecules* **2004**, *37*, 6306.
(289) He, Y.; Wu, W.; Zhao, G.; Liu, Y.; Li, Y. *Macromolecules* **2008**, *41*, 9760.
(290) Mcculloch, I.; Heeney, M.; Bailey, C.; Genevicius, K.; Macdonald, I.; Shkunov, M.; Sparrowe, D.; Tierney, S.; Wagner, R.; Zhang, W.; Chabinyc, M. L.; Kline, R. J.; McGehee, M. D.; Toney, M. F. *Nat. Mater.* **2006**, *5*, 328.
(291) DeLongchamp, D. M.; Kline, R. J.; Lin, E. K.; Fischer, D. A.; Richter, L. J.; Lucas, L. A.; Heeney, M.; McCulloch, I.; Northrup, J. E. *Adv. Mater.* **2007**, *19*, 833.
(292) Chabinyc, M. L.; Toney, M. F.; Kline, R. J.; Mcculloch, I.; Heeney, M. *J. Am. Chem. Soc.* **2007**, *129*, 3226.
(293) Kline, R. J.; DeLongchamp, D. M.; Fischer, D. A.; Lin, E. K.; Richter, L. J.; Chabinyc, M. L.; Toney, M. F.; Heeney, M.; McCulloch, I. *Macromolecules* **2007**, *40*, 7960.
(294) Hwang, I.-W.; Kim, J. Y.; Cho, S.; Yuen, J.; Coates, N.; Lee, K.; Heeney, M.; Mcculloch, I.; Moses, D.; Heeger, A. J. *J. Phys. Chem. C* **2008**, *112*, 7853.
(295) Parmer, J. E.; Mayer, A. C.; Hardin, B. E.; Scully, S. R.; McGehee, M. D.; Heeney, M.; McCulloch, I. *Appl. Phys. Lett.* **2008**, *92*, 113309.
(296) Fuller, L. S.; Iddon, B.; Smith, K. A. *J. Chem. Soc., Perkin Trans. 1* **1997**, 3465.
(297) Xiao, C.; Zhou, H.; You, W. *Macromolecules* **2008**, *41*, 5688.

(298) Watanabe, H.; Kumagai, J.; Tsurugi, H.; Satoh, T.; Miura, M. *Chem. Lett.* **2007**, *36*, 1336.
(299) Zhao, C.; Zhang, Y.; Ng, M.-K. *J. Org. Chem.* **2007**, *72*, 6364.
(300) Zhao, C.; Chen, X.; Zhang, Y.; Ng, M.-K. *J. Polym. Sci., Part A: Polym. Chem.* **2008**, *46*, 2680.
(301) Chen, C. P.; Chan, S. H.; Chao, T. C.; Ting, C.; Ko, B. T. *J. Am. Chem. Soc.* **2008**, *130*, 12828.
(302) Chan, S. H.; Chen, C.-P.; Chao, T.-C.; Ting, C.; Lin, C.-S.; Ko, B.-T. *Macromolecules* **2008**, *41*, 5519.
(303) Tierney, S.; Heeney, M.; McCulloch, I. *Synth. Met.* **2005**, *148*, 195.
(304) Wong, K.-T.; Chao, T.-C.; Chi, L.-C.; Chu, Y.-Y.; Balaiah, A.; Chiu, S.-F.; Liu, Y.-H.; Wang, Y. *Org. Lett.* **2006**, *8*, 5033.
(305) Dhanabalan, A.; van Duren, J. K. J.; van Hal, P. A.; van Dongen, J. L. J.; Janssen, R. A. J. *Adv. Funct. Mater.* **2001**, *11*, 255.
(306) van Duren, J. K. J.; Dhanabalan, A.; van Hall, P. A.; Janssen, R. A. J. *Synth. Met.* **2001**, *121*, 1587.
(307) Hao, Z.; Iqbal, A. *Chem. Soc. Rev.* **1997**, *26*, 203.
(308) Bürgi, L.; Turbiez, M.; Pfeiffer, R.; Bienewald, F.; Kirner, H.-J.; Winnewisser, C. *Adv. Mater.* **2008**, *20*, 2217.
(309) Wienk, M. M.; Turbiez, M.; Gilot, J.; Janseen, R. A. J. *Adv. Mater.* **2008**, *20*, 2556.
(310) Wienk, M. M.; Turbiez, M. G. R.; Struijk, M. P.; Fonrodona, M.; Janssen, R. A. J. *Appl. Phys. Lett.* **2006**, *88*, 153511.
(311) Wienk, M. M.; Struijk, M. P.; Janssen, R. A. J. *Chem. Phys. Lett.* **2006**, *422*, 488.
(312) Zoombelt, A. P.; Fonrodonda, M.; Wienk, M. M.; Sieval, A. B.; Hummelen, J. C.; Janssen, R. A. J. *Org. Lett.* **2009**, *11*, 903.
(313) Kooistra, F. B.; Mihailetchi, V. D.; Popescu, L. M.; Kronholm, D.; Blom, P. W. M.; Hummelen, J. C. *Chem. Mater.* **2006**, *18*, 3068.
(314) Ono, K.; Tanaka, S.; Yamashita, Y. *Angew. Chem., Ind. Ed. Engl.* **1994**, *33*, 1977.
(315) Karikomi, M.; Kitamura, C.; Tanaka, S.; Yamashita, Y. *J. Am. Chem. Soc.* **1995**, *117*, 6791.
(316) Bundgaard, E.; Krebs, F. C. *Macromolecules* **2006**, *39*, 2823.
(317) Bundgaard, E.; Krebs, F. C. *Sol. Energy Mater. Sol. Cells* **2007**, *91*, 1019.
(318) Peng, Q.; Lu, Z.-Y.; Huang, Y.; Xie, M.-G.; Han, S.-H.; Peng, J.-B.; Cao, Y. *Chem. Mater.* **2004**, *37*, 260.
(319) Kim, J. H.; Lee, H. *Chem. Mater.* **2002**, *14*, 2270.
(320) Peng, Q.; Park, K.; Lin, T.; Durstock, M.; Dai, L. *J. Phys. Chem. B* **2008**, *112*, 2801.
(321) Loewe, R. S.; McCullough, R. D. *Chem. Mater.* **2000**, *12*, 3214.
(322) Smith, A. P.; Smith, R. R.; Taylor, B. E.; Durstock, M. F. *Chem. Mater.* **2004**, *16*, 4687.
(323) Hou, J.; Tan, Z.; He, Y.; Yang, C.; Li, Y. *Macromolecules* **2006**, *39*, 4657.
(324) Henckens, A.; Knipper, M.; Polec, I.; Manca, J.; Lutsen, L.; Vanderzande, D. *Thin Solid Films* **2004**, *451*, 572.
(325) Henckens, A.; Colladet, K.; Fourier, S.; Cleij, T. J.; Lutsen, L.; Gelan, J.; Vanderzande, D. *Macromolecules* **2005**, *38*, 19.
(326) Nguyen, L. H.; Günes, S.; Neugebauer, H.; Sariciftci, N. S.; Banishoeib, F.; Henckens, A.; Cleij, T.; Lutsen, L.; Vanderzande, D. *Sol. Energy Mater. Sol. Cells* **2006**, *90*, 2815.
(327) Ashraf, R. S.; Shahid, M.; Klemm, E.; Al-Ibrahim, M.; Sensfuss, S. *Macromol. Rapid Commun.* **2006**, *27*, 1454.
(328) Hou, Y.; Chen, Y.; Liu, Q.; Yang, M.; Wan, X.; Yin, S.; Yu, A. *Macromolecules* **2008**, *41*, 3114.
(329) Huo, L. J.; He, C.; Han, M.; Zhou, E.; Li, Y. F. *J. Polym. Sci., Part A: Polym. Chem.* **2007**, *45*, 3861.
(330) Cho, N. S.; Park, J.-H.; Lee, S.-K.; Lee, J.; Shim, H.-K.; Park, M.-J.; Hwang, D.-H.; Jung, B.-J. *Macromolecules* **2006**, *39*, 177.
(331) Tang, W.; Kietzke, T.; Vemulamada, P.; Chen, Z.-K. *J. Polym. Sci., Part A: Polym. Chem.* **2007**, *45*, 5266.
(332) Brun, M.; Demadrille, R.; Rannou, P.; Pron, A.; Travers, J.-P.; Grévin, B. *Adv. Mater.* **2004**, *16*, 2087.
(333) Demadrille, R.; Delbosc, N.; Kervella, Y.; Firon, M.; de Bettignies., R.; Billon, M.; Rannou, P.; Pron, A. *J. Mater. Chem.* **2007**, *17*, 4661.
(334) Demadrille, R.; Firon, M.; Leroy, J.; Rannou, P.; Pron, A. *Adv. Funct. Mater.* **2005**, *15*, 1547.
(335) Hayashi, S.; Tanaka, M.; Hayashi, H.; Eu, S.; Umeyama, T.; Matano, Y.; Araki, Y.; Imahori, H. *J. Phys. Chem. C* **2008**, *112*, 15576.
(336) Rochford, J.; Chu, D.; Hagfeldt, A.; Galoppini, E. *J. Am. Chem. Soc.* **2007**, *129*, 4655.
(337) Feng, J.; Zhang, Q.; Li, W.; Li, Y.; Yang, M.; Cao, Y. *J. Appl. Polym. Sci.* **2008**, *109*, 2283.
(338) Huang, X.; Zhu, C.; Zhang, S.; Li, W.; Guo, Y.; Zhan, X.; Liu, Y.; Bo, Z. *Macromolecules* **2008**, *41*, 6895.
(339) Masai, H.; Sonogashira, K.; Hagihara, N. *Bull. Chem. Soc. Jpn.* **1971**, *44*, 2226.
(340) Guo, F.; Kim, Y. G.; Reynolds, J. R.; Schanze, K. S. *Chem. Commun.* **2006**, 1887.
(341) Schanze, K. S.; Silverman, E. E.; Zhao, X. *J. Phys. Chem. B* **2005**, *109*, 18451.
(342) Wong, W.-Y.; Wang, X.-Z.; He, Z.; Chan, K.-K.; Djurisić, A. B.; Cheung, K.-Y.; Yip, C.-T.; Ng, A. M.-C.; Xi, Y. Y.; Mak, C. S. K.; Chan, W.-K. *J. Am. Chem. Soc.* **2007**, *129*, 14372.
(343) Wong, W.-Y.; Wang, X.-Z.; He, Z.; Djurišić, A. B.; Yip, C.-T.; Cheung, K.-Y.; Wang, H.; Mak, C. S. K.; Chan, W.-K. *Nat. Mater.* **2007**, *6*, 521.
(344) Gilot, J.; Wienk, M. M.; Janssen, R. A. J. *Nat. Mater.* **2007**, *6*, 704.
(345) Wu, P.-T.; Bull, T.; Kim, F. S.; Luscombe, C. K.; Jenekhe, S. A. *Macromolecules* **2009**, *42*, 671.
(346) Liu, L.; Ho, C.-L.; Wong, W.-Y.; Cheung, K.-Y.; Fung, M.-K.; Lam, W.-T.; Djurišić, A. B.; Chan, W.-K. *Adv. Funct. Mater.* **2008**, *18*, 2824.
(347) Mei, J.; Ogawa, K.; Kim, Y.-G.; Heston, N. C.; Arenas, D. J.; Nasrollahi, Z.; McCarley, T. D.; Tanner, D. B.; Reynolds, J. R.; Schanze, K. S. *ACS Appl. Mater. Interfaces* **2009**, *1*, 150.
(348) Baek, N. S.; Hau, S. K.; Yip, H.-L.; Acton, O.; Chen, K.-S.; Jen, A. K.-Y. *Chem. Mater.* **2008**, *20*, 5734.
(349) Cravino, A.; Sariciftci, N. S. *J. Mater. Chem.* **2002**, *12*, 1931.
(350) Cravino, A.; Sariciftci, N. S. *Nat. Mater.* **2003**, *2*, 360.
(351) Zhang, F.; Svensson, M.; Anderson, M. R.; Maggini, M.; Bucella, S.; Menna, E.; Inganäs, O. *Adv. Mater.* **2001**, *13*, 1871.
(352) Ramos, A. M.; Rispens, M. T.; van Duren, J. K. J.; Hummelen, J. C.; Janssen, R. A. J. *J. Am. Chem. Soc.* **2001**, *123*, 6714.
(353) Tan, Z.; Hou, J.; He, Y.; Zhou, E.; Yang, C.; Li, Y. *Macromolecules* **2007**, *40*, 1868.
(354) Zhan, X.; Tan, Z.; Domercq, B.; An, Z.; Zhang, X.; Barlow, S.; Li, Y.; Zhu, D.; Kippelen, B.; Marder, S. R. *J. Am. Chem. Soc.* **2007**, *129*, 7246.
(355) Frey, J.; Bond, A. D.; Holmes, A. B. *Chem. Commun.* **2002**, 2424.
(356) Hou, J.; Zhang, S.; Chen, T. L.; Yang, Y. *Chem. Commun.* **2008**, 6034.
(357) Rispens, M. T.; Sánchez, L.; Beckers, E. H. A.; van Hal, P. A.; Schenning, A. P. H. J.; El-ghayoury, A.; Peeters, E.; Meijer, E. W.; Janssen, R. A. J.; Hummelen, J. C. *Synth. Met.* **2003**, *135*, 801.
(358) Drees, M.; Hoppe, H.; Winder, C.; Neugebauer, H.; Sariciftci, N. S.; Schwinger, W.; Schäffler, F.; Topf, C.; Scharber, M. C.; Zhu, Z.; Gaudiana, R. *J. Mater. Chem.* **2005**, *15*, 5158.
(359) Jenekhe, S. A.; Chen, X. L. *Science* **1998**, *279*, 1903.
(360) Newman, C. R.; Frisbie, C. D.; da Silva Filho, D. A.; Brédas, J.-L.; Ewbank, P. C.; Mann, K. R. *Chem. Mater.* **2004**, *16*, 4436.
(361) Dimitrakopoulos, C. D.; Malenfant, P. R. L. *Adv. Mater.* **2002**, *14*, 99.
(362) Murphy, A. R.; Fréchet, J. M. J. *Chem. Rev.* **2007**, *107*, 1066.
(363) Cravino, A.; Schilinsky, P.; Brabec, C. J. *Adv. Funct. Mater.* **2007**, *17*, 3906.
(364) Veenstra, S. C.; Loos, J.; Kroon, J. M. *Prog. Photovoltaics* **2007**, *15*, 727.

CR900182S